POLITECNICO DI MILANO

School of Industrial and Information Engineering
Department of Chemistry, Materials and Chemical Engineering "G. Natta"
Master of Science in Materials Engineering and Nanotechnology

EFFECTIVENESS OF CALCIUM NITRATE AS CORROSION INHIBITOR IN CONCRETE

Supervisor: Professor Marco ORMELLESE

Co-supervisor: Professor Fabio BOLZONI

Master Thesis by:

Marta ZERBI – ID 854190

Academic Year 2016/2017

Abstract
English

The main purpose of the present work is the investigation of a new class of inorganic concrete corrosion inhibitors, identified by calcium nitrate, that may represent the replacement for the well-established nitrite inhibitor, affected by toxicity issues. The research focused on the demonstration of an eventual beneficial effect on chlorides and carbonation-induced corrosion, that are the main reasons of concrete degradation. The concrete environment was simulated through alkaline synthetic pore solutions (pH 12.6), where calcium nitrate inhibitor was admixed in 0.1 mol/L and 0.3 mol/L concentrations; for comparison purposes, equivalent solutions were developed by adding calcium nitrite, in the same concentrations, and without any inhibitors (as reference).

Periodic free corrosion potential measurements on immersed steel samples identified a delayed effect on the metal passivation development induced by the presence of nitrate ions in the solution. Indeed, an absent calcium nitrate inhibitive effectiveness was demonstrated through potentiodynamic polarization tests on solutions contaminated by chlorides ions (0.1 mol/L and 0.3 mol/L dosages). Long-term potentiostatic polarization measurements confirmed and demonstrated, in a more reliable way, the complete calcium nitrate inhibitive ineffectiveness on chloride-induced corrosion: a decrease of 66% on the critical chloride threshold was observed with 0.1 mol/L nitrate concentration, compared to the reference test. The absence of any rebars corrosion inhibition can be related to the slow and feeble metal passivation development induced by the presence of nitrate ions. Instead, calcium nitrite showed the well-known good inhibition effect on chloride-induced corrosion: increased critical chloride threshold by 63% was observed with 0.1 mol/L nitrite concentration.

A moderate calcium nitrate delayed effect on the carbonation process diffusion through concrete was assessed on three different cement Series: CEM I 52.5R, CEM II/B-S 52.5 and CEM II/B-M 42.5. The nitrate compound, admixed to the cement paste in 4% by weight of cement dosage, seem to be sufficient for a CO_2 diffusion reduction by at least 15%, especially regarding the first and the third Series. These results were obtained through the periodic carbonation depth monitoring on concrete samples placed into a carbonation chamber (4% CO_2 concentration), to accelerate the process. They are comparable with corresponding measurements on concrete samples exposed to the aerated external atmosphere. The complete absence of calcium nitrate inhibitive effect on rebars carbonation-induced corrosion was finally demonstrated: linear polarization resistance measurements showed comparable reinforcements corrosion rates on carbonated concrete samples compared to the reference ones.

Abstract
Italiano

Lo scopo principale di questo lavoro di tesi risiede nella ricerca di una nuova classe di inibitori di corrosione inorganici per il degrado del calcestruzzo. È possibile indentificare nel nitrato di calcio un possibile candidato come sostituto al ben noto ed efficiente nitrito, colpito tuttavia da problemi di tossicità. La ricerca si è focalizzata maggiormente sullo studio di un'eventuale azione inibitiva da parte del nitrato sulla corrosione delle armature in acciaio indotta da cloruri e da carbonatazione, essendo queste le principali cause di degrado del calcestruzzo armato. L'ambiente interno del cemento è stato simulato con soluzioni alcaline artificiali (pH 12.6), a cui è stato aggiunto l'inibitore nitrato in concentrazioni 0.1 mol/L e 0.3 mol/L. Come confronto, sono state create soluzioni equivalenti con l'aggiunta di nitrito di calcio (nelle stesse concentrazioni) e senza alcun inibitore (come riferimento).

La misura periodica dei potenziali di libera corrosione sui campioni di armatura immersi nelle diverse soluzioni alcaline ha permesso di individuare un effetto ritardante da parte del nitrato nello sviluppo del film passivo di ossido sulla superficie metallica. Infatti, a seguito della contaminazione da cloruri (in concentrazioni 0.1 mol/L e 0.3 mol/L), è stata riscontrata una totale assenza di inibizione in questo tipo di soluzioni durante le prove di polarizzazione potenziodinamica. Test a lungo termine di polarizzazione potenziostatica hanno confermato e dimostrato, in modo più affidabile, la completa inefficacia del nitrato di calcio come inibitore di corrosione da cloruri: un calo del 66% nella concentrazione critica di cloruri rispetto al riferimento è stato osservato in presenza di ioni nitrato in dosaggio 0.1 mol/L. Questa assenza di efficacia inibente può essere ricondotta al lento e debole sviluppo di passività indotto dalla presenza del nitrato di calcio nelle soluzioni alcaline. Al contrario, la buona efficacia dello ione nitrito come inibitore di corrosione è stata confermata, riscontrando un aumento del 63% nella concentrazione critica di cloruri in presenza del composto inibente in dosaggio 0.1 mol/L.

Il nitrato di calcio ha dimostrato, invece, un effetto benefico nella diffusione del processo di carbonatazione all'interno del cemento. Sono state esaminate le profondità di carbonatazione su tre tipi di cemento (CEM I 52.5R, CEM II/B-S 52.5 e CEM II/B-M 42.5), a seguito della contaminazione da CO_2, sia accelerata (in camera di carbonatazione al 4% di CO_2) che realistica (con campioni esposti all'atmosfera). Sono stati ottenuti risultati comparabili, secondo i quali il nitrato di calcio risulta indurre un effetto ritardante nella penetrazione del gas all'interno del cemento: aggiungendo alla pasta cementizia il composto al 4% rispetto al peso di cemento è stato riscontrato un calo minimo del 15% nella diffusione del processo di carbonatazione, specialmente

nei cementi CEM I 52.5R e CEM II/B-M 42.5. Infine, per quanto riguarda la corrosione delle armature, a seguito della completa carbonatazione del cemento, sono state effettuate misure di velocità di corrosione su provini armati, esposti all'atmosfera, con le stesse composizioni sopra descritte. È possibile dimostrare che l'aggiunta di nitrato di calcio non induca alcun effetto inibente: velocità di corrosione confrontabili o persino più gravose rispetto ai campioni di riferimento sono state riscontrate tramite le misure della resistenza di polarizzazione durante la tecnica di polarizzazione lineare.

Table of contents

Abstract English I

Abstract Italiano II

Introduction 1

Chapter 1. Corrosion in concrete 3

1.1 Concrete general aspects 3

1.2 Mechanism of corrosion 5

1.2.1 Corrosion process 7

1.2.2 Polarization curves 8

1.3 Chloride-induced corrosion 11

1.3.1 Critical chloride threshold 12

1.3.2 Chloride penetration 13

1.3.3 Pitting corrosion 14

1.4 Carbonation-induced corrosion 15

1.4.1 Penetration of carbonation 16

1.4.2 Corrosion in carbonated concrete 17

1.5 Prevention and repair for concrete corrosion 18

1.5.1 Concrete quality 18

1.5.2 Additional protection measures 19

Chapter 2. Corrosion inhibitors 21

2.1 Effect on the service life 22

2.2 Inhibition mechanism 23

2.2.1 Effect on chloride-induced corrosion 24

2.2.2 Effect on carbonation-induced corrosion 25

2.2.3 Inhibitor effectiveness 26

2.3 Nitrite-based inhibitors 26

2.3.1 Inhibiting mechanism 27

2.3.2 Effectiveness 28

2.3.3 Effect on concrete properties 30
2.4 Nitrate-based inhibitors 30
2.4.1 Inhibiting mechanism 31
2.4.2 Effectiveness 33
2.4.3 Effect on concrete properties 36
Chapter 3. Experimental methods 38
3.1 Potentiodynamic tests in solution 39
3.1.1 Materials and instrumentation 40
3.1.2 Test procedure 43
3.2 Potentiostatic tests in solution 47
3.2.1 Materials and instrumentation 48
3.2.2 Test procedure 50
3.3 Tests in concrete 52
3.3.1 Concrete compositions 52
3.3.2 Concrete samples 54
3.3.3 Carbonation monitoring 56
3.3.4 Corrosion monitoring 57
Chapter 4. Experimental results 59
4.1 Potentiodynamic tests in solution 59
4.1.1 Reproducibility 60
4.1.2 Reference solution 61
4.1.3 Nitrite inhibited solution 63
4.1.4 Nitrate inhibited solution 67
4.2 Potentiostatic tests in solution 69
4.2.1 Reference solution 70
4.2.2 Nitrite solution 72
4.2.3 Nitrate solution 74
4.2.4 Mixed nitrite-nitrate solution 76
4.3 Carbonation monitoring on concrete samples 78
4.3.1 Accelerated carbonation monitoring 78
4.3.2 Real carbonation monitoring 80
4.4 Rebars corrosion monitoring 81

4.4.1 Free corrosion potential 82
4.4.2 Linear polarization resistance 83

Chapter 5. Discussion 85

5.1 Effect on the steel passivation 85
5.2 Effect on the passivity range 87
5.3 Effectiveness on chloride-induced corrosion 89
5.3.1 Pitting potential 89
5.3.2 Repassivation potential 91
5.3.3 Passive current density 92
5.3.4 Critical chloride threshold 94
5.4 Effectiveness on carbonation-induced corrosion 97
5.4.1 Accelerated carbonation monitoring 97
5.4.2 Real carbonation monitoring 100
5.5 Effectiveness on rebars corrosion 102
5.5.1 Free corrosion potential monitoring 103
5.5.2 Penetration rate 104

Conclusions 106

Bibliography 109

Appendix A - Cyclic polarization curves 115

A.1 Reference solutions 115
A.2 Nitrite inhibited solutions 117
A.3 Nitrate inhibited solutions 119

List of figures

Fig. 1.1 Dimensional range of solids and pores in hydrated cement paste [9]. 4
Fig. 1.2 Representation of water present in capillary pores [1]. 5
Fig. 1.3 Tuutti's model of steel reinforcement corrosion in concrete [12]. 6
Fig. 1.4 Example of concrete delamination due to carbonation induced corrosion [82]. 7
Fig. 1.5 Electrochemical process of rebars corrosion in concrete [83]. 8
Fig. 1.6 Anodic polarization curve of steel in non-carbonated concrete without chlorides [1]. 9
Fig. 1.7 Cathodic polarization curves in alkaline concrete: (a) aerated; (b) wet, (c) completely saturated with water [1]. 9
Fig. 1.8 Corrosion condition of passive steel in concrete, under different environmental conditions [1]. 10
Fig. 1.9 Chloride-induced corrosion in marine environment [84]. 11
Fig. 1.10 Schematic representation of pitting corrosion of steel in concrete [1]. 14
Fig. 1.11 Anodic and cathodic polarization curves with different chloride contents. 15
Fig. 1.12 Rate of concrete carbonation as a function of relative humidity of the environment [12]. 16
Fig. 1.13 Corrosion condition of steel in carbonated concrete in equilibrium with environments of different relative humidity. 17

Fig. 2.1 Influence of the inhibitor on the service life. 22
Fig. 2.2 Effect of the anodic inhibitor. 23
Fig. 2.3 Effect of the cathodic inhibitor. 24
Fig. 2.4 Nitrite anion [85]. 26
Fig. 2.5 Corrosion rate trend in function of $[NO_2^-]/[Cl^-]$ ratio [32]. 29
Fig. 2.6 Nitrate ion [49]. 31
Fig. 2.7 Results of linear polarization resistance tests [6]. 34
Fig. 2.8 Carbonation results in Franke et al. work [65]. 36

Fig. 3.1 Example of potentiodynamic curve. 40
Fig. 3.2 ASTM cell configuration. 41
Fig. 3.3 Picture of the ASTM cell configuration. 41
Fig. 3.4 Carbon steel specimen and stainless steel holder 42
Fig. 3.5 Schematic view of the specimen assembly. 44
Fig. 3.6 Specimen assembly picture. 44
Fig. 3.7 Cell cover. 48
Fig. 3.8 Schematic view of the cell assembly. 49
Fig. 3.9 Picture of the potentiostatic cell assembly. 49
Fig. 3.10 Specimen assembly. 51
Fig. 3.11 Picture of the specimen assembly. 51
Fig. 3.12 Plain concrete prism. 54
Fig. 3.13 Reinforced concrete specimen. 55

Fig. 3.14 Reinforced concrete specimen section. 55
Fig. 3.15 Example of phenolphthalein test on concrete section 56

Fig. 4.1 Examples of the potentiodynamic curves reproducibility. 61
Fig. 4.2 Potentiodynamic curves of reference solutions. 62
Fig. 4.3 Visual inspection of pitting initiation. 63
Fig. 4.4 Potentiodynamic curves of solutions with 0.1 mol/L nitrite concentration. 64
Fig. 4.5 Potentiodynamic curves of solutions with 0.3 mol/L nitrite concentration. 66
Fig. 4.6 Potentiodynamic curves of solutions with 0.1 mol/L nitrate concentration. 67
Fig. 4.7 Potentiodynamic curves of solutions with 0.3 mol/L nitrate concentration. 68
Fig. 4.8 Current density drop of potentiostatic reference test. 71
Fig. 4.9 Current density drop of potentiostatic nitrite test. 73
Fig. 4.10 Current density drop of potentiostatic nitrate test. 75
Fig. 4.11 Example of carbonation depth measurement. 79
Fig. 4.12 Free corrosion potentials of the reinforced concrete samples 82
Fig. 4.13 Polarization resistances of the reinforced concrete samples. 84

Fig. 5.1 Free corrosion potentials trend as function of time before potentiodynamic tests. 86
Fig. 5.2 Current densities in the potentiostatic tests. 87
Fig. 5.3 Potentiodynamic curves of nitrate chlorides-free solutions with different immersion times. 88
Fig. 5.4 Oxygen evolution potentials of potentiodynamic tests. 88
Fig. 5.5 Pitting potentials as function of the chlorides concentration in potentiodynamic tests. 90
Fig. 5.6 Repassivation potentials as a function of the chlorides concentration. 92
Fig. 5.7 Anodic passive current densities of potentiodynamic tests. 93
Fig. 5.8 Percentage of the corroded sample as a function of the chlorides concentration. 94
Fig. 5.9 Corroded samples percentage with the hypothetic nitrite 0.05 mol/L concentration solution. 95
Fig. 5.10 Critical chloride threshold for the four potentiostatic tests. 96
Fig. 5.11 Carbonation depths as a function of $(\text{time})^{1/2}$ in accelerated carbonation monitoring. 98
Fig. 5.12 Coefficient K for the carbonation depth in accelerated tests (Serie I: CEM I 52.5R; Serie II: CEM II/B-S 52.5; Serie III: CEM II/B-M 42.5). 99
Fig. 5.13 Carbonation depths measures of concrete samples exposed to atmosphere. 100
Fig. 5.14 K coefficients of the real carbonation depth measurements (Serie I: CEM I 52.5R; Serie II: CEM II/B-S 52.5; Serie III: CEM II/B-M 42.5). 101
Fig. 5.15 K coefficients scatter plot of real and accelerated carbonation depth monitoring. 102
Fig. 5.16 Free corrosion potentials of the rebars embedded in concrete samples. 103
Fig. 5.17 Corrosion penetration rates of the rebars in carbonated concrete samples. 105

Fig. A.1 Potentiodynamic characteristic curves of reference solutions. 116
Fig. A.2 Potentiodynamic curves of calcium nitrite inhibited solutions in 0.1 mol/L and 0.3 mol/L concentrations. 119
Fig. A.3 Potentiodynamic characteristic curves of calcium nitrate inhibited solutions in 0.1 mol/L and 0.3 mol/L concentrations. 121

List of tables

Tab. 3.1 Synthetic pore solutions composition. 42
Tab. 3.2 Solutions composition of series 1 day of immersion. 45
Tab. 3.3 Solutions composition of series 3 days of immersion. 45
Tab. 3.4 Solution compositions of series 7 days of immersion. 46
Tab. 3.5 Potentiostatic tests solutions composition. 50
Tab. 3.6 Concrete specimens code. 53
Tab. 3.7 Concrete compositions. 53

Tab. 4.1 Pitting and repassivation potentials of reference potentiodynamic tests. 62
Tab. 4.2 Pitting and repassivation potentials of potentiodynamic tests with 0.1 mol/L nitrite. 65
Tab. 4.3 Pitting and repassivation potentials of potentiodynamic tests with 0.3 mol/L nitrite. 66
Tab. 4.4 Pitting and repassivation potentials of potentiodynamic tests with 0.1 mol/L nitrate. 68
Tab. 4.5 Pitting and repassivation potentials of potentiodynamic tests with 0.3 mol/L nitrate. 69
Tab. 4.6 Chlorides additions in potentiostatic reference solution. 71
Tab. 4.7 Initiation times of the potentiostatic reference solution. 72
Tab. 4.8 Chlorides additions in potentiostatic nitrite solution. 73
Tab. 4.9 Initiation times of the potentiostatic nitrite solution. 74
Tab. 4.10 Inhibitor and chlorides additions in potentiostatic nitrate solution. 75
Tab. 4.11 Initiation times of the potentiostatic nitrate solution. 76
Tab. 4.12 Inhibitors and chlorides additions in potentiostatic mixed nitrite-nitrate solution. 77
Tab. 4.13 Initiation times of the potentiostatic mixed nitrite-nitrate solution. 77
Tab. 4.14 Carbonation depths (mm) measurements for accelerated tests. 79
Tab. 4.15 Carbonation depths (mm) measurements for real monitoring tests. 80

Introduction

Reinforced concrete is a versatile, economical and successful construction material: *"the combination of high compression strength of concrete and high tensile properties of reinforcing steel gives an ideal composite material which offers, compared to other materials, a wide range of applications in structural engineering"* [1].

Worldwide, more concrete is used than any other man made material: every year, the global consumption of cement is on the rise; it was estimated a global market consumption of about 50 billion tons of cement in 2017 [2]. The big demand of reinforced concrete in construction engineering stays on its ability to be durable and strong, with high performances throughout its service life. However, in some cases it does not act adequately due to poor design, poor construction or inadequate material selection to withstand the environmental conditions to which it is subjected [3]. An affected or limited state of serviceability is thus consequent. The corrosion of the steel reinforcements is globally the major problem of premature infrastructure collapses and its study gained considerable importance at the end of 1980s [4]. The economic loss and damage caused by the corrosion of steel in concrete makes it presumably the largest single infrastructure problem facing industrialized countries. Billions of dollars are spent every year in protecting and replacing corrosion damages [3].

The highly alkaline pore solution (pH around 13), formed during cement hydration, allowed to protect the steel reinforcements embedded inside concrete, promoting their passivation. Nevertheless, the passivity condition can decay (i.e. depassivation effect) with consequent breakdown of the protecting oxide layer on the rebars surface. The two main reasons are attributed to the presence of chlorides at the carbon steel surface, in a content higher than a critical threshold, and to the concrete pore solution pH reduction, generated by the reaction with atmospheric carbon dioxide (CO_2). Once corrosion has initiated, the reduction of reinforcements cross section and the concrete cover cracking and spalling arise, leading to structural complications. Measures to prevent the reinforcements damage or to keep it within tolerable limits are necessary during the design lifetime of the structure. For instance, using high quality concrete, adopting long curing times and adequate cover dimensions, or introducing new additional prevention methods that have been developed and successfully exploited in the recent years (i.e. blended cements, corrosion inhibitors, external coatings, corrosion resistant rebars, cathodic protection) [1].

Among these methods, inhibitors have been widely applied for preventing corrosion in many and varied technical fields for years, due to their low costs and easy handling [5]. Indeed, they can delay the corrosion initiation time and reduce its propagation rate. Corrosion inhibitors can be added to the concrete mixture as liquid additives to prevent corrosion, or they can be applied, as repair technique, on the hardened concrete surface, enabling them to migrate toward the steel reinforcements.

The effectiveness of corrosion inhibitors for reinforced concrete structures affected by chloride and carbonation-induced corrosion has been studied at PoliLapp, Laboratory of Corrosion of materials “P. Pedeferri”, Politecnico di Milano, in the last 15 years. Besides the well-established effective nitrite-based inhibitor, new organic and inorganic substances have been investigated as alternative to overcome the safety and environmental issues related to nitrites. More recently, nitrate ions was suggested as possible alternative, by virtue of its harmless and compatibility with the concrete matrix, enough to be commonly used as set accelerator [6].

In this work, the fundamental aspects of concrete degradation and reinforcements corrosion are described, focusing on the preventative and repair techniques commonly adopted; significant emphasis was given to inorganic corrosion inhibitors and in particular, to nitrite and nitrate-based compounds. A detailed state of the art regarding these two inhibitors was drafted.

Since considerable divergent opinions about reliable inhibition effectiveness on concrete corrosion of nitrate ions were encountered in literature, the purpose of the present work was to demonstrate an eventual inhibition effect of calcium nitrate as concrete admixture inhibitor. The experimental section of the thesis concerns the investigation of nitrate effect on chloride-induced corrosion and carbonation attack, that are the two main reasons of concrete degradation nowadays. The adopted experimental methods were selected according to previous researches present in literature; in this way, it has been possible to make a comparison with the obtained results. Nitrate-based inhibitor effectiveness for chloride-induced corrosion was determined using simulating concrete pore solutions and correlating the corresponding results in presence of nitrite-based inhibitor or without any admixture; in addition, reinforced and plain concrete samples were adopted to investigate the inhibition effectiveness in carbonation-induced corrosion.

Chapter 1.
Corrosion in concrete

Concrete is a composite material characterized by aggregates and porous cement paste, the reaction product of cement with additional mixing water. It is normally reinforced with embedded carbon steel rebars: the reinforcements introduction into the cement paste allows to protect the steel from atmospheric aggressive species, preventing various type of degradation.

1.1 Concrete general aspects

The constitutive element of cement is a mixture of limestone and clay raw materials: calcium silicates and aluminates are the main components. In presence of water, the mineral powder forms colloidal hydrated products with very low solubility. Cement paste solidification is mainly induced by the hydration of aluminates that react firstly; silicates hydration gives rise to calcium silicate hydrates formation, a rigid gel, known as C-S-H gel. It is characterized by very small particles with a layered structure of thin spacing, lower than 2 nm, and a big surface area (100-700 m^2/g): due to this conformation, C-S-H gel can give considerable strength to the cement paste [1]. During hydration, an aqueous solution of calcium, sodium and potassium hydroxides ($Ca(OH)_2$, NaOH, KOH) is formed and accumulates inside the pores. The chemical composition of the pore solution depends on concrete constituents; however, because of the high alkalinity of the dissolved species, the solution pH ranges from 12 to 14 [3].

In aerated, chloride-free, alkaline solutions, with pH > 11.5, carbon steel passivates because a protective oxide film forms [7]. This is what happened in rebars inside concrete: the alkalinity of the pore solution is sufficient to guarantee a stable passivity condition and a metal corrosion rate practically nil. The passive layer is only few nanometres thick and it is probably part metal oxide-hydroxide and part mineral coming from cement; it is a dense and impenetrable film that can prevent corrosion instauration [8]. However, the passivating environment is not always maintained: concrete carbonation and chloride attack are the two conditions that compromise the protective layer integrity.

An additional protective effect of cement on rebars consists of a physical barrier, called concrete cover, that protects the metal slowing down the aggressive species penetration. The diffusion of oxygen, water or aggressive ions (like chlorides) from atmosphere to the carbon steel surface can leads to metal corrosion instauration, so to concrete degradation. The transport processes of fluids and ions inside concrete are the crucial factor for its durability; the diffusion of these substances is related to the concrete properties (porosity and presence of cracks), on their binding with the cement paste, as well as on the environmental conditions at the surface of concrete [1]. Interconnected pores of different sizes are always created during cement paste hydration: durability of concrete is strictly connected to the dimension and distribution of these voids.

Pores are classified into macropores, capillary pores and gel pores (Fig. 1.1). The latter constitute the interlayer spaces of C-S-H gel and they do not affect cement permeability because they range from few nm to several nm in dimension.

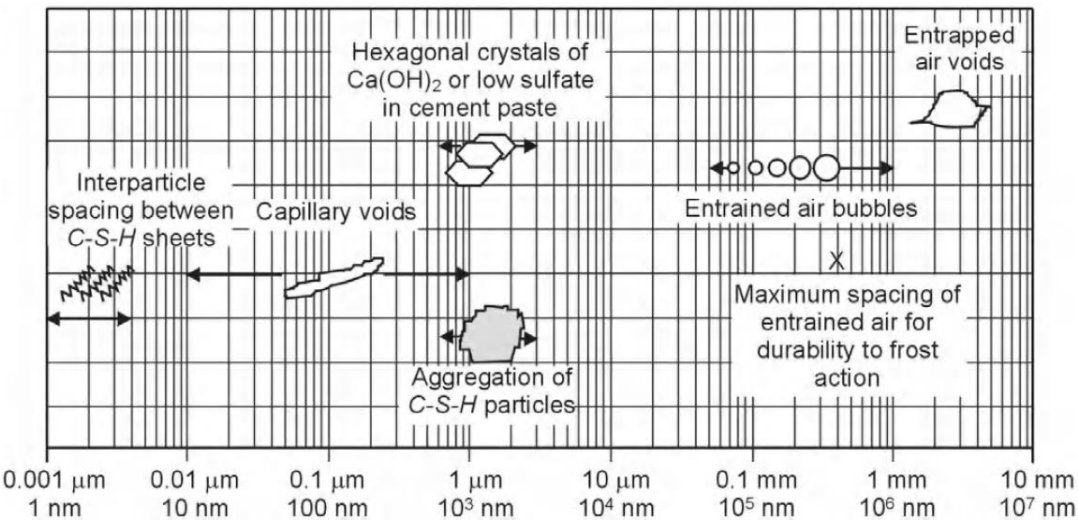

Fig. 1.1 *Dimensional range of solids and pores in hydrated cement paste* [9].

Bigger voids are characterized by capillary pores, not filled space by solid hydrate products. They can have different sizes according to the water/cement ratio (*w/c*) adopted: low ratios are preferred because they assure voids of tens of nm, not critical dimension for aggressive species penetration. On the contrary, macropores are relevant for concrete durability and rebars protection because they can reach few mm of dimension; they are typically induced by entrapped air during mixing and not removed by compaction of fresh concrete [9]. Pores size and distribution is important as well as the amount of aqueous solution contained in it; the diffusion of aggressive species into concrete depends on the transport properties of water.

For concrete exposed to atmosphere, the water content inside pores is related to the relative humidity of the environment, in absence of wetting and under equilibrium conditions. Inside capillary voids, water is firstly adsorbed on their surface and then, with the relative humidity increase, it fills up the pores, starting with the smallest and then moving to the larger ones, as illustrated in Figure 1.2. Diffusion of aggressive species in gaseous phase is related to the water content inside pores. In presence of complete water-filled pores, interconnected with each other, gas diffusion is hindered; contrary, it is facilitated by voids with water only adsorbed on surface.

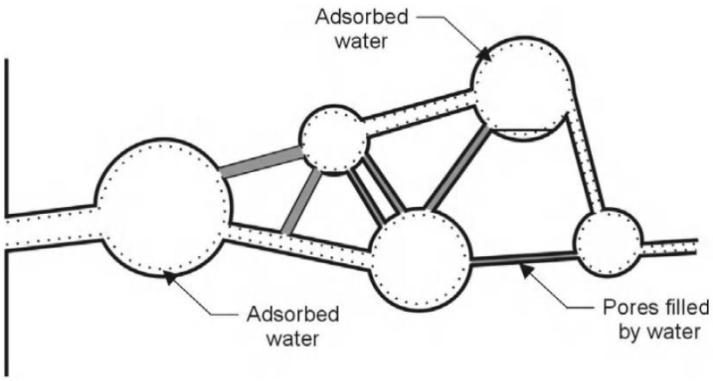

Fig. 1.2 *Representation of water present in capillary pores* [1].

For what concerns ions diffusion kinetic, it is promoted by the presence of water free from surface capillary tensions: its transport properties are similar to those of a bulk solution [1].

The main effective measures to take for the improvement of concrete durability are based on a good concrete cover dimensioning and suitable mix design selection: it includes the proper choice of water/cement ratio, cement type, dimension and size distribution of aggregates. Additional protective measures can be applied in the admixture to decrease concrete permeability, such as fluidizers, plasticizers and inhibitors [10].

1.2 Mechanism of corrosion

In aggressive environments, concrete structures have a life expectancy which is strongly limited by the corrosion of their steel reinforcement. The spontaneous protection of metallic rebars due to the alkalinity of concrete matrix can decay, over time, because of two main causes [11]:

- **Chloride contamination -** It occurs when concrete is in contact with chloride containing environments. The ions can diffuse inside the matrix and reach the reinforcements; if their

concentration at the surface of carbon steel exceeds a critical threshold, the protective layer may be locally destroyed, inducing local corrosion.

- **Carbonation process -** It is induced by concrete reaction with the carbon dioxide (CO_2) contained in the atmosphere. The process causes the change of pore solution pH from pH > 13 to pH < 9: in this condition, carbon steel loses its passivity [1]. The reaction starts from the concrete surface and then proceeds through the concrete cover until reaching the reinforcements, inducing the passive layer breakdown. Corrosion starts in presence of water and oxygen and affects the whole steel surface.

The service life of a concrete reinforced structure can be divided in two distinct phases (Fig. 1.3): corrosion initiation, which is the time required for carbonation or chlorides penetration to reach the carbon steel rebars and produce passivity breakdown; corrosion propagation is the subsequent phase starting from corrosion attack onset [12].

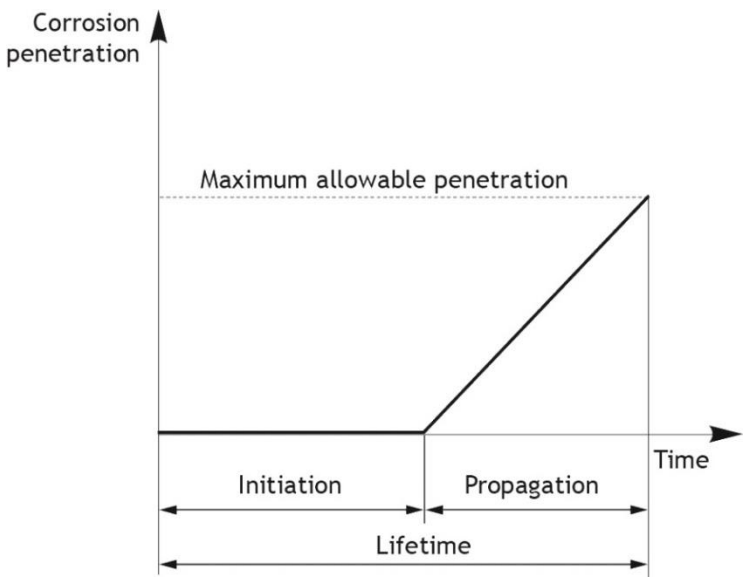

Fig. 1.3 *Tuutti's model of steel reinforcement corrosion in concrete* [12].

The kinetic of the two phases is variable and dependent on many factors: during initiation stage, the velocity of processes is governed by aggressive species ability of diffusion inside concrete. The rate of ingress of carbon dioxide and chloride contaminants depends on the quality of concrete cover and on the environmental condition at its surface [1]. Once the passive layer is destroyed, corrosion phenomena occur if water and oxygen are present at the rebars surface; propagation rate can vary considerably depending on temperature and humidity.

Rebars corrosion rate is measured generally in μm/y and it can be considered negligible if it is below 2 μm/y: in this condition, no structural consequences are expected for common structures with standard lifetimes [13]. When the corrosion rate exceeds this limit, corrosion products accumulate at concrete-reinforcement interface; they are mix of iron oxides that occupy a much greater volume (even 6 times bigger) than that of iron they are derived from. Consequently, the corrosion products can produce tensile stresses inside concrete cover, causing its cracking, spalling or complete delamination, as shown in Figure 1.4.

Fig. 1.4 *Example of concrete delamination due to carbonation induced corrosion* [82].

1.2.1 Corrosion process

Once the passive layer of rebars breaks down, because of both chloride contamination and carbonation, corrosive process develops if water and oxygen are present at the metal surface. When steel in concrete corrodes, it oxidises the iron atoms producing a couple of electrons; this is the so called anodic reaction:

$$Fe \rightarrow Fe^{2+} + 2e^{-} \tag{1}$$

The produced electrons are consumed at the surface of carbon steel by water and oxygen, giving rise to the cathodic reaction:

$$2e^{-} + H_2O + \frac{1}{2}O_2 \rightarrow 2OH^{-} \tag{2}$$

The anodic and cathodic reactions are only the first steps for the creation of rust: the iron ions produced in (1) are soluble in the pore solution and, in presence of hydroxide ions, they create the iron hydroxides ($Fe(OH)_2$, $Fe(OH)_3$, $Fe_2O_3 \cdot H_2O$) that represent corrosion product, i.e. rust [3]. This mixture of products is the cause of concrete cracking and spalling because of a significant volume increase at concrete-reinforcements interface.

The complete electrochemical process is illustrated in Figure 1.5: the electrons migration occurs from anodic to cathodic side passing through the metal; the ions diffusion is possible inside the concrete matrix because of water presence.

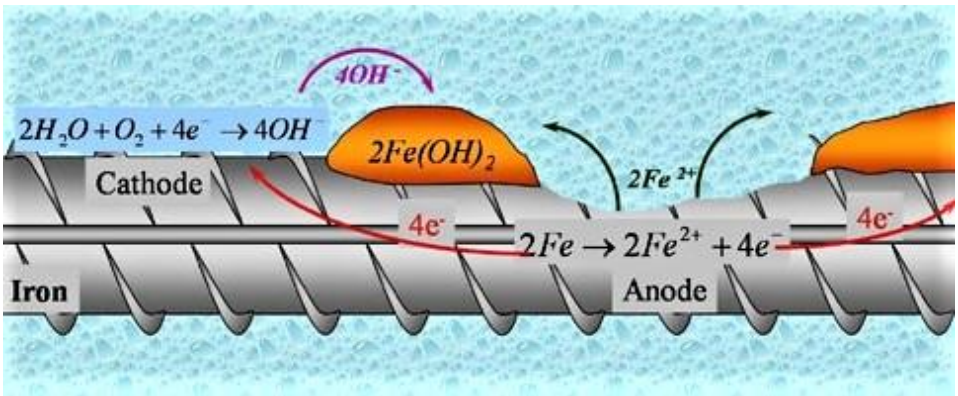

Fig. 1.5 *Electrochemical process of rebars corrosion in concrete* [83].

If any of the chemical reactions or transport mechanisms do not take place, the corrosive phenomenon is completely blocked. Corrosion rate is thus determined by the slowest process among the four partial ones.

1.2.2 Polarization curves

The rate at which the anodic and cathodic process takes place depends on the potential (*E*). The corrosion behaviour of the reinforcement can be described by means of polarization curves that relate the potential and the anodic or cathodic current density.

In non-carbonated concrete without chlorides, carbon steel is passive and its behaviour is represented in Figure 1.6, a typical anodic polarization curve. The potentials are measured with respect to a saturated calomel reference electrode (SCE) (potential +244 mV with respect the standard hydrogen electrode).

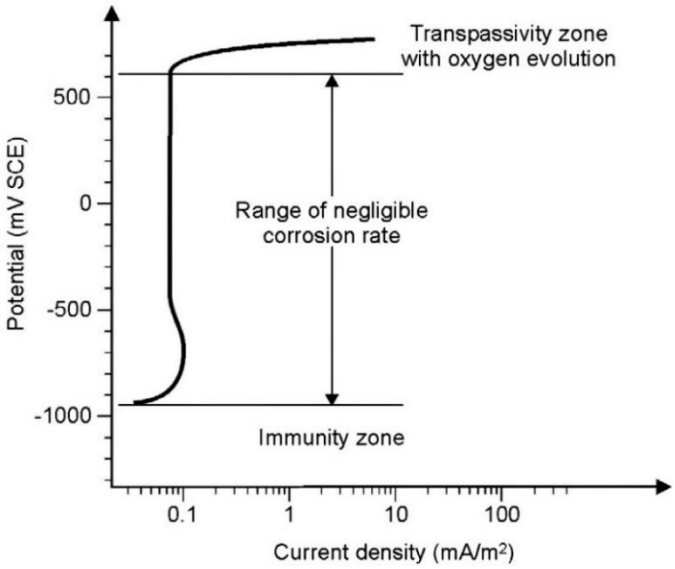

Fig. 1.6 *Anodic polarization curve of steel in non-carbonated concrete without chlorides* [1].

Iron inside concrete is in condition of immunity for potentials below –1 V SCE: metal dissolution is thermodynamically improbable. In the range of –800 mV and +600 mV potentials, the steel creates a passive film that protects it completely: in this condition, the corrosion rate is negligible. Above the passivity range, the metal is in transpassivity condition: oxygen may be produced on its surface according to the anodic reaction of oxygen evolution:

$$2H_2O \rightarrow O_2 + 4H^+ + 4e^- \tag{3}$$

The kinetics of oxygen reduction is described by the cathodic polarization curves *a* and *b* shown in Figure 1.7.

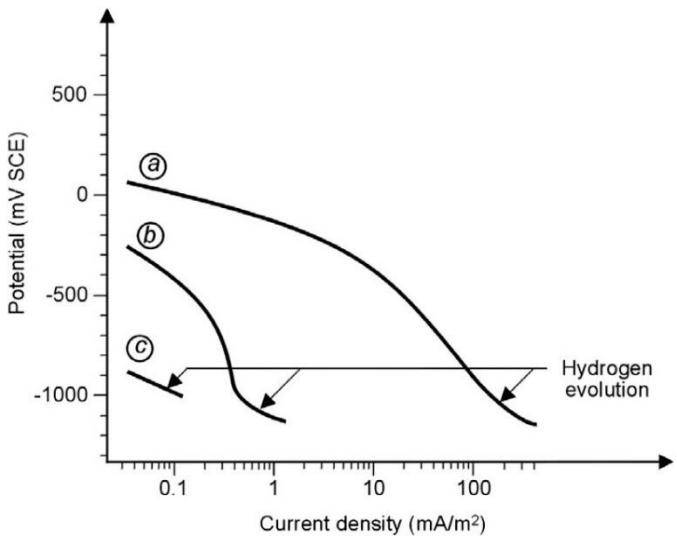

Fig. 1.7 *Cathodic polarization curves in alkaline concrete: (a) aerated; (b) wet, (c) completely saturated with water* [1].

Even if the equilibrium potential of the oxygen reduction inside concrete (pH about 13) is approximately at +200 mV SCE, the reaction has significant rates only at potentials below 0 mV SCE. This occurs because the rate of the cathodic process depends on the oxygen availability at the surface of carbon steel; cathodic polarization curves are thus depending on the ability of the gaseous specie to diffuse inside concrete. As the atmospheric relative humidity increases, the oxygen diffusivity to rebars is limited by the progressive saturation of concrete: cathodic polarization curves shift at lower potentials. If concrete is completely saturated with water (RH 100%), the only cathodic process possible is hydrogen evolution because of the oxygen complete absence (curve *c*) [1].

From cathodic and anodic polarization curves, it is possible to determine the condition of rebars corrosion in various situations: corrosion rate (i_{corr}) and corrosion potential (E_{corr}) are identified by the intersection of anodic and cathodic curves. Figure 1.8 shows the corrosion condition of a carbon steel reinforcement embedded in non-carbonated concrete in the three different atmospheric conditions.

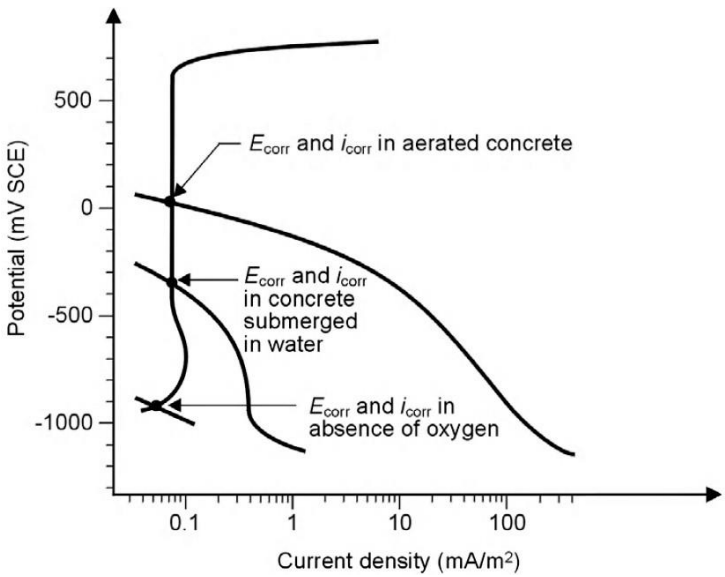

Fig. 1.8 *Corrosion condition of passive steel in concrete, under different environmental conditions* [1].

Generally, with concrete exposed to atmosphere, the rebars condition has a corrosion potential around 0 mV SCE; this potential value drops to lover value, below –400 mV SCE, for concrete immersed in water because of the decreasing of oxygen supply to the steel surface. When oxygen is totally lacking, the potential may even decrease to values below –900 mV SCE and the cathodic process will lead to hydrogen evolution. Under these conditions, the steel is subjected to a corrosion rate that is practically nil [1].

1.3 Chloride-induced corrosion

Chloride-induced corrosion is the most severe reason of reinforcements deterioration and consequent concrete degradation according to the statistical analysis in [14]. Modern design codes for reinforced concrete structures impose restrictions on the amount of chloride that may be introduced from raw materials inside the concrete matrix: in some structures built in the past, chlorides have been added in the concrete mix because of their good settled accelerant properties, causing premature extensive corrosion damages [15]. Today, the maximum allowed chloride content is ruled by the European standard “EN 206”, that imposes the limit at 0.2-0.4% of chloride ions by mass of binder for reinforced concrete [16].

The other main source of chloride in concrete is penetration from the environment; this occurs mainly in marine environments (Fig. 1.9) and in bridge slabs when de-icing salts are spread.

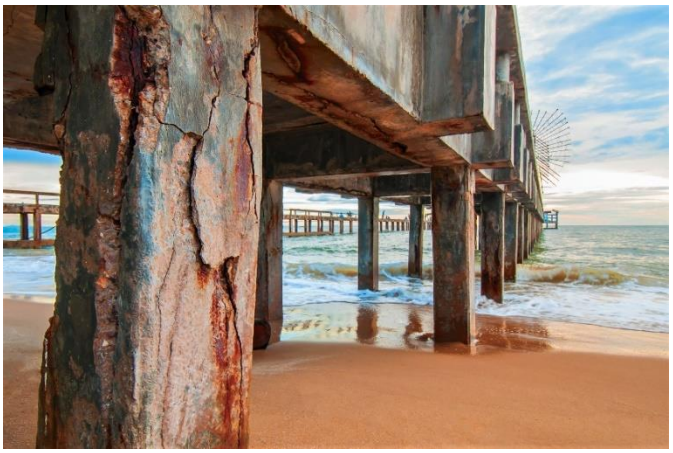

Fig. 1.9 *Chloride-induced corrosion in marine environment* [84].

Corrosion of carbon steel reinforcements can only take place once the chloride content in the surrounding concrete has reached a threshold value (Par. 1.3.1); the diffusion of chloride ions from the external environment through the concrete matrix is characterizing the initiation phase. Subsequently, propagation of the corrosive phenomenon occurs once chlorides lead to the local breakdown of the protective oxide film of the reinforcement in alkaline concrete: a consequent localized corrosion attack, called pitting, establishes [1].

1.3.1 Critical chloride threshold

Initiation of pitting corrosion takes place when chloride content at the surface of reinforcement reaches a threshold value, the critical chloride content. A certain time is required for the breakdown of the passive film: from a practical point of view, the initiation time can be considered as the time when the carbon steel rebar is characterized by an average sustained corrosion rate higher than 2 mA/m^2, i.e. when corrosion rate is no more negligible. The chloride threshold can be defined as the chloride amount required to reach this corrosion condition [17]. For this reason, the assessment of the critical chloride content is a key element in predicting the service life of structures exposed to chloride containing environments; in fact, one possible definition of concrete service life is the time required for transport processes to reach this threshold level [18].

Chloride threshold value is usually represented by the ratio of chloride, defined as the percentage of the total chloride content relative to the weight of cement, to the concentration of hydroxyl ions in the pore solution. The probability of significant corrosion increases as the $[Cl^-]/[OH^-]$ ratio in the pore solution raises above a certain value [19]. Because the critical chloride value can only be defined on a statistical basis, $[Cl^-]/[OH^-]$ reported values cover an extremely wide range. The reason for this variety of different results stays on the dependence of chloride penetration into concrete on several parameters: they are related both on the concrete (e.g. type of cement, *w/c* ratio, moisture content, etc.) and on the environment (e.g. chloride content, temperature, etc.) [1]. But the main factors that have a remarkable influence on the chloride threshold are identified on the concrete pH, related to the hydroxyl ions concentration, on the potential of the steel and on the presence of voids at the rebar/concrete interface.

Over the years, several studies about the assessment on the chloride threshold value for concrete structured were performed: the obtained results range from 0.2% of chloride content by weight of cement until a maximum value of 1.5% by weight of cement. Nevertheless, the European standard limits the chloride content to less than 0.4% for reinforced concretes, properly because this uncertainty [18].

1.3.2 Chloride penetration

The penetration of chloride ions from the environment produces a concentration profile in the concrete matrix characterized by a high chloride content in proximity to the external surface and decreasing contents at deeper levels. This profile can be approximated, in general, with the Fick's second law [20]:

$$\frac{\partial C}{\partial t} = D \frac{\partial^2 C}{\partial x^2} \tag{4}$$

where C is the concentration of the diffusing specie (% of chlorides by mass of cement or concrete), x the distance (m) from the concrete surface and D the diffusion coefficient (m^2/s) inside concrete. This relation theoretically describes the kinetics of a non-stationary diffusion process; however, this condition is rarely met in real structures: only into concrete complete saturated with water, chloride ions can penetrate by pure diffusion [1]. Analytically solving the (4) equation, it is possible to evaluate the concentration C of the diffusive specie at any depth x, under the assumption of constant superficial concentration C_s and constant diffusion coefficient D. The analytical equation (5) is thus obtained:

$$C_x = C_S \left(1 - erf \frac{x}{2\sqrt{D_{app} \cdot t}}\right) \tag{5}$$

where: C_x is the total chloride content (% by mass of cement or concrete) at time t (s) and depth x (m) from the concrete surface; D_{app} is the apparent diffusion coefficient for chloride (m^2/s) and C_s corresponds to the surface chloride content (% by mass of cement or concrete).

The use of the apparent diffusion coefficient (D_{app}) is required to better describe the penetration of chloride ions inside concrete: since it depends on the concrete permeability and cement type, it considers also the penetration of specie due to capillary adsorption. If D_{app} and C_s are known and can be assumed as constant in time, it is possible to evaluate the evolution of the chloride profile in concrete and estimate the time t at which a precise chloride threshold will be reached and corrosion will initiate.

1.3.3 Pitting corrosion

Chloride-induced corrosion initiation is characterized by a local breakdown of the protective oxide film on the reinforcement in alkaline concrete; subsequent localized corrosion attack takes place and the morphology of the phenomenon is that typical of pitting shown in Figure 1.10.

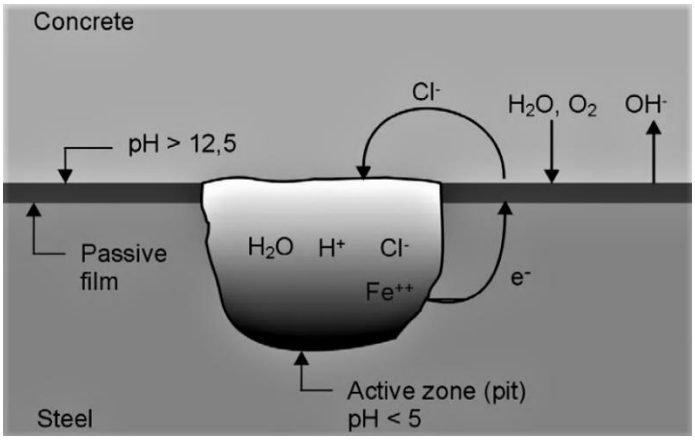

Fig. 1.10 *Schematic representation of pitting corrosion of steel in concrete* [1].

The zones where the film fails behave as anodes (active zones), while the adjacent ones remain passive and become cathodic (passive zone), hosting the oxygen reduction reaction. Current circulation is established from the anodic side to the cathodic one: this flow both increases the chloride content (chloride, being negatively charged ions, migrate to the anodic region) and lowers the alkalinity (acidity is produced by the hydrolysis of corrosion products inside the pits) [1]. In this way, the aggressiveness of the anodic zones is enhanced and the cathodic side is strengthened. Therefore, corrosion propagation can be considered autocatalytic, reaching very high penetration rates, up to 1 mm/y.

During chloride-induced corrosion attack the anodic polarization curve of rebars modifies: as the chloride content at the steel surface increases, the passivity range shortens because the upper limit, which is called “pitting potential” (E_{pit}), passes from about +600 mV SCE to –300 mV SCE (Fig. 1.11) [21]. It is possible to note that the reduction of the anodic pitting potential does not constitute a problem, since the intersection with the cathodic curve coincides to current density values no more negligible. As the chloride content increases, the rebars corrosion condition corresponds to higher current densities, thus greater penetration rates. This can lead, in the short term, to unacceptable reinforcements section reductions, compromising the concrete service life.

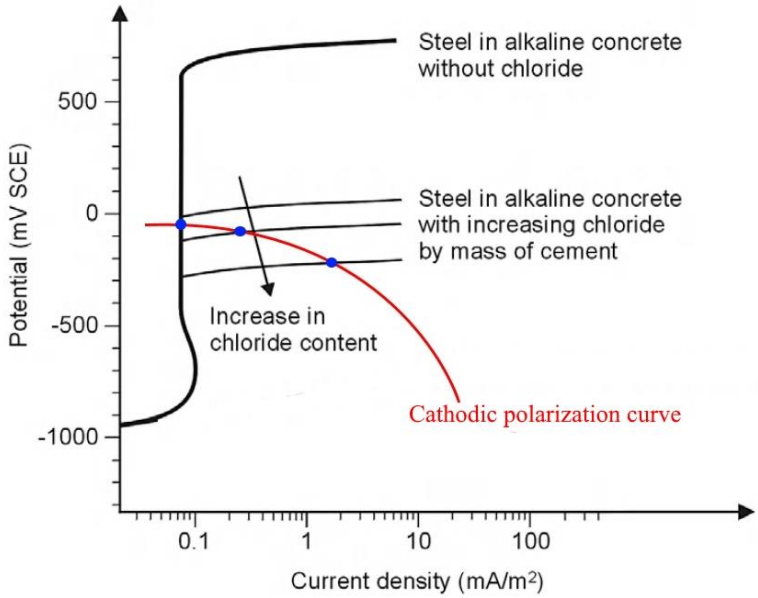

Fig. 1.11 *Anodic and cathodic polarization curves with different chloride contents.*

To stop the propagation of the corrosion attack after initiation, it is necessary to decrease the rebar potential to a value more negative than E_{pit}, called "protection potential" (E_{pro}): the interval of potentials between E_{pit} and E_{pro} is characterized by the fact that it does not allow any attack initiation, but, if the corrosion phenomena has already begun, it permits its propagation. E_{pro} varies, like E_{pit}, with chloride level, pH and temperature [1].

1.4 Carbonation-induced corrosion

Carbonation-induced corrosion is the second cause of concrete degradation according to the "Statistical analysis of factors influencing corrosion in concrete structures" [14]. Contrary to chloride-induced corrosion, the attack is generalized, involving the whole rebars surface.

Carbonation is the result of the interaction of carbon dioxide gas (CO_2) in the atmosphere with the alkaline hydroxides of the pore solution contained in concrete; the reaction can be schematized as follow:

$$CO_2 + Ca(OH)_2 \xrightarrow{H_2O,\,NaOH} CaCO_3 + H_2O \qquad (6)$$

Carbon dioxide content in the atmosphere varies from 0.04% in rural zones to 0.2% in cities; as carbon dioxide proceeds to react with the calcium (and other) hydroxides, it induces the pH of the pore solution to drop from its normal values around 13, to values approaching neutrality [3]. In

this condition, the steel passivity is destroyed and the reinforcements corrodes in humid carbonated concrete as if they were in direct contact with water [22].

1.4.1 Penetration of carbonation

Carbonation reaction starts at the external concrete surface and penetrates inside concrete producing a low pH front. Its penetration rate tends to decrease in time according to the following equation:

$$d = K \cdot t^{\frac{1}{n}} \tag{7}$$

where *d* is the depth of carbonation (mm) and *t* is time (years). often exponent *n* is approximately equal to two and, therefore, a parabolic trend can be considered: $d = K \cdot \sqrt{t}$. The coefficient K (mm/years$^{1/2}$) can be assumes as a measure of the carbonation rate for given concrete and environmental conditions.

The rate of carbonation penetration is thus depending on both environmental factors and properties related to the concrete. In particular, it varies with the concrete humidity: diffusion of carbon dioxide is made possible by the presence of aerated pores, so, not completely filled by water. Consequently, the diffusion rate of CO_2 decreases with an increase in concrete humidity; however, the carbonation reaction (7) occurs only in presence of water, making it negligible with dry concrete [1]. Carbonation rate may be correlated to the environmental humidity as shown in Figure 1.12.

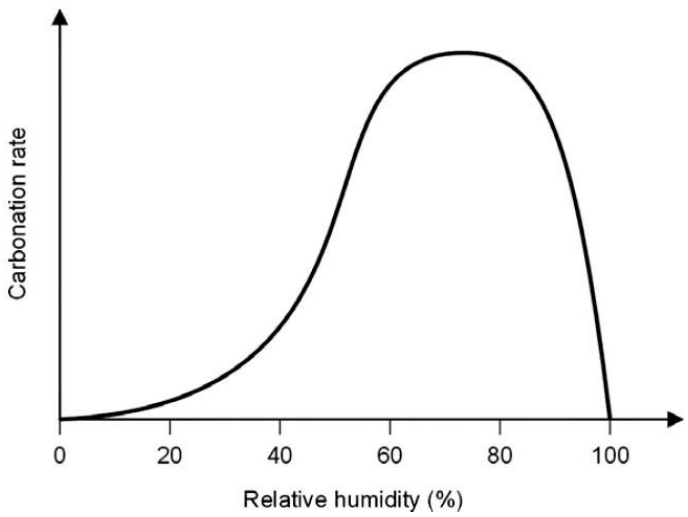

Fig. 1.12 *Rate of concrete carbonation as a function of relative humidity of the environment* [12].

The interval of relative humidity most critical for promoting carbonation is from 60% to 70%. Wet and dry cycles will accelerate carbonation attack by allowing the carbon dioxide penetration during the dry condition (unsaturated pores with water) and supplying water in wet situation [3].

The concrete composition is an additional factor that mainly affects carbonation penetration: the permeability of concrete influences the diffusion of carbon dioxide through the cover. A decrease in capillary porosity of the hydrated cement paste slows down the carbonation penetration; this can be produced by reducing the water/cement ratio during the cast combined with a properly concrete curing [1].

1.4.2 Corrosion in carbonated concrete

The initiation time of carbonation-induced corrosion is the time required for the carbonation front to reach the reinforcements, so to penetrate a depth equal to the thickness of the concrete cover. In presence of oxygen and water the corrosion process can take place on the whole surface of carbon steel in contact with the carbonated concrete, as a generalized attack. The almost neutral environment of carbonated concrete compromises the passivity condition of steel, hindering the formation of the passive film [1]. The change from passive to active behaviour due to pH decrease is shown in Figure 1.13: the anodic polarization curve progressively shifts to lower potential values with an almost linear trend.

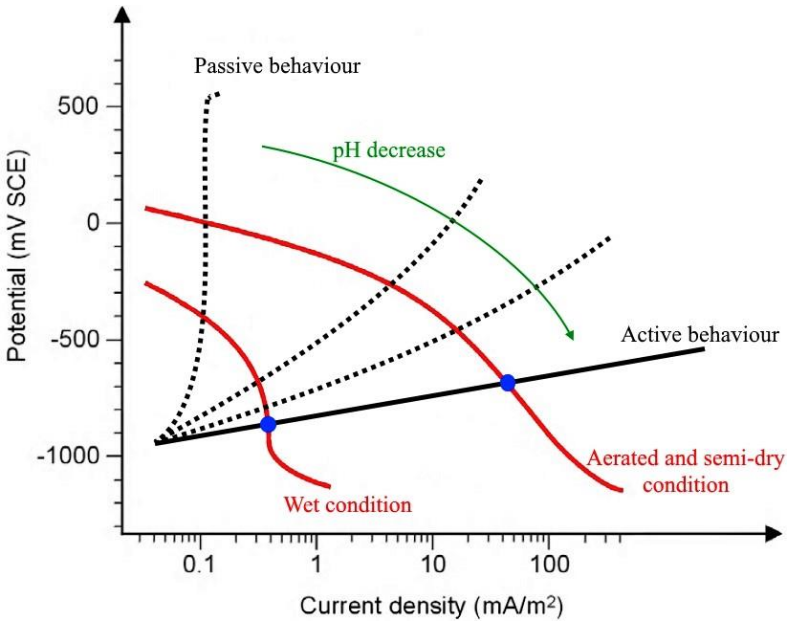

Fig. 1.13 *Corrosion condition of steel in carbonated concrete in equilibrium with environments of different relative humidity.*

The cathodic polarization trend is similar to that observed in alkaline concrete (Fig. 1.7), with different curves according to the environmental conditions.

The condition of corrosion (intersection between anodic and cathodic curves) changes with the progressive loss of passive condition stability: as the carbonation attack arises, decreasing the concrete pH, rebars corrosion current density is increased until no more negligible values. In presence of concrete in aerated or semi-dry environments, the corrosion condition is more aggressive because of the significant oxygen availability. It was demonstrated that the reinforcements corrosion rate in carbonated concrete reached maximum values in aerated environments with relative humidity around 90%; approaching to 100% humidity value, corrosion rates dropped [23].

1.5 Prevention and repair for concrete corrosion

The first requirement to achieve the good durability of concrete structures must begin at the design phase, involving conception, structural details, and material selection. Prevention further emerges during the concrete preparation, placement, compaction and curing; it will continue throughout the entire service life with programmed inspections, monitoring and maintenance. The evaluation of the environmental aggressiveness is a key factor for a good design of concrete structure: the environment is considered as the sum of chemical and physical actions to which the concrete is exposed and that result in effects on the concrete and its reinforcements [1]. For each environmental condition, the European standard “EN 206” provides a guide for composition and properties of concrete to assure 50 year lifetime [16].

1.5.1 Concrete quality

The preventative measures taken firstly during the design phase concern the general “concrete quality”, which includes its composition and the care with which it is executed [24]. Among the concrete quality items, it is possible to emphasize:

- **Water/cement ratio -** It is a key factor in mixture proportion to determine the capillary porosity of the cement paste and thus its resistance to aggressive species penetration.

Therefore, a low ratio is the primary choice to obtain an impervious concrete to either carbonation or chloride penetration.

- **Cement content -** The increase in cement content, on one hand, leads to a higher amount of water, which increases workability of the mixture, but, on other hand, also increases the risk of cracking due to hydration heat or drying shrinkage.

- **Type of cement -** Also the cement type affects the concrete porosity and permeability; for example, at the same conditions, blended and blast furnace cements are most resistant to chloride penetration.

- **Curing -** Curing affects primarily durability and mechanical strength.

- **Cover thickness -** As concrete cover becomes thicker, the barrier to the various aggressive species moving toward the reinforcements increases. The time for corrosion initiation is thus delayed.

1.5.2 Additional protection measures

In the special conditions of strong environmental aggressiveness or impossibility to have an adequate concrete cover thickness, additional protection techniques are required to guarantee the durability of concrete structures. One possible solution is the use of surface treatments, like coatings, applied on new structures, as preventative measure, or to existing constructions, as repair. The main action of surface treatments is to slow down the penetration of aggressive species, increasing the initiation time, especially for chloride-induced corrosion [1].

Acting directly on the corrosion resistance of rebars, it is possible to work on the material selection: the choice of reinforcing bars with a higher corrosion resistance than carbon steel can be advantageous when long service life is required in very aggressive environments. Stainless steels and galvanized steels are two examples.

One of the most effective measure for concrete service life promotion is the use of cathodic protection (CP): it is an electrochemical technique that induces a polarization of the carbon steel rebars, through direct current input, to potential values lower to that typical of corrosion. In this way, the metal corrosion rate is reduced until complete stop. This technique is widely used to

protect and repair structures affected by aggressive chloride-induced corrosion, even when the critical threshold value is already reached. The only drawbacks are the high costs related to the continuous current supply and to the implant installation measures.

To overcome these problems, since the 1990s, cathodic prevention (CPrev) was applied to new structures that would presumably be contaminated by chlorides. It is performed with the same features of CP, but from the beginning throughout the entire service life of the structure. In this way, the corrosion initiation is retarded and, in addition, costs related to the installation and the current supply are reduced [3].

Corrosion inhibitors are used primary to prevent chloride-induced corrosion: they are organic or inorganic substances that in contact with the cement matrix, they can inhibit the corrosion of the rebars. They can be introduced in small quantity to the concrete paste before casting, or to mortars used for restoration, or sprayed on the surface to migrate to the reinforcement.

Chapter 2.
Corrosion inhibitors

Steel reinforced concrete structures are affected by several degradation phenomena, many of them induce the trigger of rebars corrosion. It is necessary to take preventing measures to keep within tolerable limits the damages that can limit the design lifetime of the structure. Besides electrochemical techniques, the use of corrosion inhibitors is nowadays continuing to attract attention [10]. They have been used successfully in steel pipelines and tanks for many decades; however, their use in concrete is very recent and often limited [25]. Corrosion inhibitors may be a good alternative to other protection methods or classical repair techniques due to their lower cost and easy application [25]. In this context, only corrosion inhibitors that prolong the service life due to chemical or electrochemical interaction with the reinforcements are considered.

According to the International standard "ISO8044" corrosion inhibitors can be defined as "chemical substance that when present in the corrosion system at a suitable (preferably small) concentration decreases the corrosion rate, without significantly changing the concentration of any corrosive agent" [26]. The substances used as inhibitors can be both of organic and inorganic nature; they can be classified according to the application method [1]:

- **Admixed corrosion inhibitors (ACI) -** They are added to the fresh concrete as an additive. According to the general service life model of Tuutti (Figure 1.3), these inhibitors can extend the initiation time and/or reduce the corrosion rate during the propagation phase. This type of substances is used as preventative technique.

- **Migrating corrosion inhibitors (MCI) -** They are applied on the surface of hardened concrete during the initiation period; their penetration through the concrete cover is required for the reinforcements protection, promoting the reduction of the corrosion rate. In this case, they are considered as curative repair technique.

2.1 Effect on the service life

Corrosion inhibitors have the ability to increase the service life of a concrete structure working on its initiation time and propagation rate. The service life of a structure can be represented by the Tuutti diagram, that in presence of corrosion inhibitors is modified according to their action, as shown in Figure 2.1.

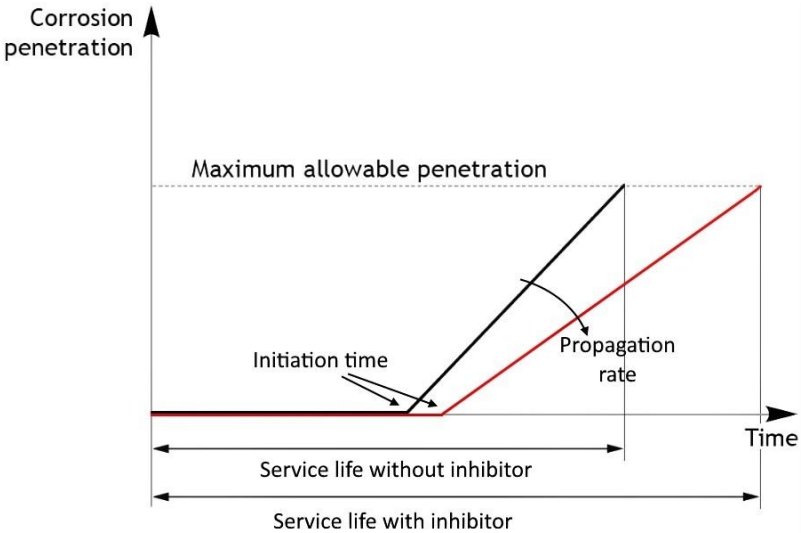

Fig. 2.1 *Influence of the inhibitor on the service life.*

The inhibitor can act firstly on the corrosion initiation time: a barrier effect, induced by its presence inside the concrete matrix, can limit the diffusion of aggressive species toward the reinforcements. The delay on initiation time can also be related to a strengthening mechanism of the rebars passive layer; the chloride threshold value can be thus increased.

Corrosion inhibitor can further influence the corrosion propagation phase, by producing a reduction in the rebars corrosion rate after its initiation. Therefore, the effect of corrosion inhibitors is to ensure a service life of the concrete structure equal or greatest then the one designed. To do this, an effective inhibitor must satisfy the compatibility with the concrete matrix, without affecting the properties of both fresh and hardened concrete, and with the environment: no problems of toxicity and environmental impact must be present [3].

2.2 Inhibition mechanism

The inhibition of steel reinforcements corrosion inside concrete structures is focused on the hindrance of the electrochemical corrosion process (Par. 0): if any of the chemical reaction or transport mechanism do not take place, the corrosion phenomena is completely blocked. The protection mechanism of corrosion inhibitors acts exactly on these processes; according to the reaction that they hinder, they can be classified into [25]:

- **Anodic inhibitors -** They work on the anodic reaction of steel dissolution by maintaining the passivity condition on the rebars surface. They modify the anodic polarization curve increasing the corrosion potential of metal: its corrosion current density is thus decreased, as shown in Figure 2.2.
  The most commonly used anodic inhibitor is nitrite, especially of calcium, but also of sodium [25].

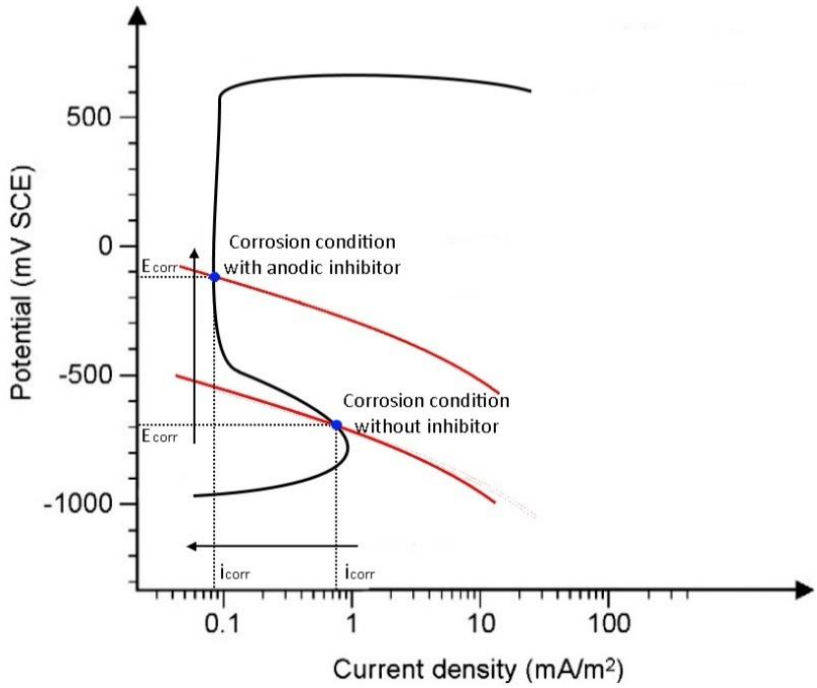

Fig. 2.2 *Effect of the anodic inhibitor.*

- **Cathodic inhibitors -** They act on the cathodic reaction on the steel surface. In alkaline environments, like in concrete, the cathodic reaction is characterized by oxygen reduction: cathodic inhibitors increase the cathodic potential, decreasing the metal corrosion condition (both the potential and the current density values), as shown in Figure 2.3.

The most commonly used are the hydroxide or carbonate of sodium, which are supposed to increase the pH near the steel and reduce the oxygen transport, by accumulating on the metal surface [27].

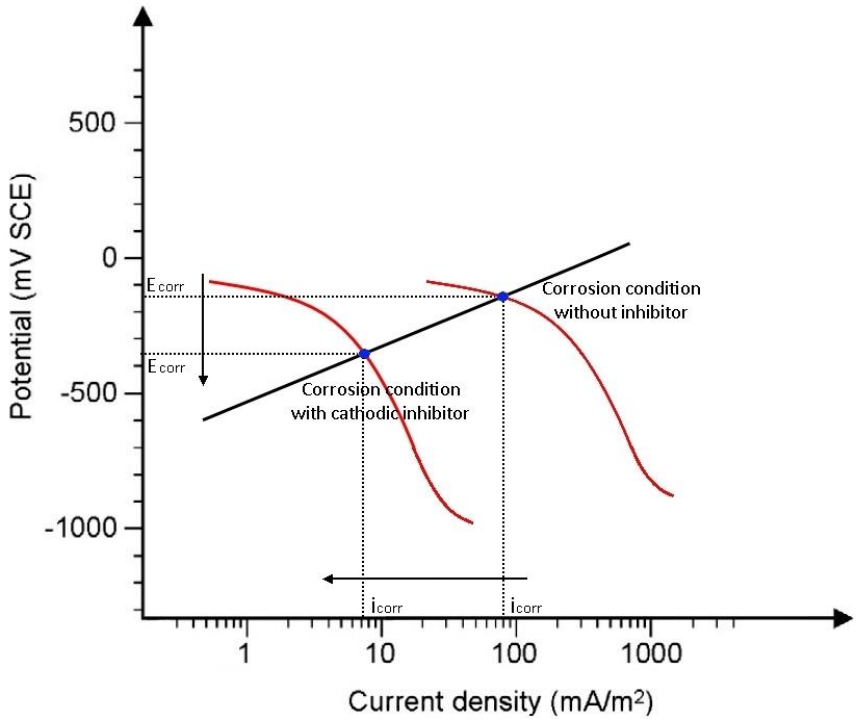

Fig. 2.3 *Effect of the cathodic inhibitor.*

- **Mixed inhibitors -** They work at both the anodic and the cathodic side, reducing the corrosion rate without significantly changing the corrosion potential: by the adsorption of these substances on the steel surface, it is possible to create a film that works as barrier for oxygen reduction and iron dissolution. They are usually organic molecules with polar groups (amine, hydroxyl or carboxylic groups), responsible for the surface adsorption [25]. The main problem with organic materials is that they act as severe set retarded, compromising the curing phase of concrete [3].

2.2.1 Effect on chloride-induced corrosion

The initiation of rebars corrosion process related to chloride contamination is trigger by the overcoming of the threshold chloride concentration able to breakdown the oxide passive film on the steel surface. Localized corrosion (pitting) starts with a very rapid propagation rate, that can be considered autocatalytic. Corrosion inhibitors for chloride-induced attack are thus acting on the

initiation time only: once the steel passive layer is locally destroyed, no inhibition can act on the corrosion propagation.

According to Elsener [10], the anodic potential at which localized corrosion starts, pitting potential, is related to chloride ions concentrations:

$$E_{pit} = C - Blog(a_{Cl^-}) \tag{8}$$

with C and B constants and a_{Cl^-} chlorides activity.

Efficient corrosion inhibitors increase the pitting potential, reaching values higher than the corrosion potential, avoiding pitting initiation. Therefore, they act decreasing the chloride concentration at the steel surface and preventing the pit formation with different mechanisms [10]: for instance, they can adsorb on the steel surface avoiding the chlorides accumulation; in alternative, they can increase or buffer the concrete pH in proximity to the reinforcements, hindering the pit development.

2.2.2 Effect on carbonation-induced corrosion

Carbonation is a concrete deterioration mechanism based on the CO_2 reaction with the concrete components and the subsequent depassivation of the steel rebars due to a pH change. Carbonation is primary a migration process; therefore, an efficient inhibitor acts on the concrete permeability hindering the penetration of this aggressive substance to the reinforcements.

In carbonation-induced corrosion, inhibitors can act on both initiation time and propagation rate: as binding inhibitors or “pore blocking”, some substances modify the concrete permeability delaying the complete concrete cover carbonation. In alternative, after reached carbonation, anodic and cathodic inhibitors can act on the rebars corrosion condition, decreasing the corrosion current density.

2.2.3 Inhibitor effectiveness

The effectiveness of a corrosion inhibitor (ξ_{corr}) is defined as the reduction of the corrosion rate as follows:

$$\xi_{corr} = 100 \cdot \frac{C_{rate} - C_{rate\text{-}inhibit}}{C_{rate}} \tag{9}$$

where C_{rate} is the corrosion rate in the absence of inhibitor and $C_{rate\text{-}inhibit}$ is the corrosion rate in presence of inhibitor.

Inhibitor effectiveness depends on a variety of factors such as the nature and concentration of the chemical substance, the type and surface condition of the metallic reinforcements, the composition of the aggressive environment, and the atmospheric temperature [1]. For each inhibitor compound it is possible to identify the minimum effective concentration above which its inhibiting effect appears. According to the impact on the corrosion rate, an inhibitor can be classified in safe and unsafe: a safe inhibitor is a substance that do not induce any corrosion rate increase if applied in concentration lower than the minimum effective one; on the other hand, unsafe inhibitors can activate corrosion enhancement with inadequate dosages.

2.3 Nitrite-based inhibitors

Inorganic nitrite compounds (NO_2^-, Fig. 2.4) are anodic inhibitors among the most extensively used admixed corrosion inhibitor, their effectiveness in chloride aggressive environments was widely proved [3][10][28].

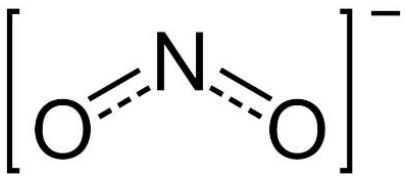

Fig. 2.4 *Nitrite anion* [85].

Nitrite-based compounds were primarily used to increased setting and hardening of concrete, rather than to inhibit corrosion [5].

The first literature reference regarding the investigation on nitrite as concrete inhibitor is dated in the late 1950s in the Soviet Union, where a mixture of nitrite and nitrate (NO_3^-) of sodium and $CaCl_2$ were used as a protection strategy against corrosion caused by de-icing salts [29][5]. Due to loss in compressive strength and risk of alkali-aggregate reactions, calcium nitrite ($Ca(NO_2)_2$) was investigated [28].

Commercial calcium nitrite was introduced only in the middle of the 1970s in Japan and United States and it was used for years [30][31][32]; the firs patent was awarded in 1977 for commercial application of nitrite-based inhibitor [25]. Over the 1980s and 1990s, the technique was enhanced: nitrite-based inhibitors were used as protection strategy in large structures, like viaducts and bridges, worldwide [33][34]. Even though calcium nitrite has proven to be an efficient corrosion inhibitor, it has a big commercial disadvantage: nitrites are toxic and environmentally hostile, therefore, they are highly regulated in Europe [28][35].

2.3.1 Inhibiting mechanism

Being an anodic inhibitor, nitrite-based compound directly interferes with the anodic dissolution reaction of steel during chloride or carbonation-induced attack.

Several hypotheses have been advanced considering a steel passivation effect induced by nitrite presence [5][36]. Nitrite ions, dissolved in the alkaline pore solution, react with the ferrous ions of the reinforcements forming stable iron oxides that preserve the surface passive layer. The redox reactions (10) and (11) show the mechanism:

$$2Fe^{2+} + 2OH^- + 2NO_2^- = 2NO \uparrow + \gamma\text{-}Fe_2O_3 + H_2O \tag{10}$$

$$Fe^{2+} + OH^- + NO_2^- = NO \uparrow + \gamma\text{–}FeOOH \tag{11}$$

Ferrous ions (Fe^{2+}) are oxidized to ferric ions (Fe^{3+}), forming a passivating ferric oxide layer on the steel surface because they are insoluble in the alkaline pore solution and block the transport of ferrous ions into the concrete electrolyte [10]. Nitrite (oxidation state +3) is reduced to nitrogen monoxide (NO, oxidation state +2), a gaseous specie that evaporates at ambient temperature and pressure.

The nitrite inhibitory effect is based on its ability to reduce itself, oxidising the ferrous ions: nitrite is not integrated into the passivity film, but it competes against chloride [37]. The redox reactions are much more rapid than the oxidation of ferrous ions through chloride ions complex formation; nitrite ions induce thus the formation of a stable passive layer even in the presence of chlorides [38]. The influence of the corrosion inhibitor on the oxidising reaction kinetic induces an increase in the pitting potential.

A second hypothesis suggested that the effectiveness of nitrite corrosion inhibitors stays on the creation of a passive oxide layer on the reinforcement surface of different nature. The mechanism is equivalent to the theory illustrated above: nitrite ions reduction to nitrogen monoxide and ferrous ions oxidation to ferric hydroxide ($Fe(OH)_3$) [39][40]. The proposed mechanism may be described by the two half-reactions:

Reduction: $$NO_2^- + H_2O + e^- \rightarrow NO + 2OH^- \quad (12)$$

Oxidation: $$Fe(OH)_2 + OH^- \rightarrow Fe(OH)_3 + e^- \quad (13)$$

They are combined to give the total reaction:

$$Fe(OH)_2 + NO_2^- + H_2O \rightarrow Fe(OH)_3 + NO + OH^- \quad (14)$$

The corrosion inhibiting effect of calcium nitrite is degenerative in nature: the unbound nitrite ions decrease in concentration as they react with ferrous ions to stabilize the passivation of steel reinforcements [28]. Another problem related to this type of inhibitors is their leaching from concrete; however, it only regards poor quality concretes [10].

2.3.2 Effectiveness

The effectiveness of nitrite based inhibitors for chloride-induced corrosion or carbonated concrete strictly depends on the nitrite ions concentration in proximity to the steel reinforcements. The dosage of the inhibitor is ruled by reasons of compatibility with concrete, both fresh and hardened, but also by economic motivations.

As illustrated in Paragraph 2.3.1, if chloride ions are present in the concrete pore solution, nitrites will compete with them forming ferritic ions and the passive layer on the reinforcements surface.

Hence, the inhibitor concentration required for protection is determined by the level of chlorides to which the concrete structure will be exposed, determined by the atmospheric aggressiveness [28]. The effectiveness of nitrite corrosion inhibition in chloride-induced attack can be evaluate considering the molar ratio between the nitrite and chloride ions concentrations, $[NO_2^-]/[Cl^-]$. It was reported in literature that molar ratios higher than 0.5-0.6 are required to prevent corrosion [10][41].

An experimental work confirmed that after 5 years, concrete samples with nitrite concentrations higher than the required one were still in passivity condition [42]. In the plot of the work [32], it was reported the rebars corrosion rates in function of $[NO_2^-]/[Cl^-]$ molar ratio (Fig. 2.5). The results confirmed that a molar ratio higher than 0.8 is required to be far from the corrosion initiation zone.

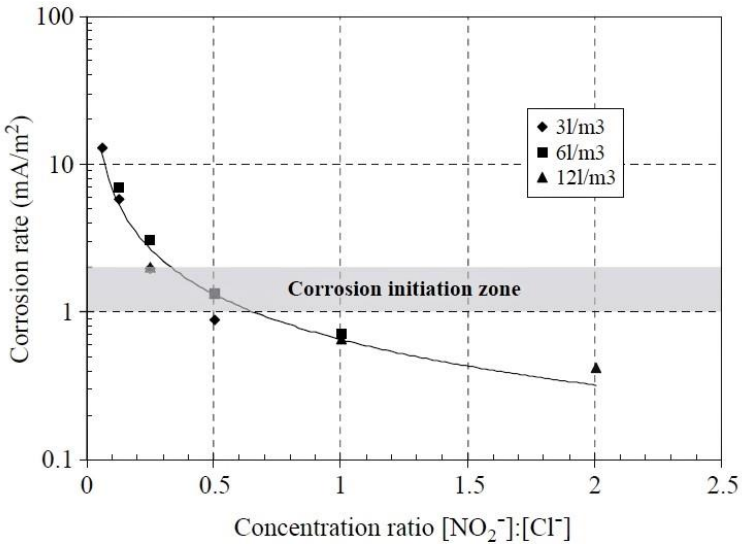

Fig. 2.5 *Corrosion rate trend in function of $[NO_2^-]/[Cl^-]$ ratio* [32].

The inhibition effect of nitrite-based corrosion inhibitor was remarkable also for what concerns the chloride threshold value: the critical threshold was raised by an increase in the dosage of corrosion inhibitor, ranging from 0.22% to 1.95% by weight of cement, considering that inhibitor-free specimens produced values ranging from 0.2% to 0.4% [32].

In carbonated and chloride-free concretes, nitrites act as corrosion inhibitors as well: experimental studies in synthetic pore solutions and carbonated concrete samples demonstrated that 3% of calcium nitrite by weight of cement can protect the steel reinforcements against generalized corrosion [10]. Creating the passive layer by the oxidation of ferrous ions, it can induce the repassivation of the rebars surface, limiting the corrosion rate. In presence of combined carbonated

concrete and chloride rich environment, nitrite corrosion inhibitors were not able to achieve the complete steel repassivation: the reinforcements corroded at a rate similar to when no inhibitors were present in the mix, event with low chloride concentrations (0.3%) [43].

2.3.3 Effect on concrete properties

Admixed corrosion inhibitors are introduced into the concrete mortar during the casting, therefore they may influence the initial set, the strength development and other properties of concrete. Calcium salts of nitrite are one of the most common non-chloride setting accelerator; they took over for calcium chloride, the classical hardening accelerator, since the late 1960s [44][45]. Nitrites may even increase the hardening rate, without affecting the strength development of concrete, with an effect comparable to that obtained with calcium chloride [46].

Sodium nitrite was previously used as accelerator of setting, however a moderate to severe compressive strength loss was encountered and, in addition, sodium compounds enhanced the risk of alkali-aggregate reaction problems [47][48]. Using calcium nitrite, no susceptibility to alkali-aggregate reaction was reported [47].

Regarding the mechanical properties of the hardened concrete, the addition of calcium nitrite as corrosion inhibitor causes an increase in the compressive strength: several recent research indicate an increase of compressive strength for all mixes containing the inhibitor of 12-13% higher than the corresponding mixes without nitrite addition [25].

2.4 Nitrate-based inhibitors

The investigation of a new class of corrosion inhibitors to replace the effective calcium nitrate inhibitor caught on in the late 1980s, when European regulations started to limit its application because of toxic issues and environmental requirements [35]. As alternative to overcome these drawbacks, organic and inorganic inhibitors were studied. The requirement to incorporate into concrete structures a non-toxic and environmental-friendly inhibitor to prevent rebars corrosion phenomena, leaded to the study of nitrate-based compounds.

Nitrate is a polyatomic ion with the molecular formula NO_3^- (Fig. 2.6); it is mainly produced for agricultural use as fertilizers because of its high solubility and biodegradability. The second major application of nitrates is as food preservatives [49].

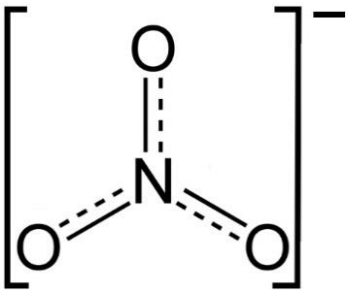

Fig. 2.6 *Nitrate ion* [49].

Compared to nitrite compounds, nitrates are cheaper and less harmful to the environment; in addition, they are commonly used as set accelerator, demonstrating their perfect compatibility with concrete mixes [50][51].

Since calcium nitrite was the most common admixed corrosion inhibitor of inorganic nature, with widely assessed efficiency, the research on an alternative nitrate-based inhibitor have been focused on calcium nitrate ($Ca(NO_3)_2$. The first research regarding these inhibitors goes back to 1987: D'yachenko et al. investigated the inhibiting efficiency of nitrate and nitrite mixes for chloride-induced corrosion of abandoned concrete samples [52]. The latter study was too primitive and immature, that it was necessary to wait the 1994 to have a complete study about calcium nitrate inhibitor [6]: Justnes et al. drafted the first theory on the inhibition mechanism, collecting all the former results as regards.

2.4.1 Inhibiting mechanism

The inhibiting mechanism of calcium nitrate for the corrosion of steel in concrete was suggested firstly by Justnes in 1994 and better clarified later, in 2000 [53]. Like nitrite, it is considered an anodic corrosion inhibitor: the typical inhibition mechanism is characterized by the suppression of the anodic reactions helping the spontaneous metal passivation or forming a barrier deposition compounds [54].

Nitrate behaviour as corrosion inhibitor can be understood through the mechanism of the related nitrite ion, which is well known. Recalling the Paragraph 2.3.1, nitrite-based inhibition was

characterized by the anodic behaviour of ferrous ions oxidation to form a protective oxide surface layer, competing thus with the aggressive chloride ions. Justnes exploited this mechanism and extended it to the nitrate behaviour; in particular, he assumed that the oxidation action of nitrate is the consequence to its easy reduction to nitrite. The two half-reactions illustrate the mechanism:

Reduction: $$2NO_3^- + 2H_2O + 4e^- \rightarrow 2NO_2^- + 4OH^- \quad (15)$$

Oxidation: $$4Fe(OH)_2 + 4OH^- \rightarrow 4Fe(OH)_3 + 4e^- \quad (16)$$

They are combined to give the total reaction:

$$2Fe(OH)_2 + NO_3^- + H_2O \rightarrow 2Fe(OH)_3 + NO_2^- \quad (17)$$

The comparison between the equation (17) and the corresponding nitrite mechanism (Eq. (14)) suggests that nitrate (NO_3^-) should be an even better inhibitor than nitrite (NO_2^-), since the amount of moles of ferrous oxide that reacts with one mole of inhibitor is doubled with respect to the nitrite reaction. Therefore, the efficiency of nitrate as corrosion inhibitor would be, theoretically, twice as high as nitrite. However, the experimental results obtained by Justnes did not confirm this enhanced inhibition efficiency: calcium nitrate did not appear to work when subjected to rapid solution tests as well as the corresponding nitrite compound [53]. This suggested that the kinetic of the redox reactions regarding nitrate may be slower than nitrite. The delay in this inhibition mechanism evolution was assessed by Justnes himself and other studies during the years [6][55][56].

An alternative and more recent hypothesis regarding the inhibiting mechanism of nitrate was suggested by Saura et al. in 2011 [57]; in particular, the behaviour and the efficiency of sodium nitrate ($NaNo_3$) was analysed in neutral and acidic environments. The starting point of this theory was still referred to nitrite inhibition mechanism with the formation of an oxide layer, insoluble in pore water, that forms a precipitation barrier on the steel surface. However, in contrast to Justnes, the authors considered a different ferrous oxide compound creation: γ- Fe_2O_3, so they referred to the corresponding nitrite equation (10). The two half equations describe the mechanism:

Reduction: $$NO_3^- + H_2O + 2e^- \rightarrow NO_2^- + 2OH^- \quad (18)$$

Oxidation: $$2Fe^{2+} + 3OH^- \rightarrow \gamma\text{-}Fe_2O_3 + 2e^- + 3H^+ \quad (19)$$

They are combined to give the total reaction:

$$2Fe^{2+} + NO_3^- + H_2O + OH^- \rightarrow \gamma\text{-}Fe_2O_3 + NO_2^- + 3H^+ \quad (20)$$

The above mechanism was assessed in simulating concrete pore solution and the γ- Fe_2O_3 formed layer was proved to be stable in alkaline environments, inducing a strong protective effect on the steel surface. Nevertheless, problems in the passive film stability were observed in neutral or low-pH solutions; as consequence, it was assumed that nitrate protective effect could be limited in carbonation-induced corrosion [57].

It is important to highlight that these two hypotheses regarding the inhibiting mechanism of nitrate compounds are not be entirely comparable, since they derive from different research conditions: different inhibitors were studied (calcium nitrate and sodium nitrate) and different test methods were adopted (Justnes worked mostly on concrete samples and Saura analysed simulating pore solutions).

2.4.2 Effectiveness

The investigation on the efficiency of nitrate-based compounds as concrete inhibitors is still today an active topic in the corrosion research. Many case studies are present in literature and most of them show conflicting results about the real inhibition effect of this substance: disagreements about effective performance and minimum dosages are common. The absence of completely shared and standardized results can be explained by the differences in the experimental procedures adopted by the authors [55].

The most significant results present in literature about the nitrate inhibition effectiveness in chloride-induced corrosion and carbonation phenomena are presented in chronological order.

The first documented beneficial effect goes back to 1995, when Meland et al. [58] investigated a deteriorated reinforced concrete structure subjected to 22 years of external contamination by calcium nitrate. They found that the steel rebars in severely nitrate-polluted areas (NO_3^- concentration higher than 1.5%) were in perfect condition with only surface rust.

In the same years, multicycle linear polarization studies were performed by Vogelsang [59] on carbon steel samples immersed in alkaline solutions simulating the concrete internal environment.

He proved that calcium nitrate and nitrite had identical corrosion inhibiting properties in pitting-induced corrosion by chlorides contamination.

Additional validation of nitrate inhibition behaviour similar to nitrite one come with Justnes and Nygaard [6]: they measured the inhibition efficiencies in chloride-induced corrosion by long-term macro cell studies in concrete samples. In this case, they worked with ordinary Portland reinforced concrete samples ($w/c = 0.55$) with calcium nitrate as admixed corrosion inhibitor. The substance dosage was chosen according to the maximum practical one for set acceleration: 3.86% of $Ca(NO_3)_2$ by weight of cement. To induce corrosion initiation by chloride attack, immersion and drying cycles on 5% NaCl solution were performed on the concrete samples. The state of rebars corrosion was revealed by linear polarization resistance tests that indicated a retarded inhibition action of calcium nitrate: only after 14 months, the measure revealed nitrate inhibition, showing corrosion rate reduction by a factor of 5 (Fig. 2.7).

Mix and terminus	R_p (Ohm)	E_{Corr} (mV)	I_{Corr} (μA/cm^2)
Calcium nitrate			
0, before exposure	19,000	-360	0.21
3.5 months	6,700±7,400	-600±30	1.3±1.1
5 months	3,200±250	-600±20	1.2±0.1
10.5 months	10,400±13,500	-330±10	1.9±2.4
14.5 months	23,400±13,600	-350±50	0.2±0.1

Fig. 2.7 *Results of linear polarization resistance tests* [6].

This study allowed thus to obtain the first data about the critical chloride threshold for calcium nitrate admixed inhibitor: 3.86% of $Ca(NO_3)_2$ by weight of cement seemed to be sufficient to protect reinforcements by aggressive environment with chloride concentration of 5%.

Later, in 2000, another Justnes' study [53] demonstrated that 2% of calcium nitrate by weight of cement was sufficient to retard chloride initiated corrosion of steel embedded in concrete. The experimental conditions corresponded to the previous Justnes' work, but different $Ca(NO_3)_2$ dosages were adopted (2% and 4% by weight of cement) and the corrosion measurements lasted more time (3 years).

Similar conclusions were achieved also by Al-Almoudi et al. [30] in 2003: the corrosion of steel reinforcements in concrete mortars was effective inhibited by calcium nitrate if contaminated by 0.8% of penetrating chloride ions. Pitting initiation was delayed and rebars corrosion rate reduced by calcium nitrate in dosages higher than 3% by mass.

Different results, in disagreement with Justnes, were obtained in a subsequent study of Dhouibi et al. [60]: electrochemical impedance spectroscopy (EIS) on concrete specimens with admixed calcium nitrate (variable concentrations of 2%, 4%, 6% by weight of cement) showed that the long-term corrosion inhibition effectiveness was not achieved. The experiment involved chloride-induced corrosion on the steel reinforcements and to initiate the attack, the samples were immersed in salt solution (5% NaCl). EIS tests demonstrated that inhibitor compounds were present at the steel surface; however, they did not prevent corrosion process to occur, at any dosages, when chlorides were present.

More recent works seem to be in line with Justnes, confirming the effective inhibition mechanism on chloride-induce corrosion of calcium nitrate at concentrations higher than 3% by weight of cement [61]. Ostnor and Justnes [62] showed effective corrosion rate reductions of steel reinforcements embedded in concrete structures exposed to marine tidal zones: adding 3% of cement mass of $Ca(NO_3)_2$, the rebars were protected against chloride-induced corrosion.

The only research that followed standard test methods was performed in 2016, when Torabzadegan et al. [63] applied the "ASTM G109-07" [64] on concrete structures with admixed calcium nitrate. They confirmed 3% by mass as sufficient dosage for effective inhibition of chloride-induced corrosion and no significant improvement was found when the inhibitor concentration was increased to 4%.

The only drawback of calcium nitrate as inhibitor against chloride-induced corrosion seems to be its delay in the protecting mechanism activation: rapid tests (potentiodynamic polarization) in simulating alkaline solutions did not show any trace of effective inhibition, since nitrates do not have enough time to exhibit their beneficial effect [55][50][56].

The evaluation of calcium nitrate as inhibitor against carbonation-induced corrosion is a more recent research topic. Since it is a well-established concrete admixture for set acceleration and the reason was suspected to be a modification in the porosity, calcium nitrate could give additional benefits. For instance, some researchers thought to evaluate its impact against carbonation-induced corrosion.

Franke et al. [65] conducted accelerated (elevated CO_2 exposure, 56 days) and non-accelerated tests to study the impact of calcium nitrate on concrete: carbonation depth results in Portland cement are reported in Figure 2.8 and they show positive impact when an inhibitor dosage higher than 2% by weight of cement was used.

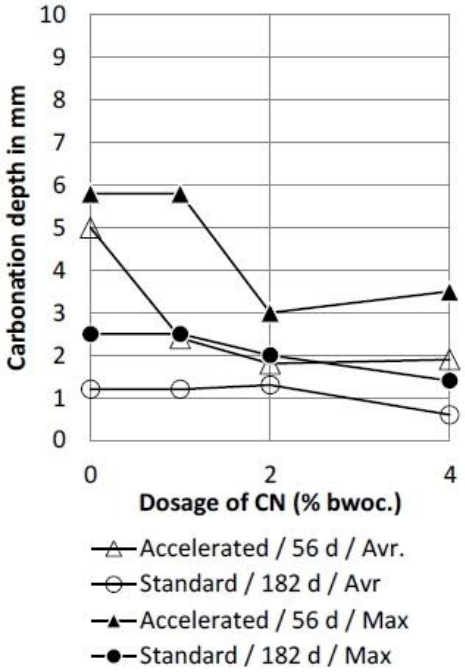

Fig. 2.8 *Carbonation results in Franke et al. work* [65].

2.4.3 Effect on concrete properties

The use of calcium nitrate as concrete admixture setting accelerator developed since the 1980s, when the formulation of chloride-free set accelerator was required to replace the widely used calcium chloride compound [51]. Calcium nitrate was proposed as a basic component for a set accelerating admixture in 1981 and during the years it was widely studied in combination with amine, as technical calcium nitrate. The effect of calcium nitrate additions on the setting properties of cement has been studied by Justnes for long: the results showed that it has in general a good efficiency between 7°C and 20°C; however, the set accelerating effects highly depend on the cement type [6][66].

Additional side effects on concrete properties have been documented and they seem to be related to modifications of the concrete porosity after the addition of calcium nitrate: compressive strength enhancements and freeze-thaw resistance improvements were found [67]. In particular, several case studies concentrated on the compressive strength enhancement consequent to the nitrate admixture; they agreed on a linear dependence of the early age compressive strength on the concentration of calcium nitrate admixed. However, in the long term, its strengthening effect becomes insufficient to consider it as a hardening accelerator [65][68].

With reference to literature, it can be concluded that calcium nitrate meets the general requirements regarding setting time and compressive strength according to the “ASTM C1582” standard [69]: the inhibitor addition in the concrete paste does not affect negatively the properties of the hardened structure [63].

Chapter 3.
Experimental methods

The purpose of the experimental section of the work is the effectiveness investigation of the nitrate based compounds (NA) as corrosion inhibitors for concrete. To compare the obtained results, the same studies were carried out with the nitrite based inhibitors (NI), whose effectiveness in alkaline environments, as well as in concrete, is largely reported in literature. Reference tests were performed with the same conditions but without any inhibitor, as control sample. The study was focused on the assessment of calcium nitrate and nitrite efficiencies as inhibitors for both chloride induced corrosion and carbonation.

The experimental work can be divided in two research sections:

- **Tests in alkaline solutions -** The internal concrete environment was recreated with a synthetic pore solution (pH 12.6) where the specimens of carbon steel rebars were immersed. These tests were used to investigate the inhibition efficiencies in chloride contamination conditions by adding the inhibitors to the alkaline solutions where a carbon steel bar was immersed. Cyclic potentiodynamic polarization and potentiostatic polarization were performed. The tests allow to gain anodic and cathodic characteristic curves, useful to understand the corrosive behaviour of rebars. The determination of these characteristic curves is more difficult in the case of real concrete specimens, because of concrete properties contaminations during the test and problems of reference electrode precision [11].

- **Tests in concrete -** The effectiveness of nitrite and nitrate compounds in the inhibition of rebars corrosion after concrete complete carbonation was evaluated on reinforced and plain specimens. Three series of different concrete compositions with dissolved inhibitors were cast; they were subjected to measurements of permeability variation of carbonation front (the plain samples) and rebars corrosion velocity (the reinforced ones).

3.1 Potentiodynamic tests in solution

The cyclic potentiodynamic polarization test is the common method used to evaluate the behaviour of metals when localized corrosion takes place [70]. In this work, it was used to measure the susceptibility to localised corrosion of the carbon steel rebar samples in chloride rich alkaline environment. Performing cyclic polarization of the metal specimen immersed in the synthetic pore solution, it was possible to identify the characteristic electrochemical parameters: pitting potential (E_{pit}), repassivation potential (E_{rep}) and passivity range.

According to the Standard Test Method "ASTM G 61", the results of the test are not to be considered as absolute values, because they do not describe quantitatively the rates of corrosion propagation that might be observed in service during a real localized attack; the main limiting aspects are the non-stationarity condition of the measurement and the potential scan velocity. However, potentiodynamic test can be useful as screening-test to rank different substances [70]. For this reason, testing different inhibitor concentrations and chloride contents in solution, it was possible to obtain the ratio of [Cl^-]/[inhibitor] concentrations for which any compound results efficient or not and compare nitrite and nitrate inhibition.

These tests are short-time screening methods, in the order of 2-4 hours, during which the potential of the metallic sample is varied with a constant scan rate: it stars from sufficiently low values, usually lower than the hydrogen evolution potential, to a prefixed value of current, when the potential is reversed in cathodic direction until the initial value is reached. Characteristic curves of current density circulating between the sample and a reference electrode were obtained as a function of the varying potential (E vs i); the plots are useful to identify the characteristic electrochemical parameters: an example is shown in Figure 3.1. The first section can be interpreted as the cathodic region (from –1.2 V Ag/AgCl to about –0.8 V Ag/AgCl) where the reaction of hydrogen evolution takes place. The passivity region can be identified when the current density reaches an almost stable value, defines as anodic passive current density; during the passive interval, the metal can be considered in passive condition. "The onset of localized corrosion is usually marked by a rapid increase of the anodic current" [70] and this defines the pitting potential: localised corrosion starts above this value. After the reversion of potential, the scan continues until the hysteresis loop closes; the repassivation potential is determined with the intersection between the backward potential and the passive range: below this value localized corrosion stops.

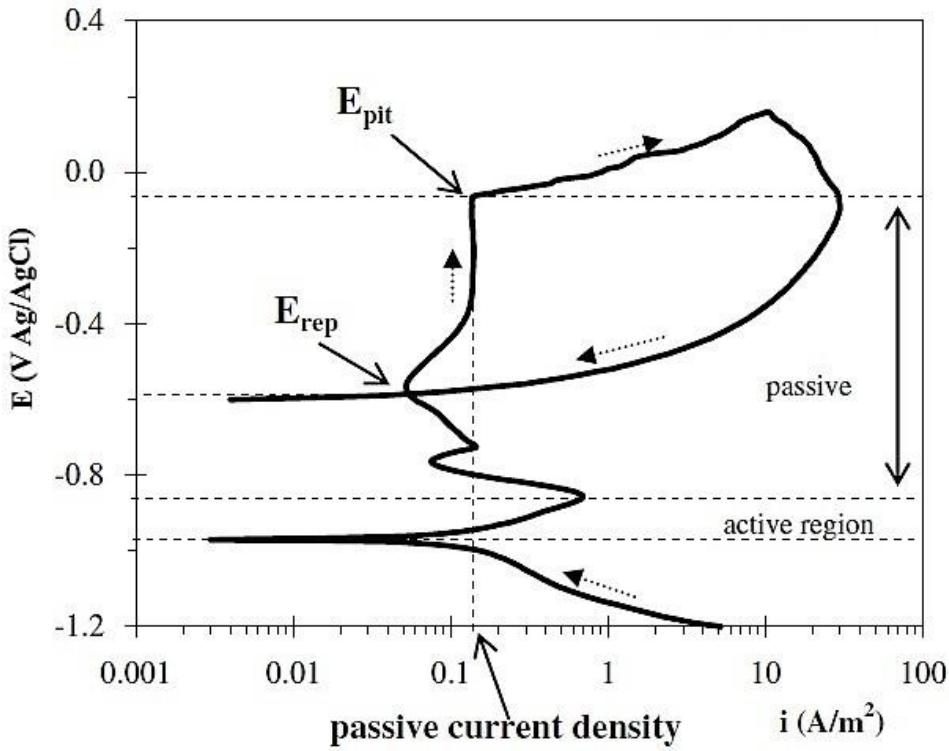

Fig. 3.1 *Example of potentiodynamic curve.*

3.1.1 Materials and instrumentation

The adopted instruments are described as follow:

- **Potentiostat -** The cyclic polarization of carbon steel specimen was performed with a Potentiostat/Galvanostat "PGSTAT 30" of Metrohm Autolab. Measures were recorded with Nova software.

- **Electrodes -** Saturated silver/silver chloride electrode (Ag/AgCl) was used as reference electrode; it is characterized by potential of +230 mV with respect to the standard hydrogen reference electrode (SHE: Saturated Hydrogen Electrode); it was connected to the "reference electrode" pole (R) of the potentiostat. For the counter-electrode activated titanium wires (Ti-MMO) were used; it was connected to the "counter-electrode" pole (C).

- **Cell -** The potentiodynamic polarization tests were carried out in standard ASTM cells (Fig. 3.2 and 3.3). The aerated conditions for the tests were maintained during the total measure time, because no chemical variations (change in pH) or physical alterations (thermal changes)

would take place in a such short experiments duration (form 2 h to 4 h). The carbon steel specimen was connected to the “working” pole of the potentiostat (W).

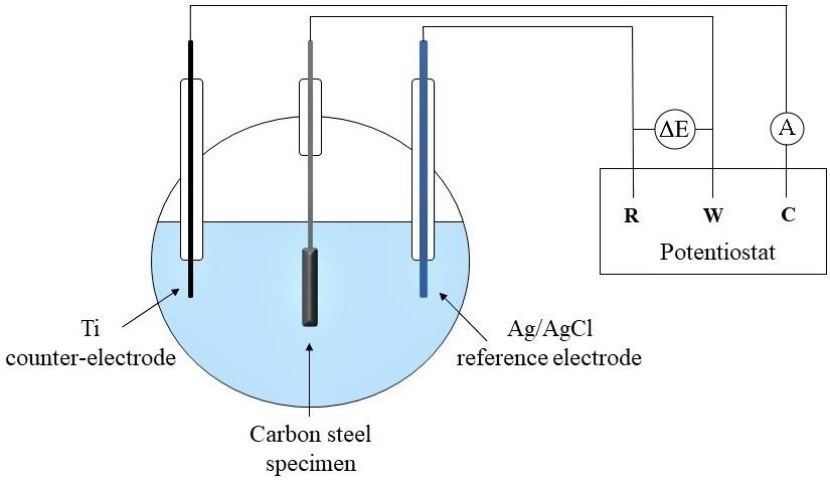

Fig. 3.2 *ASTM cell configuration.*

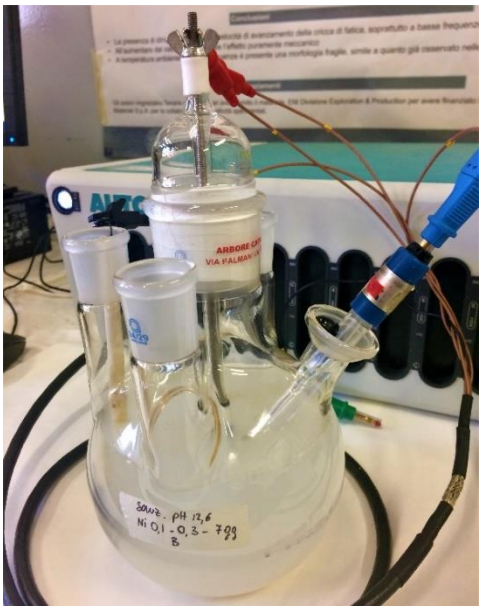

Fig. 3.3 *Picture of the ASTM cell configuration.*

- **Carbon steel specimen -** The sample is characterized by a metallic rod, 50 mm long and with 8 mm diameter, obtained machining a commercial carbon steel reinforcement with improved adhesion, complying with the European Standard “UNI EN 10080” [71] (carbon steel B450C, characteristic yield strength 450 MPa), 1 m long. On one of the two sections, a threaded hole of 4 mm diameter was made to screw a stainless steel (AISI 304) sample-holder bar (Fig. 3.4), used for electrical contact.

Fig. 3.4 *Carbon steel specimen and stainless steel holder*

- **Synthetic pore solution -** The internal environment of concrete was simulated with an alkaline solution in agreement with several experiments in literature, making possible the comparison of the obtained results with the ones historically collected. The solution consists of saturated calcium hydroxide $Ca(OH)_2$ (2 g/L) and 0.01 M of sodium hydroxide NaOH in 1 L of distilled water, to reach pH 12.6. Calcium hydroxide assures a stable solution pH because it provides an alkalinity reserve even after the addition of inorganic inhibitor compounds [72].

- **Studied inhibitors -** Different dosages of calcium nitrate $Ca(NO_3)_2$ and calcium nitrite $Ca(NO_2)_2$ inhibitors were added to the pore solution; the compounds concentrations were selected in agreement with lot of experiments present in literature: 0.1 mol/L and 0.3 mol/L both for nitrate (NA) and nitrite inhibitors (NI), quantities that do not affect the properties of settled concrete. Table 3.1 resumes the different solution compositions and, for comparison purposes, first reference tests (REF) were carried out with control solutions, i.e. without any inhibitor dissolved.

Tab. 3.1 *Synthetic pore solutions composition.*

Solution code	$Ca(OH)_2$ (mol/L)	NaOH (mol/L)	$Ca(NO_2)_2$ (mol/L)	$Ca(NO_3)_2$ (mol/L)
REF	Saturated	0.01	0	0
NI 0.1	Saturated	0.01	0.1	0
NI 0.3	Saturated	0.01	0.3	0
NA 0.1	Saturated	0.01	0	0.1
NA 0.3	Saturated	0.01	0	0.3

3.1.2 Test procedure

Potentiodynamic test, carried out at 20 °C (±2 °C), stars with the preparation of the carbon steel specimen and the synthetic pore solution.

First, the rebar sample, mounted on the stainless steel sample-holder, was sandblasted (air pressure 3-4 bar) with brownish-red corundum to remove any surface impurity and trace of rust. As reported in literature, critical chloride threshold is influenced by the sample surface preparation: the polished condition may favour the increase in chlorides level required for pitting occurrence with respect the non-polished surfaces [31][73]. Therefore, the polished state was chosen for all the samples to allow the relative comparison between obtained results in inhibited and not inhibited solutions and to stay in the as conservative condition as possible.

The synthetic pore solution was prepared in a 1 L graduated beaker; here, the previously prepared rebar specimen is immersed and, because of the alkaline pH environment, it gradually passivates, forming an oxide passive film on the surface. The sample was maintained in free corrosion condition, i.e. submerged in the solution, for different immersion times: 1 day, 3 days and 7 days; three series of tests were performed as a function of these dwell times. This immersion time variation was thought to evaluate the different nobility of the created passive film on carbon steel as a function of the persisting time inside the alkaline environment: the oxide surface layer is not immediately produced after the dipping, but it gradually forms and stabilizes. In addition, this technique was chosen to allow the nitrate inhibitor compound to exhibit its protective effect on the rebar specimen, slower with respect to the corresponding nitrite action [62].

Free corrosion potential was measured daily on the specimens immersed in the solution; this was necessary to evaluate the trend of rebar specimen passivation during time and estimate the efficiency of inhibitor compounds in the enhancement of carbon steel nobility in alkaline environments. Free corrosion potentials were measured with a voltmeter connected to the carbon steel sample and to the Ag/AgCl reference electrode immersed in the same solution.

After the immersion period, the sample was subjected to cyclic potentiodynamic test; carbon steel specimen was extracted from the solution and let dried in air. A self-adhesive tape was carefully applied on both the ends of the metallic rod to insulate the contacts with stainless steel sample-holder and to protect the transversal sections; 5 mm of lateral surface were covered on both sides. This procedure allowed to avoid any type of unwanted and uncontrolled corrosion behaviour

different than the localized one (galvanic coupling and crevice corrosion) and to obtain a net exposed surface area of 10 cm^2.

To assure a safe water-sealing during the measurement and avoid stainless steel sample-holder contact with the liquid, a drilled Teflon cylinder was mounted on the sample-holder between two O-rings. The ASTM cell glass specimen-holder was stick into the stainless steel bar and finally, the system was closed with a butterfly bolt in contact with the glass and screwed to the bar (Fig. 3.5 and 3.6).

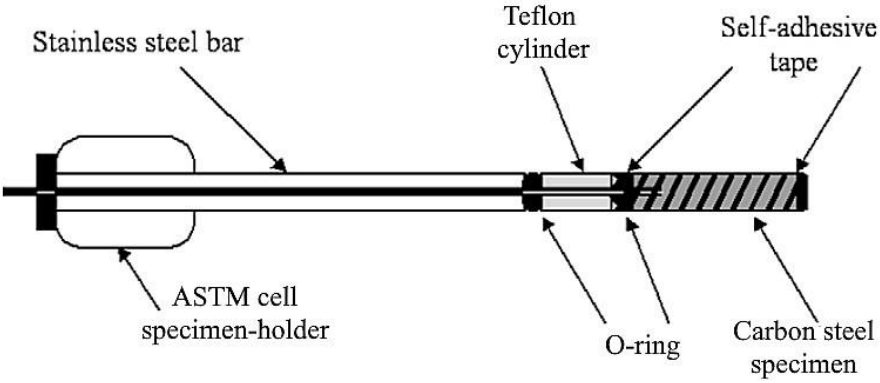

Fig. 3.5 *Schematic view of the specimen assembly.*

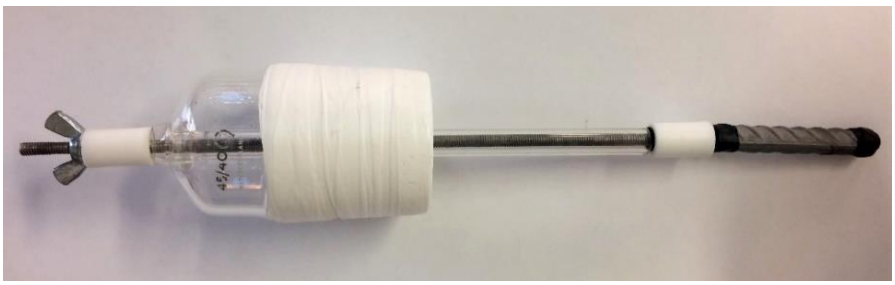

Fig. 3.6 *Specimen assembly picture.*

During the carbon steel sample drying, the addition to the solution of sodium chloride NaCl, in different quantities, were carried out under stirring. Chlorides concentrations were chosen in agreement with several works in literature: 0.1 mol/L and 0.3 mol/L, corresponding to the critical chloride threshold values of carbon steel in alkaline environment: from 0.4 % to 1 % by weight of cement [1]. A series of tests in alkaline solution without sodium chloride addition was performed to measure the potential of oxygen evolution.

The solutions composition is reported in Tables 3.2, 3.3 and 3.4, considering the three different test series according to the immersion times; for each of the two inhibitors and for reference solutions, three electrochemical tests were carried out to assure a good statistical reproducibility of the obtained results.

Tab. 3.2 *Solutions composition of series 1 day of immersion.*

Solution code	$Ca(OH)_2$ (mol/L)	NaOH (mol/L)	$Ca(NO_2)_2$ (mol/L)	$Ca(NO_3)_2$ (mol/L)	NaCl (mol/L)
REF – 0.0 – 1 d	Saturated	0.01	0	0	0
REF – 0.1 – 1 d	Saturated	0.01	0	0	0.1
REF – 0.3 – 1 d	Saturated	0.01	0	0	0.3
NI 0.1 – 0.0 – 1 d	Saturated	0.01	0.1	0	0
NI 0.1 – 0.1 – 1 d	Saturated	0.01	0.1	0	0.1
NI 0.1 – 0.3 – 1 d	Saturated	0.01	0.1	0	0.3
NI 0.3 – 0.0 – 1 d	Saturated	0.01	0.3	0	0
NI 0.3 – 0.1 – 1 d	Saturated	0.01	0.3	0	0.1
NI 0.3 – 0.3 – 1 d	Saturated	0.01	0.3	0	0.3
NA 0.1 – 0.0 – 1 d	Saturated	0.01	0	0.1	0
NA 0.1 – 0.1 – 1 d	Saturated	0.01	0	0.1	0.1
NA 0.1 – 0.3 – 1 d	Saturated	0.01	0	0.1	0.3
NA 0.3 – 0.0 – 1 d	Saturated	0.01	0	0.3	0
NA 0.3 – 0.1 – 1 d	Saturated	0.01	0	0.3	0.1
NA 0.3 – 0.3 – 1 d	Saturated	0.01	0	0.3	0.3

Tab. 3.3 *Solutions composition of series 3 days of immersion.*

Solution code	$Ca(OH)_2$ (mol/L)	NaOH (mol/L)	$Ca(NO_2)_2$ (mol/L)	$Ca(NO_3)_2$ (mol/L)	NaCl (mol/L)
REF – 0.0 – 3 d	Saturated	0.01	0	0	0
REF – 0.1 – 3 d	Saturated	0.01	0	0	0.1
REF – 0.3 – 3 d	Saturated	0.01	0	0	0.3
NI 0.1 – 0.0 – 3 d	Saturated	0.01	0.1	0	0
NI 0.1 – 0.1 – 3 d	Saturated	0.01	0.1	0	0.1
NI 0.1 – 0.3 – 3 d	Saturated	0.01	0.1	0	0.3
NI 0.3 – 0.0 – 3 d	Saturated	0.01	0.3	0	0
NI 0.3 – 0.1 – 3 d	Saturated	0.01	0.3	0	0.1
NI 0.3 – 0.3 – 3 d	Saturated	0.01	0.3	0	0.3

NA 0.1 – 0.0 – 3 d	Saturated	0.01	0	0.1	0
NA 0.1 – 0.1 – 3 d	Saturated	0.01	0	0.1	0.1
NA 0.1 – 0.3 – 3 d	Saturated	0.01	0	0.1	0.3
NA 0.3 – 0.0 – 3 d	Saturated	0.01	0	0.3	0
NA 0.3 – 0.1 – 3 d	Saturated	0.01	0	0.3	0.1
NA 0.3 – 0.3 – 3 d	Saturated	0.01	0	0.3	0.3

Tab. 3.4 *Solution compositions of series 7 days of immersion.*

Solution code	***$Ca(OH)_2$ (mol/L)***	***NaOH (mol/L)***	***$Ca(NO_2)_2$ (mol/L)***	***$Ca(NO_3)_2$ (mol/L)***	***NaCl (mol/L)***
REF – 0.0 – 7 d	Saturated	0.01	0	0	0
REF – 0.1 – 7 d	Saturated	0.01	0	0	0.1
REF – 0.3 – 7 d	Saturated	0.01	0	0	0.3
NI 0.1 – 0.0 – 7 d	Saturated	0.01	0.1	0	0
NI 0.1 – 0.1 – 7 d	Saturated	0.01	0.1	0	0.1
NI 0.1 – 0.3 – 7 d	Saturated	0.01	0.1	0	0.3
NI 0.3 – 0.0 – 7 d	Saturated	0.01	0.3	0	0
NI 0.3 – 0.1 – 7 d	Saturated	0.01	0.3	0	0.1
NI 0.3 – 0.3 – 7 d	Saturated	0.01	0.3	0	0.3
NA 0.1 – 0.0 – 7 d	Saturated	0.01	0	0.1	0
NA 0.1 – 0.1 – 7 d	Saturated	0.01	0	0.1	0.1
NA 0.1 – 0.3 – 7 d	Saturated	0.01	0	0.1	0.3
NA 0.3 – 0.0 – 7 d	Saturated	0.01	0	0.3	0
NA 0.3 – 0.1 – 7 d	Saturated	0.01	0	0.3	0.1
NA 0.3 – 0.3 – 7 d	Saturated	0.01	0	0.3	0.3

The solution pH was measured by visual inspection of litmus test to check if the alkalinity of the solution is maintained before and after the chlorides addition; the critical pH below which the passive layer of reinforcing steel immersed in alkaline solution is no more stable is around 11.5 [7].

Then, the solution is transferred from the beaker to the ASTM cell on which the specimen-holder is mounted to; the liquid level was maintained in proximity of the Teflon cylinder to avoid any liquid penetration inside the glass specimen-holder. Titanium counter-electrode and Ag/AgCl reference electrode were dipped in the solution and connected to the potentiostat.

Cyclic potentiodynamic tests were carried out starting from potential of –1.2 V Ag/AgCl: this value is definitely lower than the free corrosion potential of carbon steel in alkaline environment that in passive condition is in the range of –0.1-0 V SCE (+230 mv of potential with respect to the SHE) [7][1][74]; therefore, it was possible to evaluate the presence of eventual effects on the first cathodic section. With scan rate of 1 V/h (0.277 mV/s), the potential was increased in the anodic direction until reaching 10 mA of measured current, corresponding to a current density of about 10 A/m^2; at this point, the potential was reversed in the cathodic direction. The test finished when the repassivation condition was achieved. At the end of the measure, visual inspection of the carbon steel specimen confirmed the succeeded localized corrosion.

3.2 Potentiostatic tests in solution

Potentiostatic polarization is a long-term measurement: anodic polarization with constant potential in a quasi-stationary condition was performed on rebar samples immersed in a synthetic pore solution simulating the concrete environment. Different solution compositions were used to study the inhibition efficiency of a nitrate compound for chloride contamination corrosion in concrete; the obtained results were compared with corresponding tests without any inhibitor and with nitrite compound whose efficiency is well known in literature. The information obtained with this test is the critical chloride threshold at which localised corrosion of carbon steel specimens takes place at the fixed polarisation potential. The test can last from weeks to few months.

Potentiostatic tests give more reliable results with respect to the corresponding potentiodynamic scan: measuring for a longer period the effect of imposed constant potential in quasi-steady state condition, the corrosive behaviour of concrete rebars can be better simulated. Therefore, these measurements represent an important evaluation and eventual confirmation of the inhibitive action of the examined compounds.

3.2.1 Materials and instrumentation

- **Potentiostat -** The polarization potential was imposed with an "AMEL 1480A" potentiostat.

- **Cell -** The tests were carried out in cylindrical cells of 19 cm diameter and 15 cm of height; they are able to contain 3 L of solution. The cover of the cell, illustrated in Figure 3.7, presents 13 equidistant holes placed on a circumference of 14 cm diameter: they are required for corresponding 13 specimens' location. Additional two holes are present in the centre of the cover: the central one allows the placement of the reference electrode and the other is used to withdrawn solution samples and introduce eventual substances. A small lateral hole is required for the electrical connection of the counter-electrode.

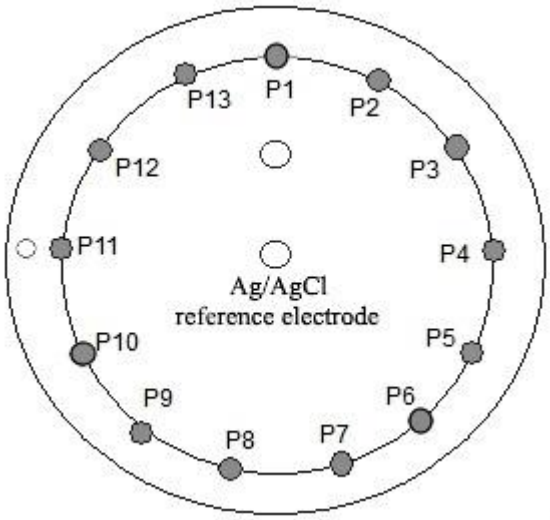

Fig. 3.7 *Cell cover.*

- **Electrodes –** Saturated silver/silver chloride electrode (Ag/AgCl) was used as reference electrode; it is characterized by potential of +230 mV with respect to the standard hydrogen reference electrode (SHE: Saturated Hydrogen Electrode).
  As counter-electrode, on the bottom of the cell was placed an activated titanium net-wire (Ti-MMO) considering the dimension of the cell and the number of specimens; the uniform circulation of current into the solution was thus guaranteed. The overall cell assembly is depicted in Figure 3.8 and 3.9.

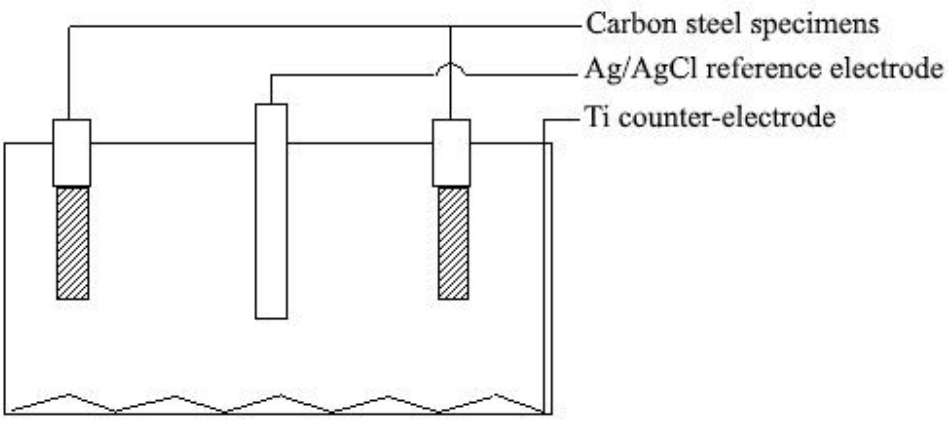

Fig. 3.8 *Schematic view of the cell assembly.*

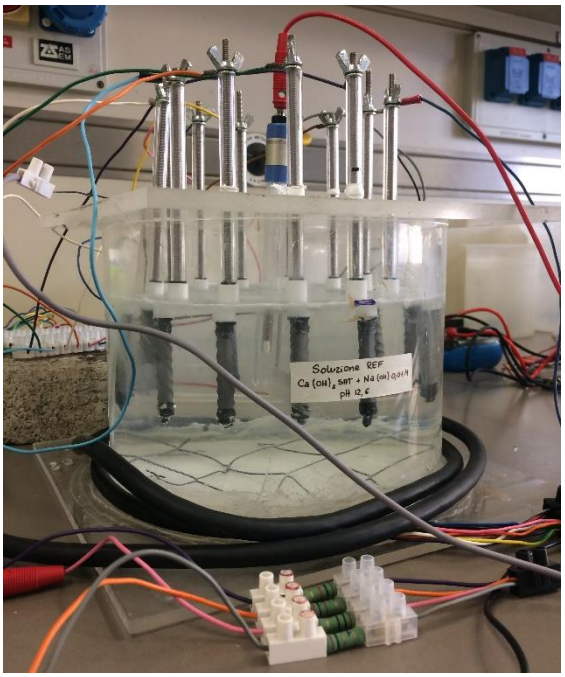

Fig. 3.9 *Picture of the potentiostatic cell assembly.*

- **Carbon steel specimens -** The preparation of the rebars samples is similar to the potentiodynamic procedure (Par. 3.1.1): 13 carbon steel (type B450C, characteristic yield strength 450 MPa) specimens of 8 mm diameter and 50 mm length, was mounted on stainless steel sample-holder bars.

- **Synthetic pore solution -** The internal environment of concrete was simulated by the same alkaline solution used in potentiodynamic tests (Par. 3.1.1); calcium hydroxide $Ca(OH)_2$ in saturated concentration (2 g/L) and 0.01 M of sodium hydroxide NaOH were dissolved in 3 L of distilled water, to reach pH 12.6. Additional inhibitors were used in the following reported compositions.

- **Studied inhibitors -** Calcium nitrate $Ca(NO_3)_2$ and calcium nitrite $Ca(NO_2)_2$ inhibitors were studied separately as inhibitor compounds; they were added to the pore solution both in 0.1 mol/L concentrations. In addition, also the inhibition efficiency of combined nitrite-nitrate was studied to investigate an eventual synergistic behaviour: it was created a third alkaline solution with components concentration of 0.05 mol/L in 1:1 molar ratio. For comparison purposes, reference tests (REF) were firstly carried out with control solutions, i.e. without any inhibitor dissolved. The four solutions composition is resumed in Table 3.5.

Tab. 3.5 *Potentiostatic tests solutions composition.*

Solution code	$Ca(OH)_2$ (mol/L)	NaOH (mol/L)	$Ca(NO_2)_2$ (mol/L)	$Ca(NO_3)_2$ (mol/L)
REF	Saturated	0.01	0	0
NI 0.1	Saturated	0.01	0.1	0
NA 0.1	Saturated	0.01	0	0.1
NA 0.05 – NI 0.05	Saturated	0.01	0.05	0.05

3.2.2 Test procedure

The potentiostatic test starts with a pre-passivation procedure during which a stable passive film creation was induced on the surfaces of all rebar specimens. The 13 sandblasted carbon steel samples were immersed in the alkaline solution and electrically connected in parallel to the potentiostat: a constant polarization potential of +200 mV Ag/AgCl was set for almost 2 days. During all the passivation time, the density of current was continuously measured with a voltmeter through a set of four parallel shunts of 1 Ω, 10 Ω, 100 Ω, 1000 Ω values, respectively. After almost 2 days, when the measured current density was lower than 1 mA/m^2, passive condition was achieved: reaching this value, the complete creation of oxide passive layer can be assured.

The 13 samples were then removed from the solution and dried in air; self-adhesive tape was carefully applied on both the ends of the metallic rod (5 mm for each side) to insulate the contacts with stainless steel sample-holder and to protect the transversal sections. Galvanic coupling and crevice corrosion were thus avoided; in addition, the net exposed surface area at this point was 10 cm^2. Later, the samples were subjected to soft sandblasting (air pressure < 2 bar) in perpendicular direction to the exposed surface: in this way, the previously formed passive film was removed without affecting the tape and the below oxide film. This procedure was performed to avoid, during

the test, any potential local corrosion attack below the protective tape, otherwise it would be favoured by the presence of heterogeneity between the active carbon steel below the self-adhesive cover and the exposed passivated metal.

To completely insulate the stainless steel bars, avoiding the contact with the alkaline solution, glass specimen-holders were used. The assembly water-sealing was guaranteed by a Teflon cylinder between two O-rings and by the blocking with a butterfly bolt, as illustrated in Figure 3.10 and 3.11. The 13 specimens were introduced in the alkaline solution without chlorides by the immersion of the sample-holder assembly in the holes of the cell cover; they were let suspended in the solution setting the liquid level in proximity to the Teflon cylinder to avoid any liquid penetration.

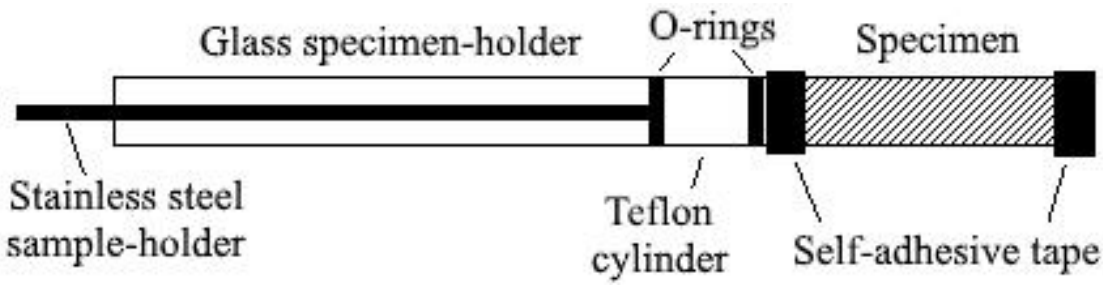

Fig. 3.10 *Specimen assembly.*

Fig. 3.11 *Picture of the specimen assembly.*

Connecting in parallel all the samples to the “working” pole of the potentiostat, the potential was fixed to 0 mV Ag/AgCl: this value was chosen considering that carbon steel reinforcement in concrete environment usually shows free corrosion potential of 0 mV SCE (+230 mv of potential with respect to the SHE) in passive condition [1][7][74]. On one specimen, the passive current density was recorded as a function of time through the ohmic drop measurement made with the set of parallel shunts (1 Ω, 10 Ω, 100 Ω, 1000 Ω). In this way, the carbon steel passivation was

assessed and the efficiency of inhibitor compounds in the enhancement of metal nobility in alkaline environment was evaluated.

After a week, when the passive current density was lower than 1 mA/m^2 and the complete passivation guaranteed, the first chlorides addition was performed. A small quantity of solution (about 100 mL) was withdrawn from the cell and the fixed quantity of sodium chloride NaCl was dissolved in it; then the liquid was reintroduced in the cell. Periodic additions of chlorides were performed at constant intervals of 80-90 hours with increasing dosage (0.05 mol/L, 0.1 mol/L, 0.2 mol/L…). The concentration value of the first chlorides addition was selected considering that carbon steel shows a critical chloride threshold of 0.6 in terms of $[Cl^-]/[OH^-]$ ratio, corresponding to 0.024 mol/L chlorides concentration in a solution of pH 12.6. The pH of the solution was measured through visual inspection of litmus test during every chlorides addition.

The current density of each carbon steel specimen was measured daily to verify if localised corrosion event was taking place. The ohmic drop at the sides of a 10 Ω shunt mounted on each sample wire was recorded: local corrosion initiation was considered in correspondence to current density values higher than 5 A/m^2. Visual inspection confirmed the corrosion attack and the corresponding sample was disconnected from the circuit. The test finishes when all the 13 samples show localized corrosion attack; the critical chloride threshold can be thus obtained.

3.3 Tests in concrete

The aim of these tests was to evaluate the nitrate inhibitive effect on the carbonation diffusion velocity in concrete and the rebars corrosion after complete carbonation of the concrete cover. For the first type of assessment, plain concrete specimens were fabricated with three different concrete mixture proportions. The same mixes were used for the reinforced samples fabrication: they were subjected to rebars corrosion measurements.

3.3.1 Concrete compositions

The fabrication of reinforced and plain concrete samples was performed in a past thesis work (2016) [75]: three different series of mixes were selected according to the European Standard “BS EN 197-1” [76]:

- Serie I – CEM I 52.5 R: ordinary Portland cement
- Serie II – CEM II/B-S 52.5 N: Portland-composite cement
- Serie III – CEM II/B-M 42.5: Portland-composite cement

For each of the three series, four different concrete types were cast with the same aggregates and workability class, but with different concentrations of inhibitors introduced into the concrete mix. Nitrite compound in 2% by weight of cement (bwoc) and nitrate compound in 2% and 4% by weight of cement were selected as inhibitor concentrations because they do not affect the properties of settled concrete. The fourth concrete type was cast without inhibitor as reference sample. 12 different concrete compositions were thus obtained: the codes to identify them are reported in Table 3.6.

Tab. 3.6 *Concrete specimens code.*

Inhibitor	***Serie I***	***Serie II***	***Serie III***
No inhibitor	I – 00	II – 00	III – 00
Nitrite 2% bwoc	I – NI – 2	II – NI – 2	III – NI – 2
Nitrate 2% bwoc	I – NA – 2	II – NA – 2	III – NA – 2
Nitrate 4% bwoc	I – NA – 4	II – NA – 4	III – NA – 4

Water to cement ratio was maintained equal to 0.6 for all the specimens; in particular, for compositions in presence of inhibitors, water concentration was calculated considering that inhibitor compounds are dissolved in different amounts in aqueous solutions.

Concrete specimens were cast in June 2016: the mix compositions are reported in Table 3.7, valid for the three series of cements.

Tab. 3.7 *Concrete compositions.*

Composition	***00***	***NI – 2***	***NA – 2***	***NA – 4***
Water (L)	4.2	3.873	3.92	4.06
Cement (kg)	7	7	7	7
Plasticizer (kg)	0.07	0.07	0.07	0.07

Inhibitor (kg)	0	0.467	0.28	0.56
Sand (kg)	14.05	14.05	14.05	14.05
Gravel (kg)	21.072	21.05	21.05	21.05

3.3.2 Concrete samples

Two types of concrete samples were cast:

- **Plain concrete specimens -** 36 prismatic concrete specimens of 15x6x6 cm dimensions were fabricated without rebars: the first 12 samples were used for carbonation diffusion measurements in accelerated condition; the other 24 prisms were placed to the external atmosphere of Milan, on the rooftop of "Dipartimento di Chimica, Materiali e Ingegneria Chimica "Giulio Natta", Politecnico di Milano", half exposed to rain and half sheltered. The latter were tested to measure the carbonation diffusion for a longer period in real aerated conditions. An example is shown in Figure 3.12.

Fig. 3.12 *Plain concrete prism.*

- **Reinforced concrete specimens -** 24 reinforced cylindrical samples were cast and exposed to the external atmosphere of Milan after the complete carbonation of the concrete cover.
  Measurements of internal rebars corrosion were performed. An example of the reinforced samples is shown in Figure 3.13.

Fig. 3.13 *Reinforced concrete specimen.*

The reinforcements are 15 cm in height and 6 cm in diameter; they present a single carbon steel rebar with the same material of the specimens used for the tests in solution (B450C, characteristic yield strength 450 MPa). The rebar is 17 mm long and it has 10 mm of diameter; an electric cable was connected at one side of the bar to allow the potential measurements. Before the cast, the bars were subjected to sandblasting to remove any superficial impurity and trace of rust. Through the application of a self-adhesive tape on both the ends, so that only a length of 10 cm was exposed to the internal concrete; this insulation was also required to avoid any contact of the bar with the external atmosphere. Figure 3.14 illustrates the section of the reinforced specimen.

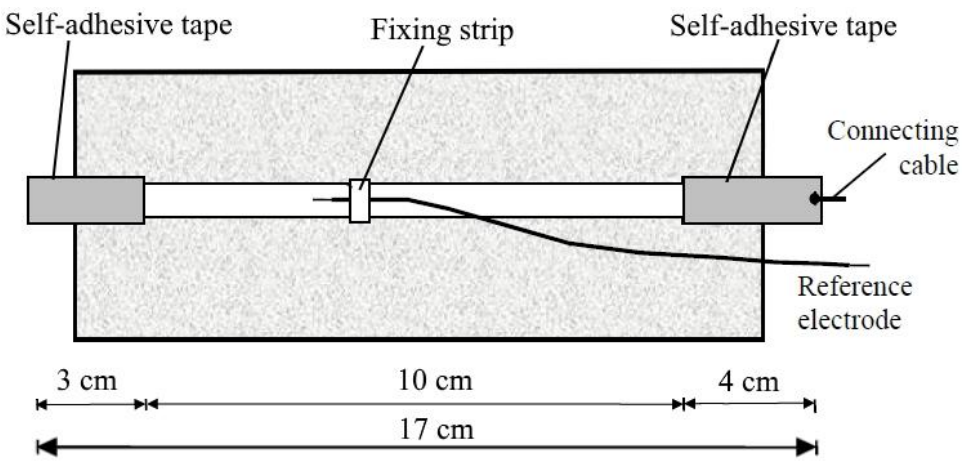

Fig. 3.14 *Reinforced concrete specimen section.*

Inside the specimen, an activated titanium (Ti-MMO) reference electrode was placed in proximity to the carbon steel rebar and a copper cable was connected to it allowing the external electrical connection. Titanium reference electrode was required for the linear polarization resistance tests used to monitor the metal corrosion (Par. 3.3.4).

3.3.3 Carbonation monitoring

Carbonation process is directly related to carbon dioxide (CO_2) diffusion inside concrete and reaction with alkaline compounds. This phenomenon is very slow in common aerated conditions because of the low concentration of CO_2 in atmosphere. For this reason, accelerated tests were performed in addition to carbonation monitoring on concrete specimens exposed to external atmosphere:

- **Accelerated carbonation monitoring -** The tests were performed introducing 12 prismatic plain samples into carbonation chamber with controlled atmosphere (room temperature and 65% RH) and at high level of carbon dioxide concentration (4%). To avoid gas diffusion from the ends of the specimens, the bases of the prism were spackled: carbon dioxide penetration was thus possible only from lateral surfaces.
  The progress of the carbonation front was measured by withdrawing the samples from the chamber at regular intervals (every two months) and subjecting them to phenolphthalein test. A transversal cut of the prisms was performed to obtain sections of few centimetres thick; the test was carried out on every surface according to the Standard "UNI 9944" [77]. Immediately after the cut, a small quantity of phenolphthalein was sprayed on the sections. The carbonated concrete does not modify its aspect; the concrete that is not yet reached by the carbonation front, reacts with the substance because of its maintained alkaline pH, changing its colour to the characteristic pink tone. In this way, for every periodic test, the evaluation of carbonation diffusion inside concrete could be performed looking at the uncoloured part dimensions, as shown in Figure 3.15.

Fig. 3.15 *Example of phenolphthalein test on concrete section*

- **Real carbonation monitoring -** Carbonation tests on the 24 prismatic samples exposed to the external atmosphere were performed with the same procedure of the prisms in carbonation chamber: transversal section cut and subsequent phenolphthalein test. The only difference is that it was necessary to wait more time for the results, because of the low kinetic of carbonation diffusion in real aerated conditions. The first measurement was taken about one year after the cast.

3.3.4 Corrosion monitoring

The evaluation of inhibitors effect on rebars corrosion after complete carbonation of the concrete cover was performed through the monitoring of free corrosion potential and polarization resistance of the carbon steel bars.

The tests were carried out on the reinforced concrete samples after the complete carbonation of their concrete cover (2.5 cm). To accelerate the process, they are placed into carbonation chamber (4% CO_2 concentration) together with the previously illustrated plain prismatic specimens. Because reinforced and plain concrete samples were cast with the same compositions, the complete carbonation of the first ones was assessed with the CO_2 penetration monitoring on the corresponding plain prisms, as described in Paragraph 3.3.3. Once phenolphthalein tests assured concrete cover carbonation, the cylindric prisms were removed from the carbonation chamber and exposed to the external atmosphere of Milan, on the rooftop of "Dipartimento di Chimica, Materiali e Ingegneria Chimica "Giulio Natta", Politecnico di Milano", part exposed to rain and part sheltered. With a variable periodicity, about every 10 days for the first two months of atmosphere exposure and then less frequently, the free corrosion potentials and polarization resistances were measured on carbon steel rebars:

- **Free corrosion potential measurement -** According to the standard "ASTM C 876" [78], rebar corrosion probability can be estimated through its free corrosion potential, measured with respect to copper sulfate reference electrode (CSE, potential of +314 mV SHE). "The numerical magnitude of the potential usually provides an indication of the presence or absence of corrosion of steel embedded in concrete; the numeric magnitude does not indicate the corrosion rate of the steel" [78]. The standard stated that measured free corrosion potentials higher than –200 mV CSE indicates low corrosion probability and with potentials lower than –350 mV CSE, the metal is in active corrosion condition.

The metal potential was recorded by a voltmeter connected to the electrical wire of the specimen and to the CSE reference electrode put in contact with the concrete surface through a wet sponge.

- **Polarization resistance measurement -** Rebars corrosion rate was evaluated through linear polarization resistance (LPR) method [79][80]. The test was performed with a Potentiostat/Galvanostat ("PGSTAT 30" of Metrohm Autolab). The internal titanium wire was used as reference electrode and a circular net of activated titanium (Ti-MMO) was placed on concrete surface over a wet sponge as counter-electrode.
  Using the linear potentiodynamic technique, rebars corrosion rates measurements were carried out: the metal potential was variated form –10 mV to +10 mV with respect to the free corrosion potential; the scan rate was set as 10 mV/min. Polarization resistance was calculated as the slope of the final linear section of the resulting curve potential vs current density (E vs i) [81]. Mean corrosion rate (mA/m^2) was then obtained through the Stern-Geary relation:

$$i_{corr} = \frac{B}{R_p} \tag{21}$$

  where R_p is the measured polarization resistance (Ω m^2) and constant B is assumed equal to 26 mV for active rebars and 52 mV for passive ones [80].
  Mean penetration rate (μm/year) can be calculated according to Faraday law: in the case of carbon steel, it is equal to i_{corr} multiplied by 1.17 factor. Since corrosion penetration lower than 1-2 μm/year can be considered negligible [1], polarisation resistance of about 10-20 Ω m^2 is the threshold value below which corrosion is significant.

Chapter 4. Experimental results

The research of a new class of non-toxic and environmental-friendly corrosion inhibitors found in calcium nitrate a promising candidate to replace the well-established effective nitrite affected by toxicity issues. The results obtained by the experimental section of the work are presented in this chapter and they are divided according to the type of test performed. As illustrated in Chapter 3, the effectiveness of nitrate-based inhibitor can be investigated with different experimental measurements to obtain distinct interpretations about the nitrate effect on concrete corrosion.

The obtained results are divided in:

- Potentiodynamic tests in solution;
- Potentiostatic tests in solution;
- Tests in concrete.

4.1 Potentiodynamic tests in solution

The cyclic potentiodynamic polarization test was used to measure the steel rebar susceptibility to localised chloride-induced corrosion in presence of nitrate inhibitor. It allowed to obtain the characteristic electrochemical parameters of steel samples in alkaline environment (pH 12.6): pitting potential (E_{pit}), repassivation potential (E_{rep}) and anodic passive current density.

Two different calcium nitrate concentrations (0.1 mol/L and 0.3 mol/L) were used in the synthetic pore solution and the obtained results were compared with corresponding tests without any inhibitor and with nitrite compound (in the same two concentrations), whose efficiency is well known in literature. Before the cyclic polarization tests, the steel samples were immersed in the alkaline solutions for different residence times: 1 day, 3 days and 7 days. Two different amounts of chloride ions (0.1 mol/L and 0.3 mol/L) were added to the solution just before the potentiodynamic scan; in addition, a series of chlorides-free solutions was used to assess the steel passive behaviour in the different inhibited conditions. As result, 45 different solutions settlements were produced (5 different inhibitors configurations, 3 chlorides concentrations and 3 immersion

times). In all the following plots, these different configurations are identified with the abbreviations:

- *REF* - reference solutions without any inhibitor;
- *NI 0.1* - inhibited solutions with calcium nitrite ($Ca(NO_2)_2$) in 0.1 mol/L concentration;
- *NI 0.3* - inhibited solutions with calcium nitrite ($Ca(NO_2)_2$) in 0.3 mol/L concentration;
- *NA 0.1* - inhibited solutions with calcium nitrate ($Ca(NO_3)_2$) in 0.1 mol/L concentration;
- *NA 0.3* - inhibited solutions with calcium nitrate ($Ca(NO_3)_2$) in 0.3 mol/L concentration.

The second number (after the dash) is referred to the chlorides dosage: *0.1* and *0.3* respectively for 0.1 mol/L and 0.3 mol/L concentrations. Additional abbreviations were used to identify the immersion time, e.g. *1 d* for one day of immersion, *3 d* for three days and *7 d* for seven days; the symbols *A, B, C* were used to identify the three identical test solutions for the triple multiplicity.

4.1.1 Reproducibility

For each of the 45 different solutions settlements, three identical potentiodynamic tests were performed to obtain a good statistical reproducibility of the results, for a total of 135 polarization measurements.

All the potentiodynamic tests showed a good reproducibility: the resulting characteristic curves (E vs i) were always quite overlapping. Some examples of good reproducibility are reported in Figure 4.1: they depict different conditions, from reference solution to the most aggressive inhibited situation (NA 0.1 – 0.3).

Considering the good reproducibility of all the multiple performed tests, only one curve for each test condition is henceforth presented; all the characteristic polarization plots are presented in the *Appendix A – Cyclic polarization curves*.

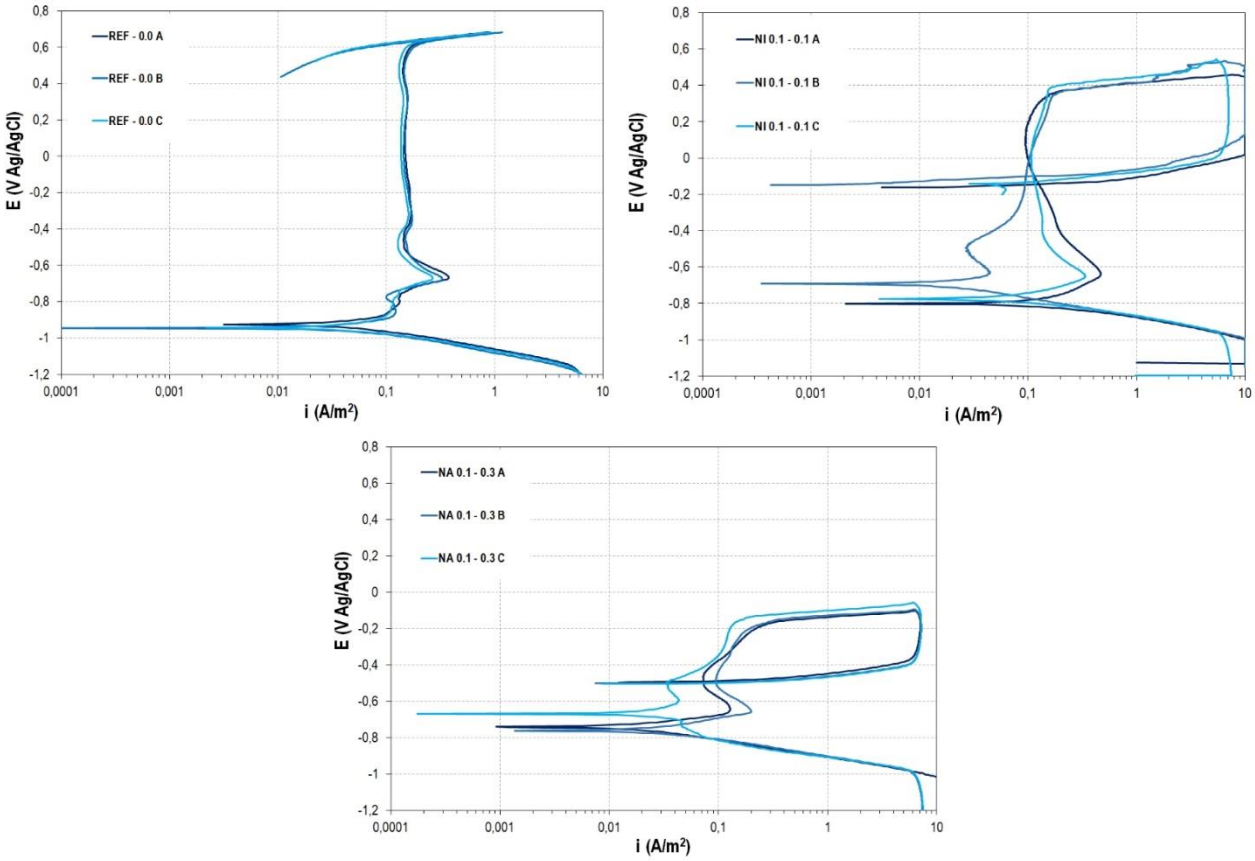

Fig. 4.1 *Examples of the potentiodynamic curves reproducibility.*

4.1.2 Reference solution

The preparation of the reference alkaline solutions is described in Chapter 3.

Here, the characteristic polarization curves are presented in three different graphs, according to the three different immersion times; for each graph, three distinct curves, as a function of the amount of chloride ions admixed to the solution, are shown. Polarization curves of one day, three days and seven days are presented in Figure 4.2.

In absence of chloride (blue curve), it is possible to identify the passive behaviour of the steel sample, for each immersion time: the potential trend shows a large passivity region with constant anodic current density around 0.1 A/m^2. In this condition, no hysteresis loops are present and the passive trend ends with oxygen evolution at potentials around 0.6 V Ag/AgCl. In presence of chlorides, the typical pitting corrosion occurs: the anodic polarization curve of rebars modifies, shortening the passivity range with increasing chlorides content. The rapid increase of the anodic current defines the onset of the localized attack, namely pitting potential (E_{pit}). The obtained pitting potentials range from –0.2 V Ag/AgCl to 0 V Ag/AgCl and they decrease with increasing chlorides

concentrations, since higher Cl^- content induce an increase in the alloy susceptibility to localized corrosion [70].

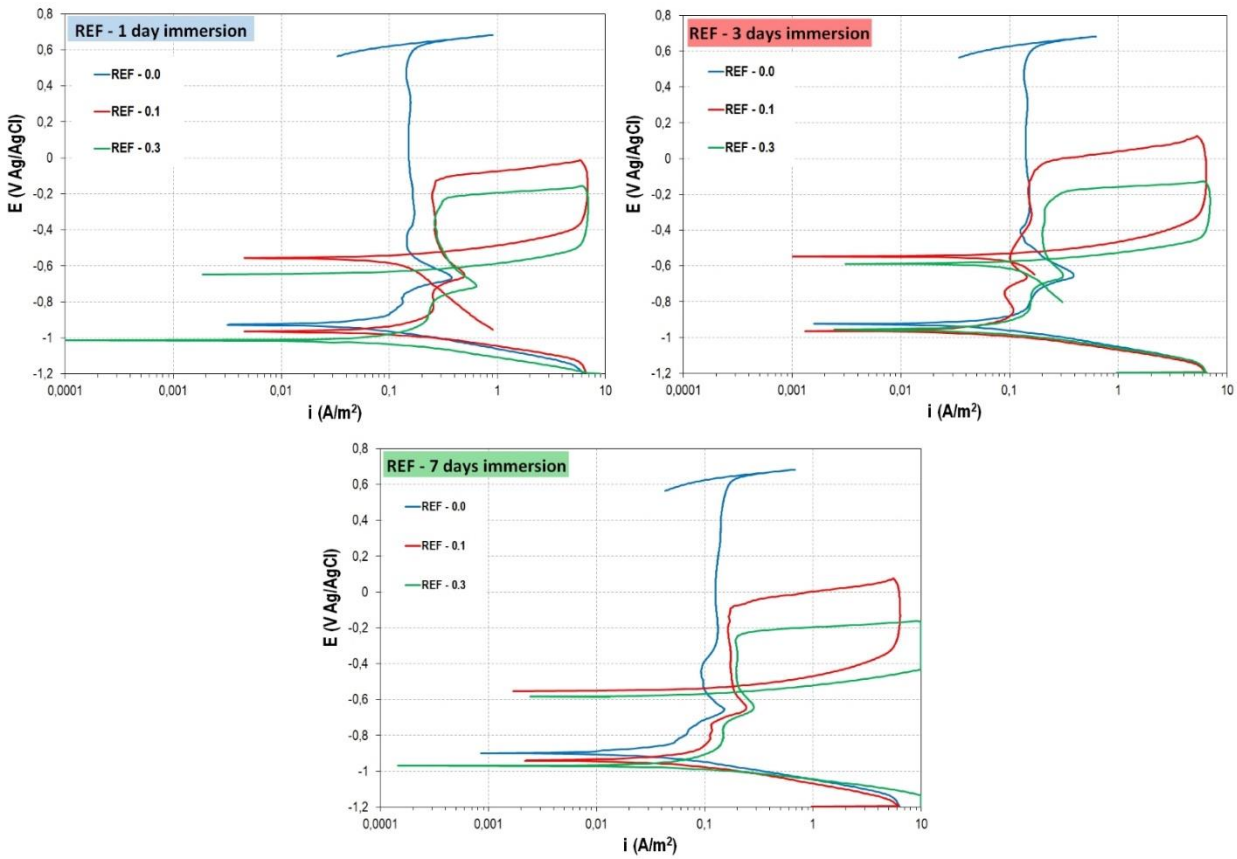

Fig. 4.2 *Potentiodynamic curves of reference solutions.*

Potentiodynamic test ends with the inversion of the potential scan, closing the hysteresis loop. The repassivation potentials (E_{rep}) can be identified as the intersection between the backward potential and the passive range and the obtained values are quite constant for each condition, around –0.5 V Ag/AgCl, suggesting an independent repassivation trend on the chloride content.

The average values of the three pitting and repassivation potentials for each condition are reported in Table 4.1; it is important to highlight that the pitting potentials in the conditions without chloride are referred to the potentials of oxygen evolution (o.e.).

Tab. 4.1 *Pitting and repassivation potentials of reference potentiodynamic tests.*

Solution code	**NaCl (mol/L)**	**E_{pit} (V Ag/AgCl)**	**E_{rep} (V Ag/AgCl)**
REF – 1 d	0	0.62 (o.e.)	-
	0.1	– 0.08	– 0.55
	0.3	– 0.18	– 0.56

	0	0.6 (o.e.)	-
REF – 3 d	0.1	– 0.05	– 0.52
	0.3	– 0.17	– 0.56
	0	0.6 (o.e.)	-
REF – 7 d	0.1	– 0.08	– 0.52
	0.3	– 0.25	– 0.57

The steel samples, after the end of the polarization measure, confirmed the localized corrosion initiation: the visual inspection of the bars demonstrated the presence of several localized pits all over the metal surface (Fig. 4.3).

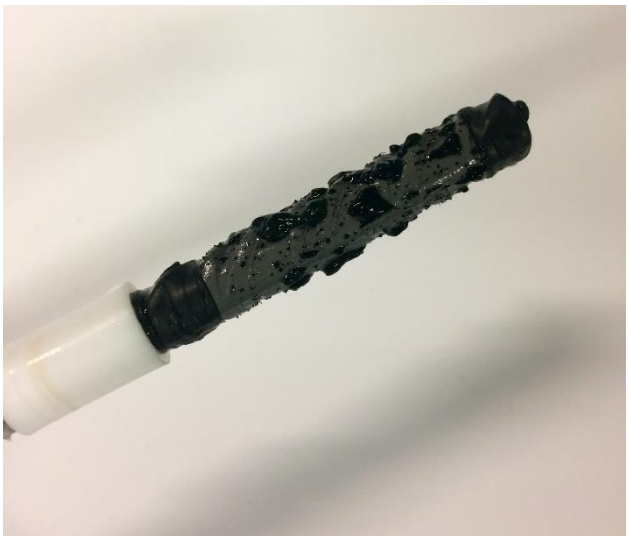

Fig. 4.3 *Visual inspection of pitting initiation.*

4.1.3 Nitrite inhibited solution

Calcium nitrite corrosion inhibitor was added to the alkaline solutions in two different concentrations: 0.1 mol/L and 0.3 mol/L. Its inhibition effect in chloride-induced corrosion is well established; therefore, polarization tests were performed for comparison purposes.

The concentrations of the chlorides additions were maintained (0 mol/L, 0.1 mol/L, 0.3 mol/L), as well as the immersion times (1 day, 3 days and 7 days).

- **Calcium Nitrite 0.1 mol/L -** The obtained characteristic polarization curves were collected in the three different plots (Figure 4.4) according to the immersion times and as a function of the added chlorides dosages.

The passive behaviour is visible in all the curves without chlorides and the evolution of oxygen still occurs at potentials around 0.6 V Ag/AgCl.

In presence of chlorides, the obtained pitting potentials become less noble with increasing salt dosage. The corrosion inhibition effect is highly evident comparing the pitting potentials with the corresponding ones of the reference solutions: with 0.1 mol/L of nitrite inhibitor, localized corrosion occurs at potentials ranging from 0.3 V to 0.5 V Ag/AgCl in presence of 0.1 mol/L chlorides concentration and around 0.1 V Ag/AgCl with 0.3 mol/L chlorides.

The potentials for the steel repassivation, in this case, seems to be dependent on the chloride content: for all the immersion times, a small decrease in the E_{rep} is visible in the condition of higher chlorides dosage.

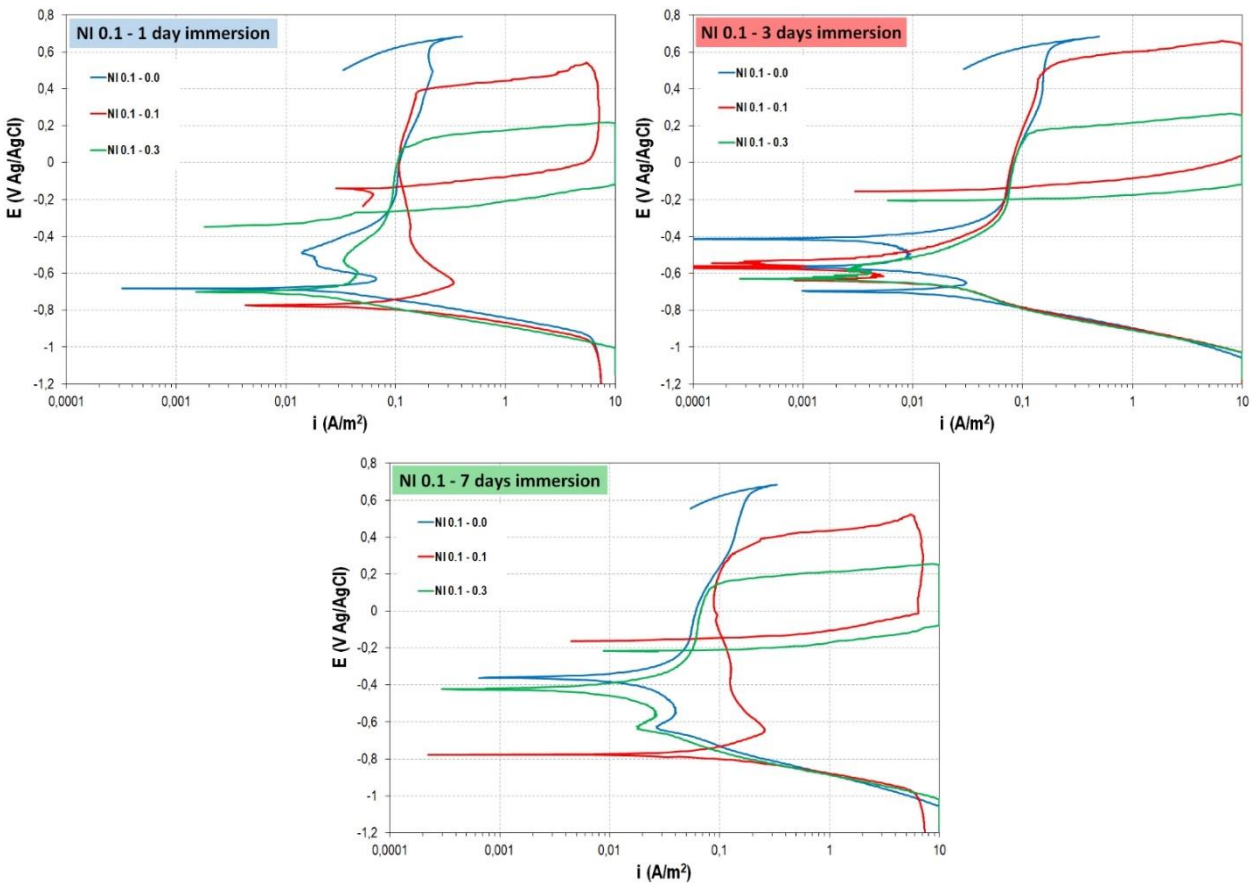

Fig. 4.4 *Potentiodynamic curves of solutions with 0.1 mol/L nitrite concentration.*

The obtained pitting and repassivation potentials are reported in the Table 4.2, considering the average of the three identical tests for each solution settlements.

Tab. 4.2 *Pitting and repassivation potentials of potentiodynamic tests with 0.1 mol/L nitrite.*

Solution code	NaCl (mol/L)	E_{pit} (V Ag/AgCl)	E_{rep} (V Ag/AgCl)
NI 0.1 – 1 d	0	0.63 (o.e.)	-
	0.1	0.4	– 0.13
	0.3	0.08	– 0.26
NI 0.1 – 3 d	0	0.62 (o.e.)	-
	0.1	0.42	– 0.13
	0.3	0.15	– 0.2
NI 0.1 – 7 d	0	0.64 (o.e.)	-
	0.1	0.38	– 0.16
	0.3	0.12	– 0.21

- **Calcium Nitrite 0.3 mol/L -** A higher concentration of nitrite inhibitor is used to verify the increasing inhibition effect. Cyclic polarization tests were performed in the same conditions (0 mol/L, 0.1 mol/L and 0.3 mol/L of chloride content) and the characteristic curves are shown in the Figure 4.5 divided in the three variable immersion times.

  The increased inhibition effect of calcium nitrate at 0.3 mol/L concentration with respect to the previous lower amount is highly visible in presence of low chlorides dosage: pitting potentials of very high nobility, around 0.6 V Ag/AgCl, were obtained at any immersion time. These potential values are quite below the evolution oxygen potential in absence of chloride, suggesting that nitrite inhibitor in this concentration allows to expand the steel passive region to nearly its maximum amplitude.

  For higher dosages of chlorides, the inhibition improvement is less visible: pitting potentials in presence of 0.3 mol/L of chlorides range from 0.1 V Ag/AgCl to 0.3 V Ag/AgCl.

  For what concerns the repassivation potentials, also in this case a small dependence on the chlorides concentration is discernible; however, no considerable variations of E_{rep} are present compared to the above 0.1 mol/L nitrite concentration.

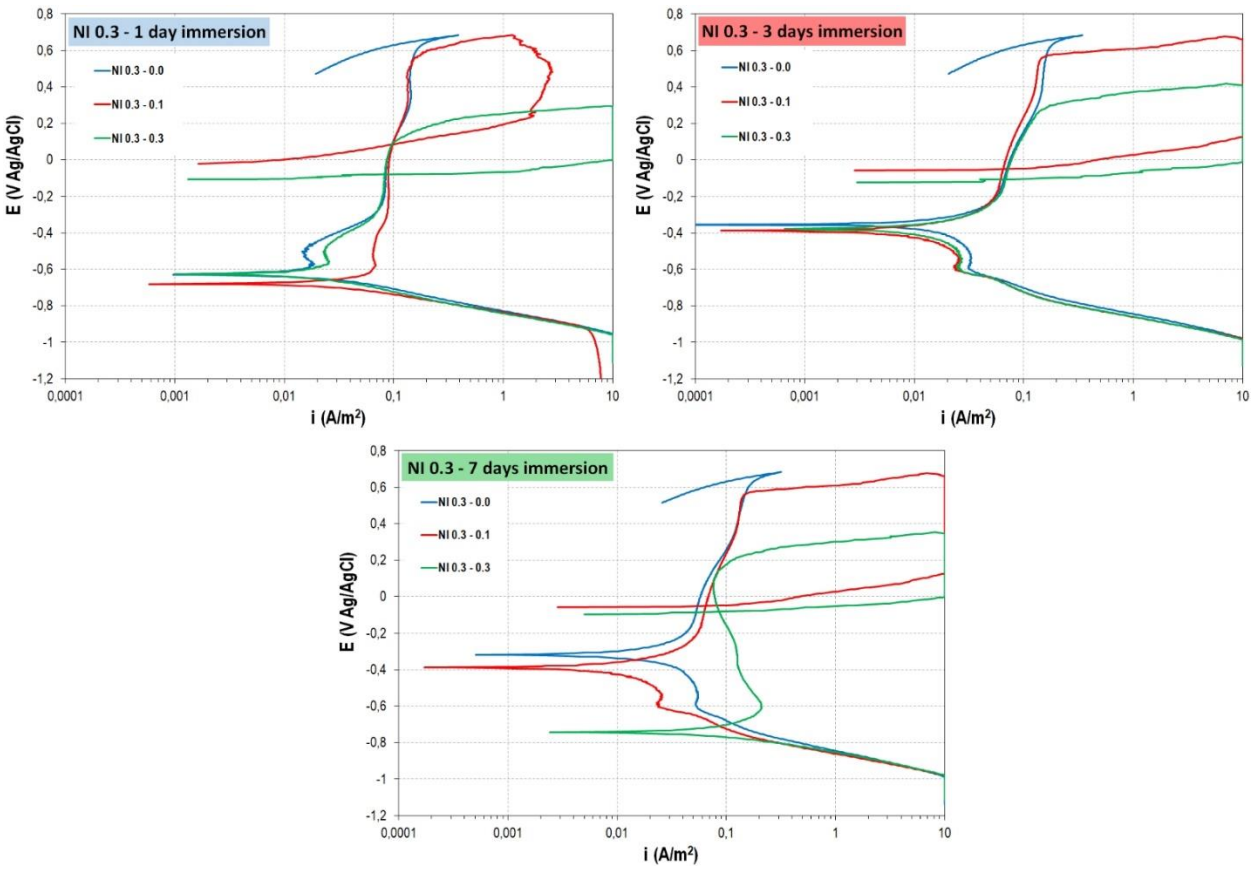

Fig. 4.5 *Potentiodynamic curves of solutions with 0.3 mol/L nitrite concentration.*

The average values of pitting and repassivation potentials are collected in Table 4.3.

Tab. 4.3 *Pitting and repassivation potentials of potentiodynamic tests with 0.3 mol/L nitrite.*

Solution code	**NaCl (mol/L)**	**E_{pit} (V Ag/AgCl)**	**E_{rep} (V Ag/AgCl)**
NI 0.3 – 1 d	0	0.63 (o.e.)	-
	0.1	0.58	0.9
	0.3	0.09	–0.1
NI 0.3 – 3 d	0	0.62 (o.e.)	-
	0.1	0.56	– 0.05
	0.3	0.29	– 0.13
NI 0.3 – 7 d	0	0.63 (o.e.)	-
	0.1	0.62	– 0.05
	0.3	0.16	– 0.09

4.1.4 Nitrate inhibited solution

Cyclic polarization tests were then performed on alkaline solutions with admixed calcium nitrate inhibitor, with two different concentrations of 0.1 mol/L and 0.3 mol/L. The measurement conditions were maintained identical to the corresponding ones with reference and nitrite inhibited solutions to ensure a good comparison.

- **Calcium Nitrate 0.1 mol/L -** The characteristic curves of the performed potentiodynamic tests were reported in Figure 4.6 divided in the three different immersion intervals.
  It is easy to anticipate that the nitrate inhibition effect in this concentration is very limited: characteristic pitting potentials are around –0.1 V Ag/AgCl in presence of chlorides concentration of 0.1 mol/L and –0.15 V Ag/AgCl with 0.3 mol/L chlorides. These results are quite analogous to the ones obtained with the reference tests and they suggest that 0.1 mol/L of calcium nitrate concentration is unable to inhibit steel chloride-induced corrosion.
  Repassivation potentials in presence of nitrate seem to be independent on the chlorides dosage, since almost constant E_{rep} values (around –0.5 V Ag/AgCl) were collected.

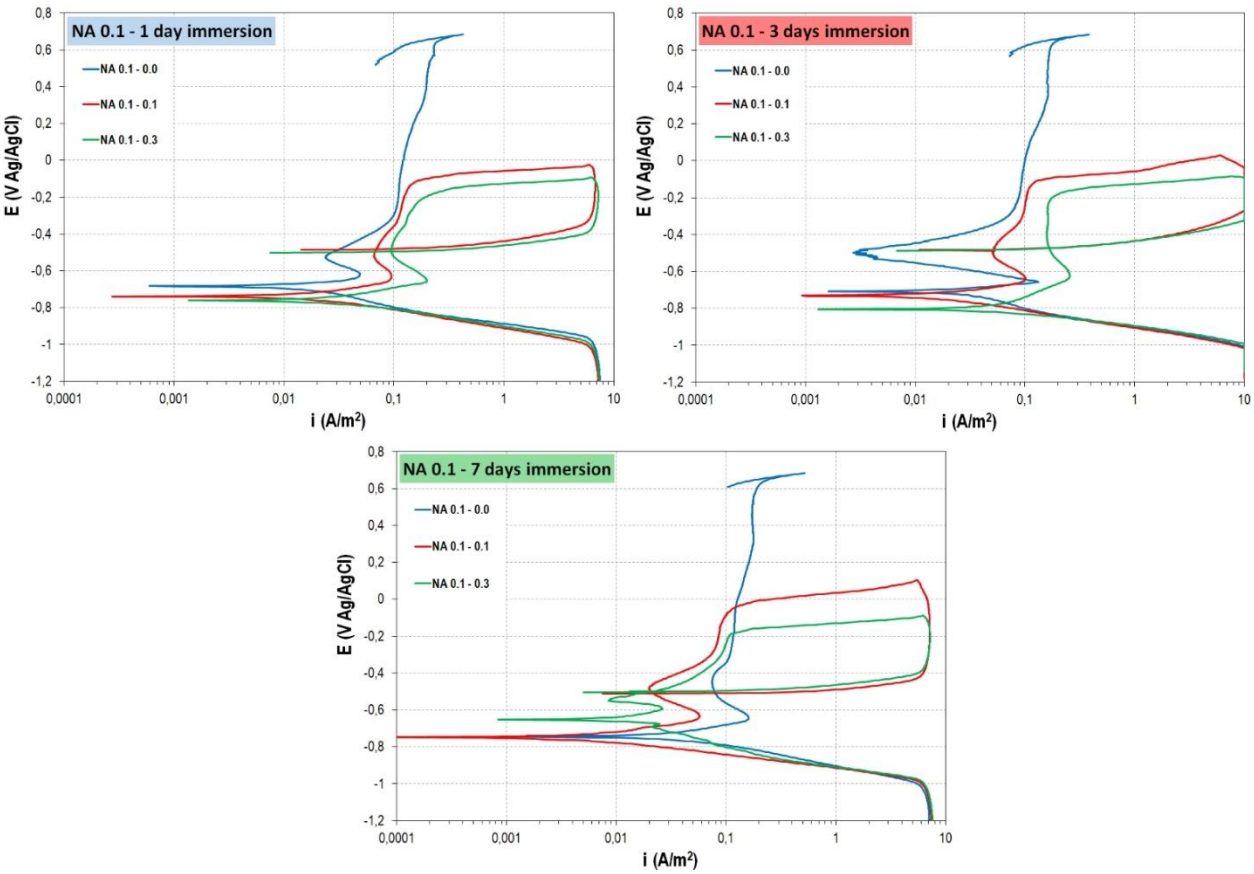

Fig. 4.6 *Potentiodynamic curves of solutions with 0.1 mol/L nitrate concentration.*

The average values of pitting and repassivation potentials derived from the characteristic polarization curves are listed in the Table 4.4.

Tab. 4.4 *Pitting and repassivation potentials of potentiodynamic tests with 0.1 mol/L nitrate.*

Solution code	NaCl (mol/L)	E_{pit} (V Ag/AgCl)	E_{rep} (V Ag/AgCl)
NA 0.1 – 1 d	0	0.64 (o.e.)	-
	0.1	– 0.13	– 0.5
	0.3	– 0.15	– 0.49
NA 0.1 – 3 d	0	0.63 (o.e.)	-
	0.1	– 0.12	– 0.49
	0.3	– 0.14	– 0.56
NA 0.1 – 7 d	0	0.62 (o.e.)	-
	0.1	– 0.09	– 0.5
	0.3	– 0.14	– 0.48

- **Calcium Nitrate 0.3 mol/L -** The investigation of a higher concentration of nitrate-basted inhibitor is presented in Figure 4.7, where the characteristic polarization curves of the alkaline solutions with 0.3 mol/L calcium nitrate dosage are reported.

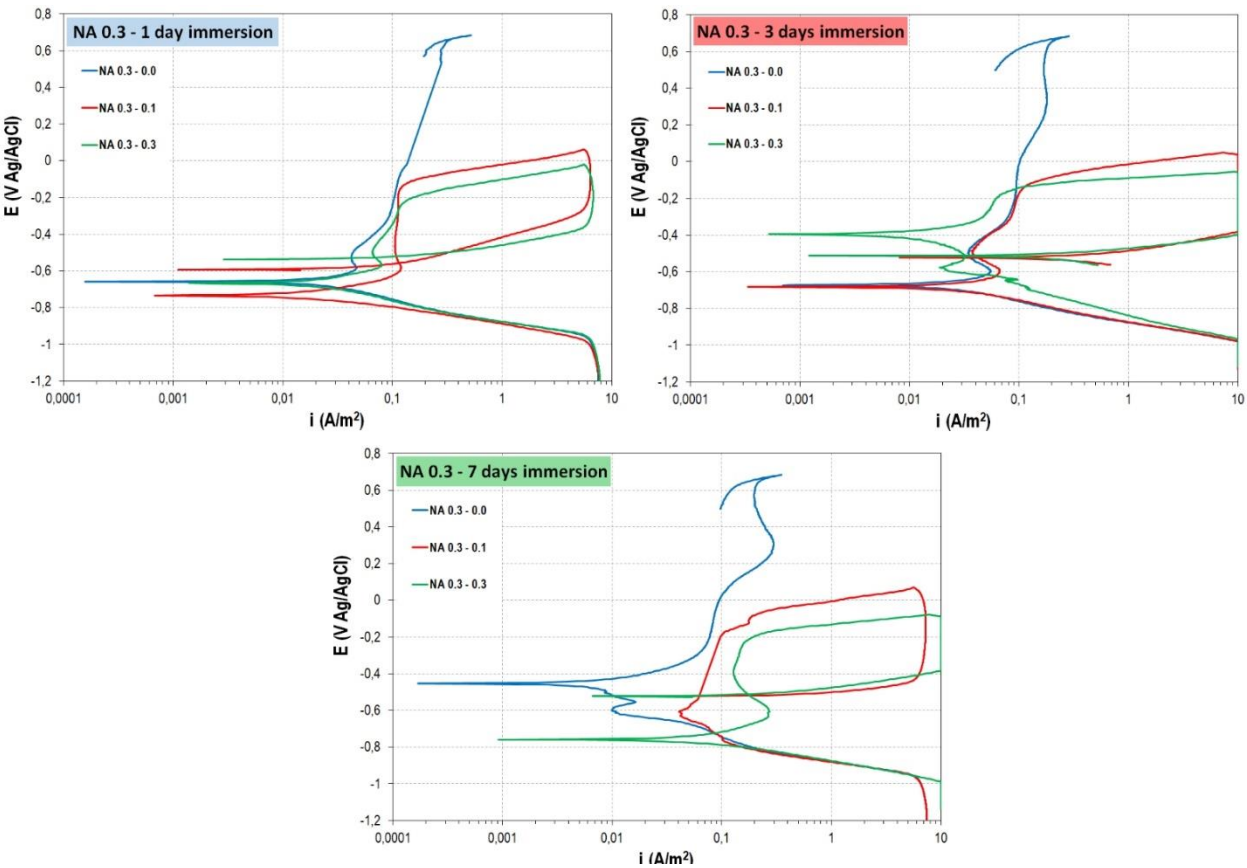

Fig. 4.7 *Potentiodynamic curves of solutions with 0.3 mol/L nitrate concentration.*

For all the immersion times, the inhibition effect is quite absent, even when an increased calcium nitrate concentration is adopted. The reported pitting potentials are quite identical to the corresponding ones referred to 0.1 mol/L calcium nitrate and reference tests: –0.1 V Ag/AgCl and –0.2 V Ag/AgCl with respectively 0.1 mol/L and 0.3 mol/L chlorides concentrations were collected. Also in this case, repassivation potentials are independent on the chlorides dosage adopted: constant E_{rep} values, around –0.5 V Ag/AgCl, were identified.

The average values of the pitting and repassivation potentials for each solution condition are reported in Table 4.5.

Tab. 4.5 *Pitting and repassivation potentials of potentiodynamic tests with 0.3 mol/L nitrate.*

Solution code	NaCl (mol/L)	E_{pit} (V Ag/AgCl)	E_{rep} (V Ag/AgCl)
NA 0.3 – 1 d	0	0.64 (o.e.)	-
	0.1	– 0.15	– 0.54
	0.3	– 0.19	– 0.51
NA 0.3 – 3 d	0	0.65 (o.e.)	-
	0.1	– 0.13	– 0.52
	0.3	– 0.16	– 0.52
NA 0.3 – 7 d	0	0.64 (o.e.)	-
	0.1	– 0.1	– 0.53
	0.3	– 0.21	– 0.5

The discussion about the comparison of inhibitors efficiencies and the effect of adopted concentrations and immersion times is accomplished in Chapter 5. Potentiodynamic polarization tests are short-time screening methods that allowed to obtain a first indication of nitrate eventual inhibition effectiveness; therefore, long-term measurements were required for more accurate results.

4.2 Potentiostatic tests in solution

Potentiostatic tests were used to obtain the passivation development rate and the critical chloride threshold at which localised corrosion of steel specimens takes place. The evaluation of nitrate inhibition effectiveness with this type of test is more accurate, since the steel samples are subjected to a more realistic situation of stationary polarization, similar to the real reinforcements condition in concrete.

The samples were immersed in different alkaline solutions simulating the concrete environment: nitrite and nitrate compounds were admixed to investigate their effect as corrosion inhibitor on the chloride threshold value. Four different synthetic pore solutions were produced; they are identified with the abbreviations:

- *REF* - reference solution without any inhibitor;
- *NI 0.1* - inhibited solution with calcium nitrite ($Ca(NO_2)_2$) in 0.1 mol/L concentration;
- *NA 0.1* - inhibited solution with calcium nitrate ($Ca(NO_3)_2$) in 0.1 mol/L concentration;
- *NI 0.05 – NA 0.05* - inhibited solution with combined calcium nitrite ($Ca(NO_2)_2$) in 0.05 mol/L concentration and calcium nitrate ($Ca(NO_3)_2$) in 0.05 mol/L concentration.

Inside each of these solutions, 13 carbon steel samples were immersed and polarized with a constant potential of 0 V Ag/AgCl, selected according to the usual free corrosion potential of reinforcements embedded in concrete. Periodic additions of chlorides were performed at constant intervals of 80-90 hours with increasing dosage (0.05 mol/L, 0.1 mol/L, 0.2 mol/L…) to assess the localized corrosion initiation.

4.2.1 Reference solution

The preparation of the reference alkaline solution and the carbon steel samples is described in Chapter 3. The prepolarization phase (+200 mV Ag/AgCl) was maintained for 2 days; then, the specimens were polarized at fixed potential (0 mV Ag/AgCl) for one week without chlorides.

During the early polarization phase, the current density of one sample was constantly recorded in function of time through the ohmic drop measurement made with a set of parallel shunts (1 Ω, 10 Ω, 100 Ω, 1000 Ω). This procedure is important to evaluate the development in time of the passive layer, correlating the obtained information with the corresponding ones proper of the inhibited solutions.

The collected current densities are reported in Figure 4.8 as a function of time: a double logarithmic scale was selected to illustrate the current density drop for long times. Since steel passive condition is achieved when the measured current density reaches values lower than 1 mA/m^2, this situation was achieved after 35 hours of static polarization at 0 V Ag/AgCl in alkaline solution without inhibitor.

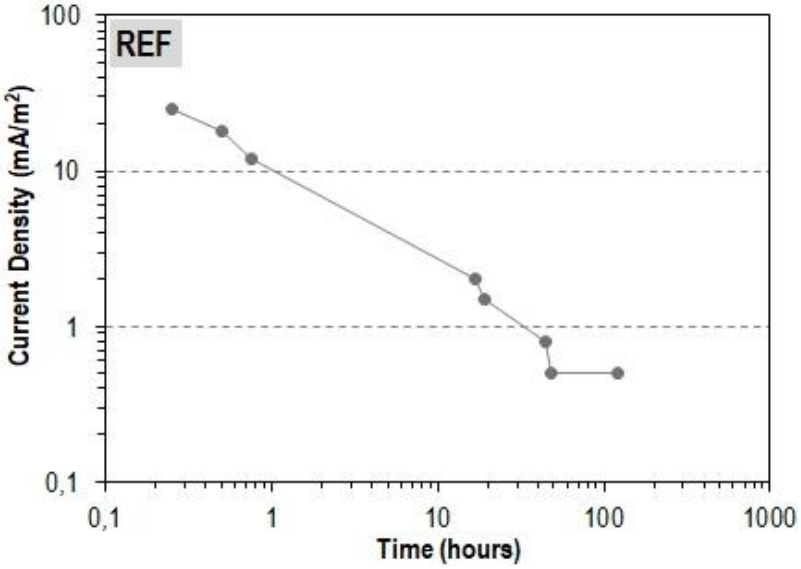

Fig. 4.8 *Current density drop of potentiostatic reference test.*

After a week, the periodic chlorides additions were performed every 80-90 hours until all the 13 samples developed localized corrosion initiation, as resumed in Table 4.6. The test lasted 19 days and the maximum chlorides concentration for pitting initiation of all the specimens was 0.3 mol/L.

Tab. 4.6 *Chlorides additions in potentiostatic reference solution.*

Date of the addition	11/10/17	19/10/17	23/10/17	26/10/17	30/10/17
Chlorides concentration (mol/L)	0	0.05	0.1	0.2	0.3

The current density of each carbon steel specimen was measured daily to verify if a localised corrosion phenomenon was taking place: recorded current density higher than 5 mA/m^2 indicates corrosion initiation. The visual inspection of the initiated steel sample verified the position of the attack, since other phenomena different than pitting corrosion could take place at the interface with the self-adhesive tape, for instance crevice corrosion. Corrosion attacks on the lateral metal surface indicate pitting events. Table 4.7 collects the corrosion times and positions for each of the 13 samples.

Tab. 4.7 *Initiation times of the potentiostatic reference solution.*

Sample number	Date	Chlorides (mol/L)	Attack position
1	21/10/17	0.05	Lateral
2	23/10/17	0.05	Lateral
3	23/10/17	0.1	Lateral
4	24/10/17	0.1	Lateral
5	24/10/17	0.1	Interface
6	25/10/17	0.1	Lateral
7	25/10/17	0.1	Lateral
8	25/10/17	0.1	Interface
9	27/10/17	0.2	Lateral
10	27/10/17	0.2	Lateral
11	28/10/17	0.2	Interface
12	29/10/17	0.2	Interface
13	30/10/17	0.3	Lateral

4.2.2 Nitrite solution

Potentiostatic test in alkaline simulating pore solution were performed with the addition of calcium nitrite inhibitor in 0.1 mol/L concentration; its well-established inhibition effectiveness was used to compare the corresponding results regarding calcium nitrate inhibitor.

The test procedure was equivalent to the potentiostatic measurement in the reference solution. The current density decreasing trend was recorded during the early polarization phase to assess the complete passivation of the steel samples; the current trend as a function of time is reported in Figure 4.9. The steel passive condition (current density lower than 1 mA/m^2), in this situation, was reached after about 40 hours from the polarization beginning.

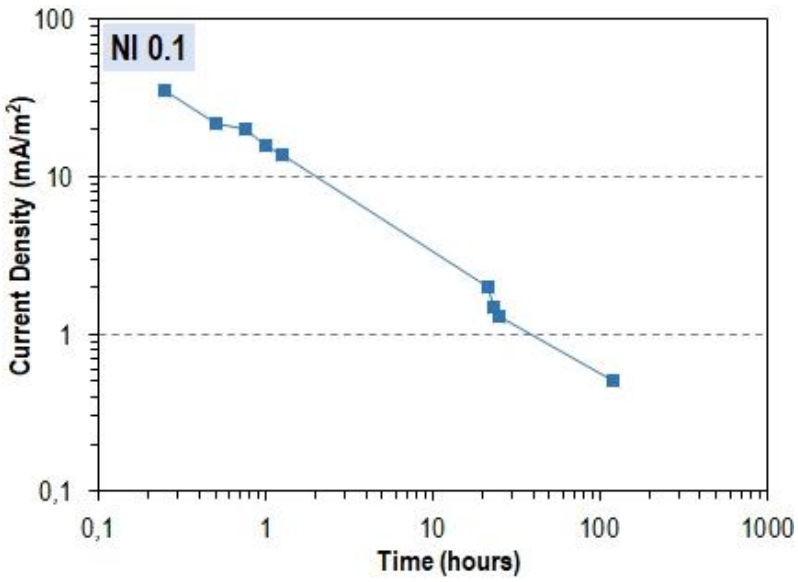

Fig. 4.9 *Current density drop of potentiostatic nitrite test.*

After a week, the periodic chlorides additions were performed every 80-90 hours until localized corrosion initiation of all the 13 samples developed, as resumed in Table 4.8. The good inhibition effect of calcium nitrate can be verified considering the delay on the pitting initiation of all the specimens: in this condition, the maximum chlorides concentration was 0.8 mol/L and the duration of the tests was 36 days.

Tab. 4.8 *Chlorides additions in potentiostatic nitrite solution.*

Date of the addition	18/10	26/10	30/10	2/11	6/11	9/11	13/11	16/11	20/11	23/11
Chlorides concentration (mol/L)	0	0.05	0.1	0.2	0.3	0.4	0.5	0.6	0.7	0.8

The initiation times (Tab. 4.9) are collected through the daily measurement of the current densities for each sample. Recorded current densities higher than 5 mA/m^2 indicate pitting initiation; the visual inspection of the corroding specimen allowed to distinguish crevice corrosion from the typical chloride-induced attack on the metal lateral surface.

Tab. 4.9 *Initiation times of the potentiostatic nitrite solution.*

Sample number	Date	Chlorides (mol/L)	Attack position
1	6/11/17	0.3	Lateral
2	10/11/17	0.4	Lateral
3	14/11/17	0.5	Lateral
4	16/11/17	0.5	Interface
5	18/11/17	0.6	Lateral
6	19/11/17	0.6	Lateral
7	20/11/17	0.7	Lateral
8	20/11/17	0.7	Lateral
9	20/11/17	0.7	Lateral
10	22/10/17	0.7	Lateral
11	22/10/17	0.7	Lateral
12	26/11/17	0.8	Lateral
13	26/11/17	0.8	Lateral

4.2.3 Nitrate solution

The effectiveness of calcium nitrate as corrosion inhibitor for chloride-induced corrosion was investigated through the potentiostatic tests after the rapid measure of potentiodynamic polarization.

The test procedure was identical of the other previous ones; however, during the early polarization step at 0 V Ag/AgCl, the recorded current density of the specimen showed an initial gradual decreasing, as expected, followed by an increase to higher values, as reported in Figure 4.10. This rising in the current density continued during time and it came to the instauration of localized corrosion on all the 13 specimens in the early 3 days, when the chlorides were still absent. The test was thus invalidated.

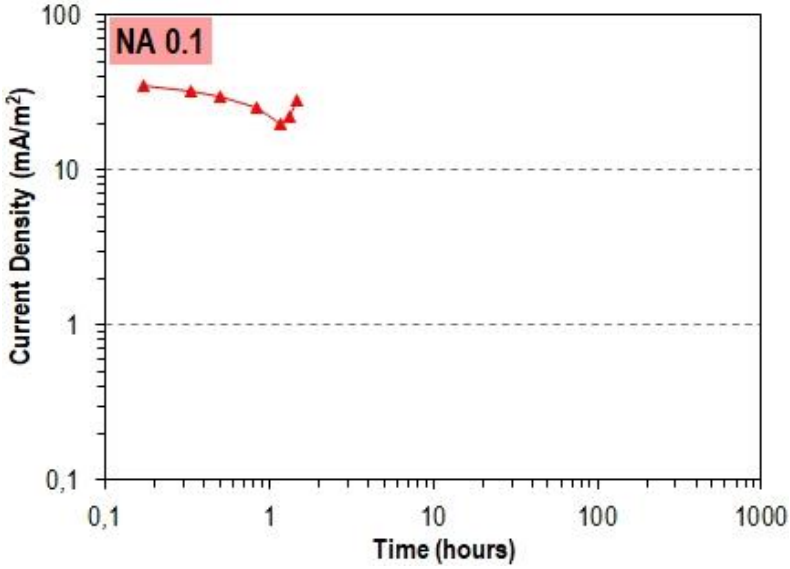

Fig. 4.10 *Current density drop of potentiostatic nitrate test.*

To overcome this problem and obtain the information about initiation times and nitrate effect on corrosion inhibition, an alternative procedure for the first stage of polarization without chlorides was investigated. For the first week of passivation at 0 V Ag/AgCl potential, the solution was used without inhibitor, to assure the formation of the passive layer without any corrosion initiations; calcium nitrate was then added to the solution and the first chlorides addition was performed after 80-90 hours. The subsequent salt additions were accomplished as usual: all the solution modifications from the beginning of the polarization are reported in Table 4.10. With this method, the information about possible effect on the current density drop during the early passivation phase were lost, since the inhibitor were added only after the complete steel passivation.

Tab. 4.10 *Inhibitor and chlorides additions in potentiostatic nitrate solution.*

Date of the addition	13/2/18	19/2/18	22/2/18	26/2/18
Nitrate concentration (mol/L)	0	0.1	0.1	0.1
Chlorides concentration (mol/L)	0	0	0.05	0.1

During the test, the current densities for all the 13 specimens was recorded daily and the initiation times were collected in Table 4.11, when the measured corrosion currents were higher than 5 mA/m^2.

Tab. 4.11 *Initiation times of the potentiostatic nitrate solution.*

Sample number	Date	Chlorides (mol/L)	Attack position
1	24/2/18	0.05	Interface
2	24/2/18	0.05	Interface
3	24/2/18	0.05	Interface
4	24/2/18	0.05	Interface
5	24/2/18	0.05	Interface
6	25/2/18	0.05	Interface
7	26/2/18	0.05	Interface
8	26/2/18	0.05	Interface
9	26/2/18	0.05	Interface
10	26/2/18	0.05	Interface
11	26/2/18	0.05	Lateral
12	26/2/18	0.1	Interface
13	26/2/18	0.1	Lateral

Several crevice corrosion phenomena initiated at the metal interface with the self-adhesive tape, they were not considered in the next statistical analysis; only two of the 13 samples showed lateral attack, typical of pitting. In addition, the samples corrosion took place at the early days of chlorides contamination in the lowest concentration; the test lasted thus just 13 days. The possible explanations for this effect are given in Chapter 5.

4.2.4 Mixed nitrite-nitrate solution

The inhibition effect of combined calcium nitrite and nitrate was investigated with the fourth potentiostatic test, in which an eventual synergistic behaviour was researched. The dosage of the two compounds was maintained in 1:1 molar ratio at a concentration of 0.05 mol/L.

To prevent the previous problems of premature corrosion instauration when nitrate was present in solution, the mix of inhibitors was added only after the complete passivation at 0 V Ag/AgCl potential of all the steel samples. Calcium nitrite and nitrate were added in 0.05 mol/L concentration after a week from the polarization beginning; subsequently, after 80-90 hours, the chlorides additions were performed with the usual periodicity, as illustrated in Table 4.12.

Tab. 4.12 *Inhibitors and chlorides additions in potentiostatic mixed nitrite-nitrate solution.*

Date of the addition	15/2/18	22/2/18	26/2/18	2/3/18	5/3/18	8/3/18
Nitrite-nitrate concentration (mol/L)	0	0.05-0.05	0.05-0.05	0.05-0.05	0.05-0.05	0.05-0.05
Chlorides concentration (mol/L)	0	0	0.05	0.1	0.2	0.3

Also in this case, the measurement of the current density drop during the steel passivation was impossible, since the inhibitors were admixed only after this phase; the information about possible effects on the passive layer formation in presence of these inhibitors were lost. The initiation times (Tab. 4.13) are collected, as usual, through the daily measure of the current densities for each sample.

Tab. 4.13 *Initiation times of the potentiostatic mixed nitrite-nitrate solution.*

Sample number	**Date**	**Chlorides (mol/L)**	**Attack position**
1	5/3/18	0.1	Lateral
2	5/3/18	0.2	Lateral
3	6/3/18	0.2	Lateral
4	6/3/18	0.2	Interface
5	6/3/18	0.2	Lateral
6	6/3/18	0.2	Interface
7	7/3/18	0.2	Lateral
8	7/3/18	0.2	Interface
9	8/3/18	0.2	Lateral
10	8/3/18	0.2	Lateral
11	8/3/18	0.2	Interface
12	8/3/18	0.2	Lateral
13	9/3/18	0.3	Lateral

For this type of solution, premature crevice corrosion phenomena were less frequent than the NA 0.1 test. This suggests that the presence of calcium nitrite limits the instauration of corrosion events localized on the interface with the self-adhesive tape and assists calcium nitrate in the corrosion inhibition. The test lasted 22 days: a small reduction of the steel susceptibility to chloride-rich environment was thus observed.

4.3 Carbonation monitoring on concrete samples

The effect of calcium nitrate on the diffusion of carbonation inside concrete was investigated on prismatic plain concrete samples. Carbonation process is directly related to the carbon dioxide (CO_2) diffusion inside concrete and its reaction with alkaline compounds: this phenomenon is very slow and, for this reason, accelerated tests were performed in addition to carbonation monitoring on concrete specimens exposed to external atmosphere.

Three different series of concrete specimens were fabricated according to the adopted cement type:

- Serie I – CEM I 52.5 R: ordinary Portland cement;
- Serie II – CEM II/B-S 52.5 N: Portland-composite cement;
- Serie III – CEM II/B-M 42.5: Portland-composite cement.

For each of these cements, four concrete types were cast with different concentrations of admixed inhibitors: calcium nitrite in 2% by weight of cement and calcium nitrate in 2% and 4% by weight of cement. The identification codes to distinguish the type of cement indicates the series number (I, II, III), followed by the below abbreviations:

- *REF*: reference sample without any inhibitor admixed;
- *NI – 2*: addition of calcium nitrite ($Ca(NO_2)_2$) at 2% by weight of cement;
- *NA – 2*: addition of calcium nitrate ($Ca(NO_3)_2$) at 2% by weight of cement;
- *NA – 4*: addition of calcium nitrate ($Ca(NO_3)_2$) at 4% by weight of cement.

The concrete specimens were cast in June 2016 in all the 12 different compositions: part of them were used for accelerated carbonation monitoring and the remaining ones were exposed to the external atmosphere of Milan, both in shielded from rain and exposed placement.

4.3.1 Accelerated carbonation monitoring

The plain concrete samples in the 12 different compositions were placed into the carbonation chamber with controlled atmosphere (room temperature and 65% RH) and at 4% of carbon dioxide concentration. The first carbonation depth measurement was performed in the previous thesis work on all the three series after about one month form the ingress into the carbonation chamber: the samples were subjected to phenolphthalein tests as illustrated in Paragraph 3.3.3. Afterwards,

every two months, the specimens were withdrawn from the chamber for the subsequent measurements. The front of the carbonation reaction was visible through the change in the concrete surface colour indicating the still unreacted core. The carbonation depth was considered as the average of the distances between the sample border and the limit of the reacted phenolphthalein, for each of the four sides of the prism, as illustrated in Figure 4.11. Once the carbonation depth has reached the core of the prism (30 mm of depth), the sample was considered completely carbonated and the tests stopped.

Fig. 4.11 *Example of carbonation depth measurement.*

The carbonation depths averages measured from March 2017 are reported in Table 4.14.

Tab. 4.14 *Carbonation depths (mm) measurements for accelerated tests.*

Days after the ingress into the chamber	127	142	229
I – 00	20	21.8	28.5
I – NI – 2	19	21.1	30
I – NA – 2	16.5	18.3	30
I – NA – 4	15	16.8	26.6
II – 00	25	30	
II – NI – 2	27	30	
II – NA – 2	26	28.3	
II – NA – 4	22.5	24.6	
III – 00	30		
III – NI – 2	30		
III – NA – 2	30		
III – NA – 4	30		

It is visible that with different series the penetration of the carbonation process was highly variable, since different cements have different permeabilities. Serie III reached complete carbonation (depth of 30 mm) just after 127 days; Serie I, on the contrary, showed the lowest CO_2 permeability, completing the carbonation process after 229 days. Serie II showed medium results, with a residence time into the carbonation chamber of 142 days.

4.3.2 Real carbonation monitoring

The monitoring of the realistic CO_2 penetration and reaction within concrete were performed on 24 plain concrete specimens exposed to the external atmosphere of Milan, they were placed on the rooftop of "Dipartimento di Chimica, Materiali e Ingegneria Chimica "Giulio Natta", Politecnico di Milano", half exposed to rain and half sheltered.

Since the carbonation diffusion in aerated conditions has a slower kinetic, the first carbonation depth measure on the samples was performed after more than one year from the atmospheric exposure beginning. The procedure for the monitoring of the carbonation front with the phenolphthalein test was equivalent to the previous one. Considering that the specimens were placed to atmosphere in September 2016, only one test for the carbonation depth was performed to date. In Table 4.15, the measured carbonation penetrations (in mm) performed on the 31st of January 2018, after 498 days, are reported. The presented data are divided according to the exposition state of the samples.

Tab. 4.15 *Carbonation depths (mm) measurements for real monitoring tests.*

Carbonation depths after 498 days (mm)	Exposed to rain	Sheltered
I – 00	2.7	3.5
I – NI – 2	2.7	4.7
I – NA – 2	2.5	4.7
I – NA – 4	2.2	4.5
II – 00	3.7	7.2
II – NI – 2	3.2	7.5
II – NA – 2	3.2	7.2
II – NA – 4	4.2	5.5
III – 00	5.5	8.5

III – NI – 2	3.2	8
III – NA – 2	3.7	8.2
III – NA – 4	3	8

It is visible that the Serie I is the less permeable to carbon monoxide diffusion; on the contrary, the penetration depths of Serie III are the highest. Although these measures are the firsts one, the results seem to be in line with the corresponding carbonation depths of the accelerated tests.

The differences between carbonation depths into concrete samples exposed to rain and sheltered are appreciable: since the repair from rain induces a more controlled atmosphere, preventing the condition of relative humidity 100%, the penetration of carbon monoxide was more favoured. Recalling Figure 1.12 (Par 1.4.1), the interval of relative humidity most critical for carbonation diffusion inside concrete is from 60% to 70%. The investigation on the effect of inhibitors and their concentration on the carbonation process diffusion, both in accelerated and in real tests, is performed in Chapter 5.

4.4 Rebars corrosion monitoring

The effectiveness of calcium nitrate as corrosion inhibitor was investigated also on its eventual inhibition effect on the corrosion rate of the steel reinforcements embedded in concrete after the complete carbonation of the cover. The analysis was performed through the monitoring of the free corrosion potentials and polarization resistances of the metallic bars inside 24 cylindric concrete samples fabricated with the 12 different concrete compositions as usual.

The carbonation of the concrete covers was performed inside the carbonation chamber (4% CO_2 concentration) together with the plain prisms; through the latter's monitoring of CO_2 penetration depths, it was possible to assess the complete cover carbonation of the corresponding reinforced cylinders. Afterward, the samples were placed at the external atmosphere of Milan, part exposed to rain and part sheltered. The free corrosion potentials and polarization resistances of the steel reinforcements were measured with a variable periodicity of about 10 days, for the first two months of atmospheric exposure, and then less frequently.

4.4.1 Free corrosion potential

The monitoring of the reinforcements free corrosion potentials is important for the evaluation of the steel rebars condition inside carbonated concrete: since the protection of the high alkalinity is lost with the carbonation, the embedded metal passes from passive to active corrosion condition, with a consequent increase in the free corrosion potential. It was possible to recognize a steel low corrosion probability with measured free corrosion potentials higher than –200 mV CSE; on the contrary, with potentials lower than –350 mV CSE, high probability of reinforcements corrosion could be assessed.

The trends of the measured potentials are reported in Figure 4.12, where three different graphs show the collected values for the three series.

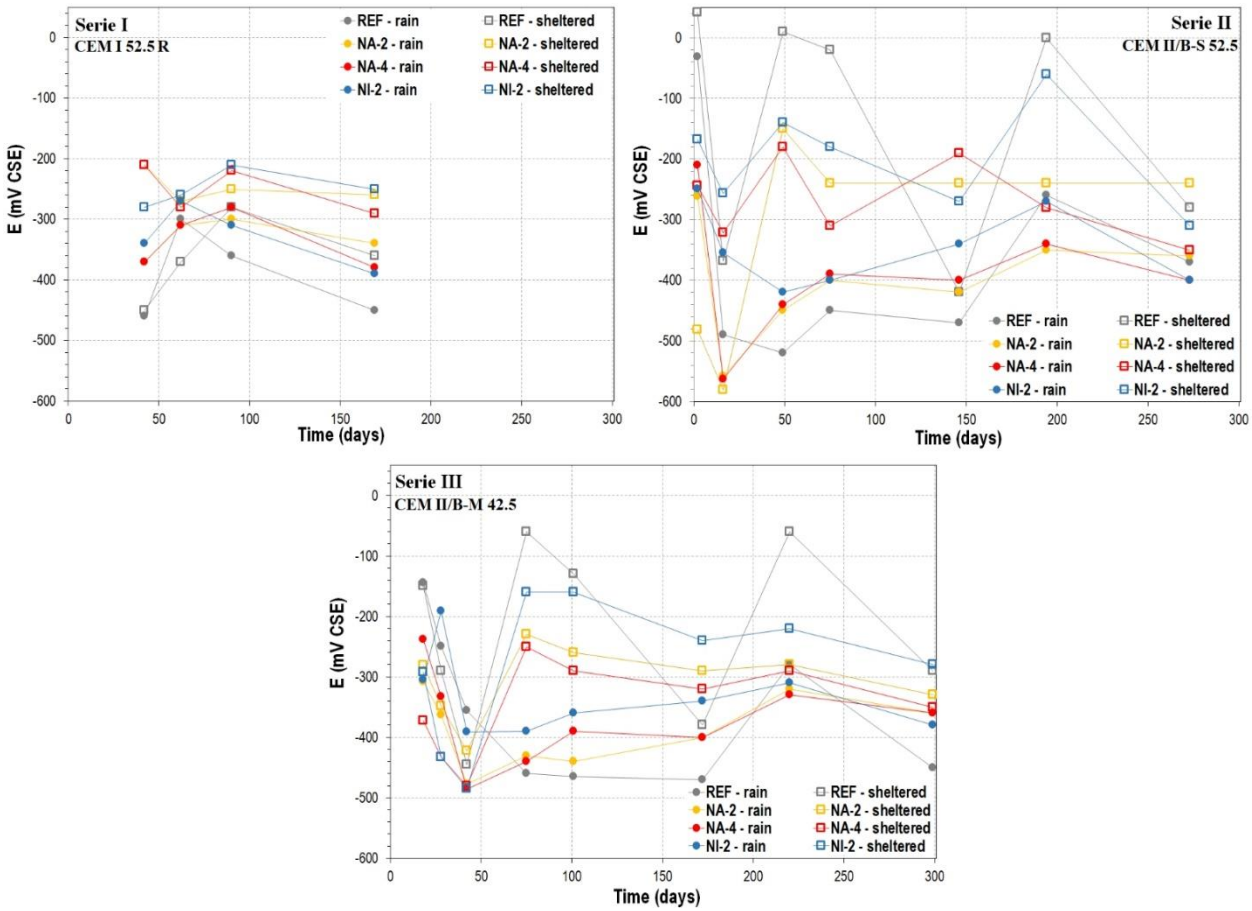

Fig. 4.12 *Free corrosion potentials of the reinforced concrete samples.*

The four different concrete compositions are divided considering the exposure state: it is visible that for all the series, the sheltered concretes showed higher free corrosion potentials values with respect to the ones exposed to rain. These results were expected, since it is accepted that the

corrosion rate of reinforcements in carbonated concrete reaches maximum values in environments with relative humidity around 90%. The samples exposed to rain, being subjected to higher relative humidity, are thus affected by more relevant reinforcements corrosion.

In addition, a general trend of the free corrosion potentials decreasing with time is noticeable and it indicates a comprehensive activation and aggravation of the progressive steel rebars corrosion. Free corrosion potential measurements give thus an indication on the corrosion aggressiveness condition and an evaluation of the oxygen content and different ohmic drop for each sample.

4.4.2 Linear polarization resistance

The monitoring of the corrosion rates of the steel reinforcements embedded in the concrete samples was performed through the linear polarization resistance tests (LPR). The measurement was described in Paragraph 3.3.4 and the obtained polarization resistances (R_p) could be related to the mean corrosion rates (mA/m^2) through the Stern-Geary relation:

$$i_{corr} = \frac{B}{R_p} \tag{22}$$

where B is a constant assumed equal to 26 mV, considering that the steels were constantly in active condition.

The measured polarization resistances are reported as a function of time in Figure 4.13, where three graphs were created for the three series. A decreasing trend along time is visible for all the measured resistances, indicating an increasing in the comprehensive corrosion rates, since i_{corr} has an inverse proportionality with R_p. Differences in the results between sheltered and exposed specimens were found: in the first case, all the steel polarization resistances were higher than the corresponding uncovered ones. This trend is again in agreement with the general consideration that environments with high relative humidity induce huge corrosion rates.

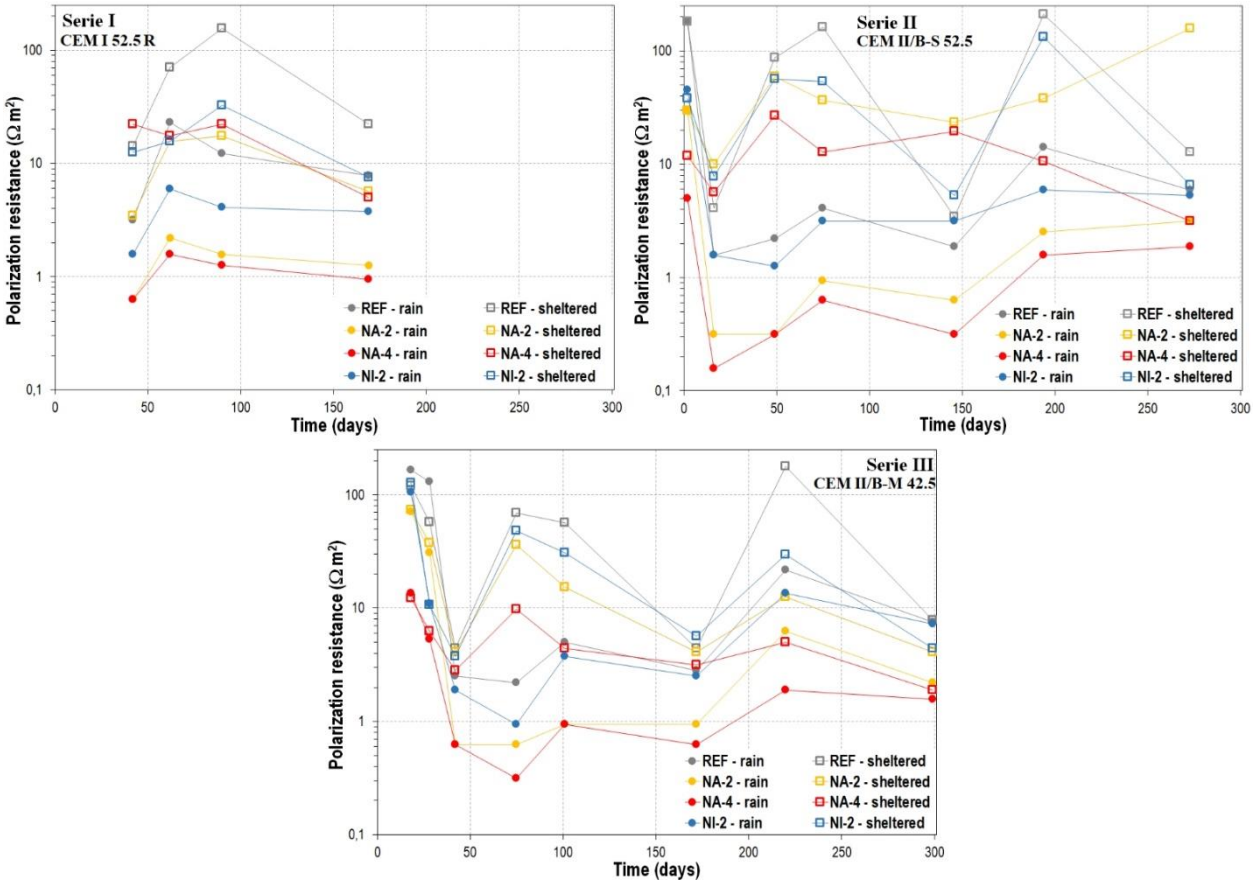

Fig. 4.13 *Polarization resistances of the reinforced concrete samples.*

The effects of the inhibitors and their concentrations on the free corrosion potentials and on the corrosion rates of carbonated concrete specimens are evaluated in Chapter 5.

Chapter 5. Discussion

The effectiveness of calcium nitrate is herein critically discussed through the analysis and the interpretation of the obtained experimental results regarding chloride and carbonation-induced corrosion.

The effect of the inhibitor admixture in concrete is analysed considering three main aspects:

- The effect on the steel reinforcements passivation
- The effect on the steel passivity interval
- The effect on the chloride-induced corrosion
- The effect on the carbonation-induced corrosion

5.1 Effect on the steel passivation

The effect of calcium nitrate as corrosion inhibitor was investigated through tests in simulating concrete pore solutions, reproducing the alkaline concrete environment: potentiodynamic and potentiostatic polarization measurements were performed. Accordingly, it was possible to monitor the development of the passive layer on the steel surface once the metallic samples were immersed into the inhibited solution.

Concerning potentiodynamic polarization tests, the measurement of the free corrosion potentials of the rebar samples allowed to evaluate the trend of steel passivation during the immersion time in the different alkaline solutions. Free corrosion potentials approaching to –0.2 V Ag/AgCl indicate a good steel passivation. Therefore, the reinforcement specimen was subjected to daily free corrosion potential measurement with respect to the saturated silver/silver chloride electrode (Ag/AgCl). The recorded potentials as function of time are reported in Figure 5.1, where different trends indicate the different solutions adopted: without inhibitors (REF), with calcium nitrite (NI) in its two concentrations (0.1 mol/L and 0.3 mol/L) and with calcium nitrate (NA) in the same two concentrations.

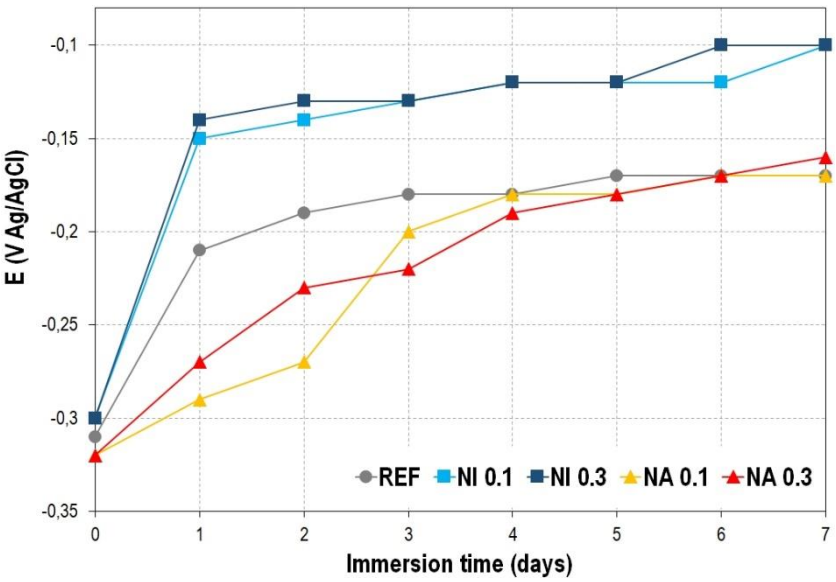

Fig. 5.1 *Free corrosion potentials trend as function of time before potentiodynamic tests.*

The increasing of all the recorded potentials indicates the development of the steel passive layer: after seven days of immersion inside the alkaline solutions, in all the five different compositions, the rebar samples can be considered in passive condition. In the early passivation phases, some differences among the inhibitors were found; in particular, delayed development of the passive layer is recorded for nitrate inhibited solutions, in both the concentrations, with respect to the reference and the nitrite inhibited solutions.

A good protection of the steel specimens is formed after just one day of immersion for the tests with NI in both the concentrations, indicating an induced fast development of the passive layer. Calcium nitrite good action as passivating anodic inhibitor was thus demonstrated: after seven days of immersion, the achieved free corrosion potentials were higher with respect to the other three solutions. However, in presence of calcium nitrate, the passivation of the steel was appreciable after higher immersion times, from three to four days. These results agree with the information present in literature: a delay in nitrate inhibition mechanism evolution, that was commonly observed in [6], [55] and [56], could be related to this slow steel passivity development induced by NA presence.

Similar conclusions in presence of nitrate was encountered also in potentiostatic tests. Here, the development of the steel passive layer could be monitored through the current density drop of the steel samples during the early phase of polarization. As reported in Chapter 4 (Par. 4.2.3), problems of premature localized corrosions were found using calcium nitrate admixture; however, few information on the steel passivity development in the first hour of polarization (before the

corrosion instaurations) allowed to make a comparison with the results in the reference and nitrite inhibited tests. The recorded current densities in the three test conditions are collected in Figure 5.2.

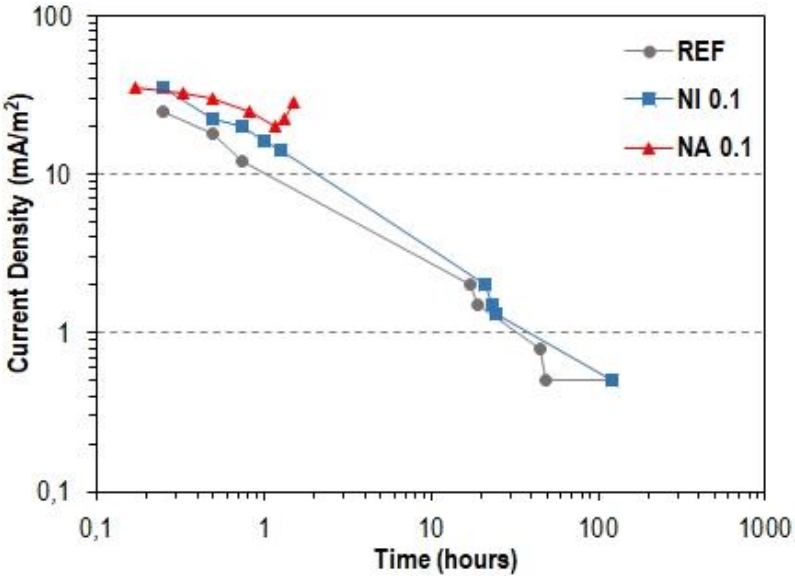

Fig. 5.2 *Current densities in the potentiostatic tests.*

The limited results of the nitrate solution allowed, nonetheless, to identify a slower initial passivity evolution with respect to REF and NI tests: they showed lower current densities than NA of respectively 10 mA/m^2 and 5 mA/m^2 after one hour of polarization at 0 V Ag/AgCl.

5.2 Effect on the passivity range

Eventual modifications of the passivity region were investigated in the characteristic plots of nitrate potentiodynamic polarization tests, after the evidence of a delayed effect on the steel passivation during the immersion time into the alkaline solution. In particular, the analysis focused on the potentiodynamic tests without any chlorides addition, where the passive interval has its maximum extent until reaching the potential of oxygen evolution.

For all the immersion times inside the alkaline nitrate-inhibited solutions (in both concentrations), the steel samples showed the characteristic trend of the passive behaviour, with a wide passive region at low current density values, as shown in Figure 5.3. For both the nitrate concentrations, the three curves are quite overlapping and do not show any effect on the oxygen evolution potential with different immersion times. This suggests that the slow steel passivation in presence of calcium

nitrate does not affect the passive behaviour of the metal, maintaining constant the passive interval extent that is thus dependent only on the solution pH.

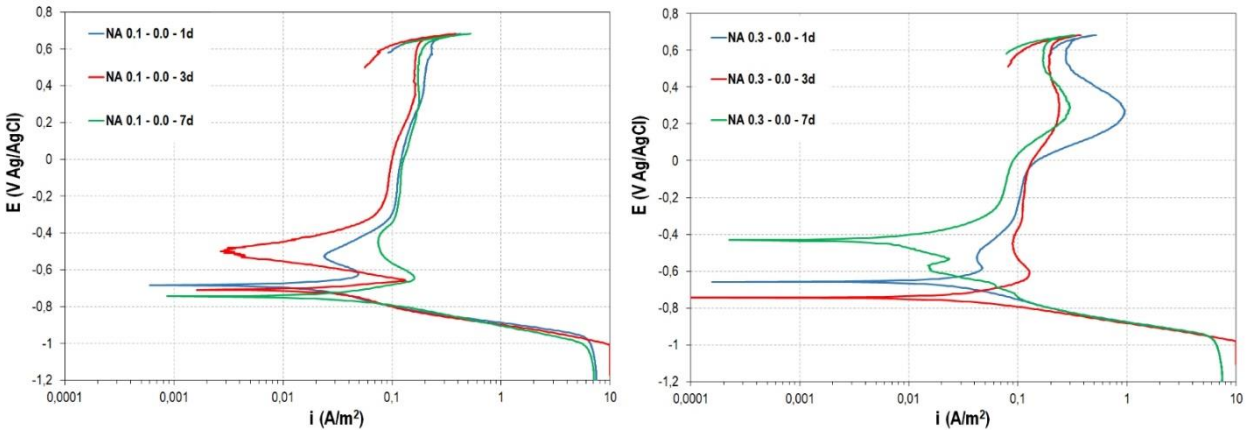

Fig. 5.3 *Potentiodynamic curves of nitrate chlorides-free solutions with different immersion times.*

A comparison with the extent of passive region in the reference and nitrite-inhibited potentiodynamic tests could be performed considering the oxygen evolution in all the solutions compositions, since the corresponding potential represents the upper limit of the passivity interval. Figure 5.4 shows the values of oxygen evolution potentials in all the potentiodynamic tests conditions: for each composition, three potential values are indicated considering the three different immersion times.

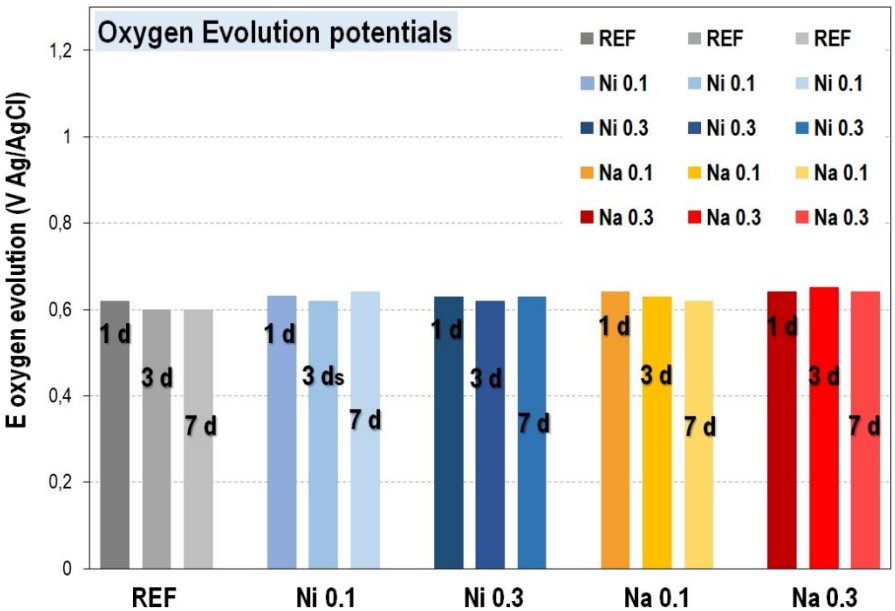

Fig. 5.4 *Oxygen evolution potentials of potentiodynamic tests.*

It is visible that the obtained oxygen evolution potentials are indistinctly around 0.6 V Ag/AgCl in all the tested solutions. No differences in the passivity intervals were thus recorded in the nitrate-inhibited solutions with respect to REF and NI solutions: the delay in the steel passivity evolution does not affect the passive region in the potentiodynamic characteristic curves.

5.3 Effectiveness on chloride-induced corrosion

Since chloride-induced corrosion is the most severe reason of reinforcements deterioration, the effectiveness of calcium nitrate as corrosion inhibitor was firstly assessed for this type of attack. Two different tests were performed to investigate the nitrate effect on the steel rebars in chloride-contaminated situations. The concrete environment was simulated through different alkaline solutions; the reinforcements samples were immersed in these solutions and they were subjected to polarization tests of cyclic potentiodynamic and potentiostatic type.

Characteristic electrochemical parameters of pitting potential (E_{pit}), repassivation potential (E_{rep}) and anodic passive current density were obtained with the first measure; indeed, the critical chloride threshold was determined with potentiostatic tests. In this way, it was possible to assess the eventual corrosion inhibition effect of calcium nitrate on the steel concrete reinforcements, indicating the inhibitor appropriate concentration as a function of the chloride contamination extent.

5.3.1 Pitting potential

Cyclic potentiodynamic tests were performed to gain an initial investigation on the effectiveness of calcium nitrate compared to tests without any inhibitor and in presence of calcium nitrite. For each condition, the analysis allowed to obtain the characteristic electrochemical parameter of pitting potential as the onset of chloride-induced localized corrosion.

The comparison of the obtained pitting potentials in the potentiodynamic polarisations of nitrate (NA), nitrite (NI) and reference solutions (REF) were reported in Figure 5.5 as a function of the admixed chlorides concentrations; they are divided in three different plots according to the adopted immersion times.

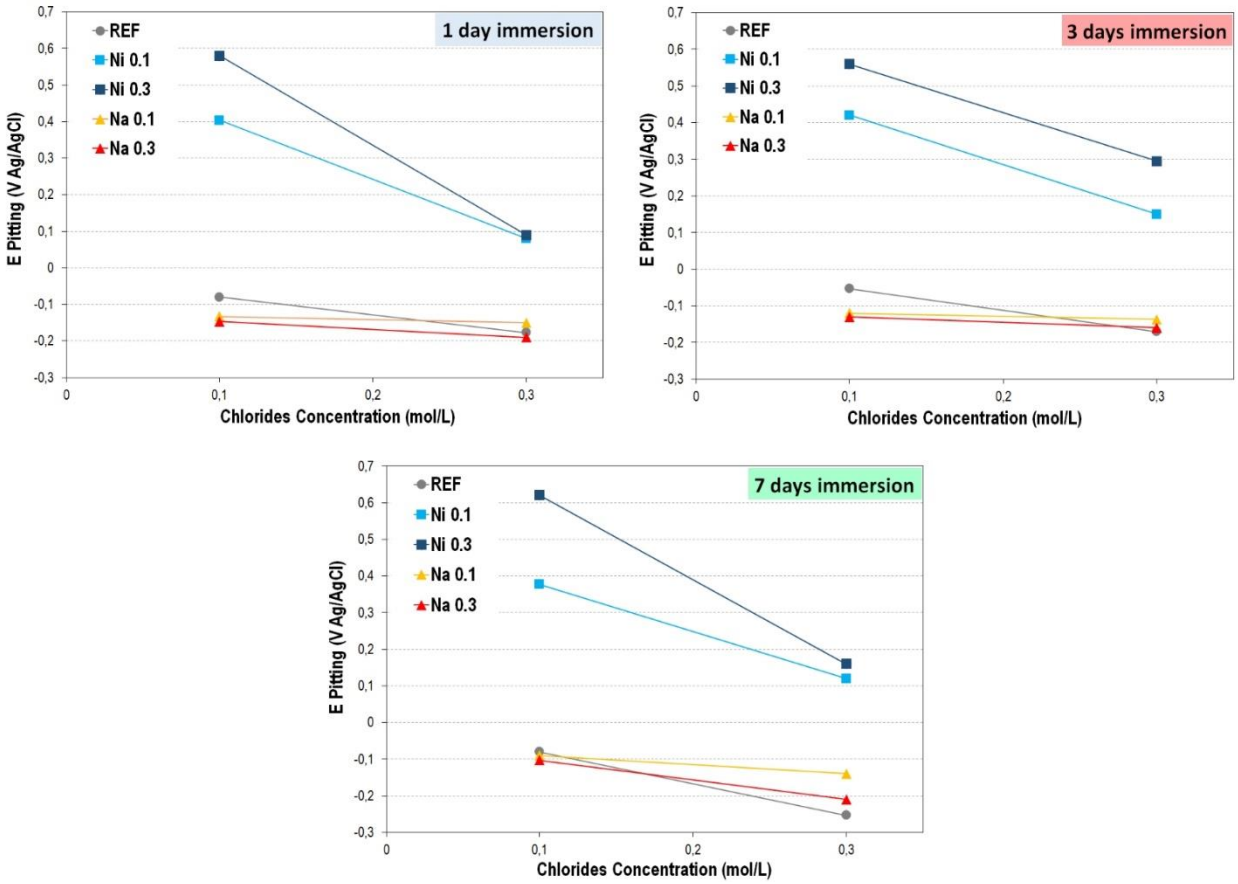

Fig. 5.5 *Pitting potentials as function of the chlorides concentration in potentiodynamic tests.*

The general decreasing of all the pitting potentials in function of the chlorides concentration is highly visible: for each solution, the passivity interval reduction is proportional to the chlorides content. As expected, the inhibitive effect of calcium nitrite is highly demonstrated: the well-known effective compound, in 0.1 mol/L concentration, showed pitting potentials of 500 mV higher with respect to the REF and NA solutions. This difference is further enhanced with increased nitrite dosage, where 700 mV of discrepancy was obtained using 0.3 mol/L inhibitor concentration.

Concerning the effectiveness of calcium nitrate as corrosion inhibitor, a general weak effect is highly noticeable; in particular, with the lowest chlorides concentration, all the obtained pitting potentials were below the corresponding REF results. This indicates that the presence of calcium nitrate in the alkaline solution worsen the steel passive behaviour, inducing a shortening of its passivity interval even greater than the one without inhibitor. The pejorative effect of NA solutions is less visible after seven days of immersion in the alkaline solution: pitting potentials similar to the REF ones were obtained. No effect is visible increasing the calcium nitrate concentration from 0.1 mol/L (yellow trend) to 0.3 mol/L (red line).

A small increasing in the obtained pitting potentials by extending the residence time of the steel samples inside the NA solutions can be observed. Characteristic values passing from –0.15 V Ag/AgCl to –0.12 V Ag/AgCl and to –0.1 V Ag/AgCl were obtained respectively for 1 day, 3 days and 7 days of immersion, regardless the calcium nitrate concentration. The explanation for this behaviour with short immersion times, can be related to the delay in the passive layer development on the sample surface in presence of calcium nitrate, as reported in literature and as shown in the free corrosion potential measurements (Fig. 5.1) to Paragraph 5.1.

The absence of any manifestation of the calcium nitrate inhibitive mechanism in these tests demonstrated the Justnes' hypothesis of slow kinetic of the protective redox reaction (23) responsible of the steel passive layer strengthening (Par. 2.4.1): with rapid measurements, e.g. potentiodynamic polarization tests, the development of the protective oxide surface layer, potentially capable to compete with the aggressive chloride ions, cannot take place [53]. As result, the obtained characteristic pitting potentials were similar to the ones achieved without any admixed inhibitor.

5.3.2 Repassivation potential

The characteristic potentiodynamic curves allowed also to identify the electrochemical parameter of repassivation potential, determined with the intersection between the backward potential and the passive interval. Since this value identifies the condition for the initiated corrosion attacks blocking, it is important for the evaluation of eventual calcium nitrate inhibition effect on chloride-induced corrosion. By experience, repassivation potentials are always more negative than the corresponding pitting potentials of at least 300 mV; all the obtained results confirmed this general rule. They are reported in Figure 5.6 for all the test conditions as a function of the chlorides concentrations; three plots are presented according to the three immersion times.

As expected, similar trends to the corresponding pitting potentials were obtained: except for NA 0.1 solution after one day of immersion, decreasing repassivation potentials with increasing chlorides concentration are visible in all the tests. This behaviour is related to the greater effort in the limitation of the evolving pitting attacks with higher amount of chlorides.

Also in these plots, the absence of any trace of corrosion inhibition in nitrate tests is clear. Compared to nitrite effect, that increases the characteristic potentials of at least 350 mV in each condition with respect to the REF results, calcium nitrate confirms its ineffectiveness as chloride-

induced corrosion inhibitor with potentiodynamic tests. No significant differences in the obtained repassivation potentials were encountered in function of the different immersion times

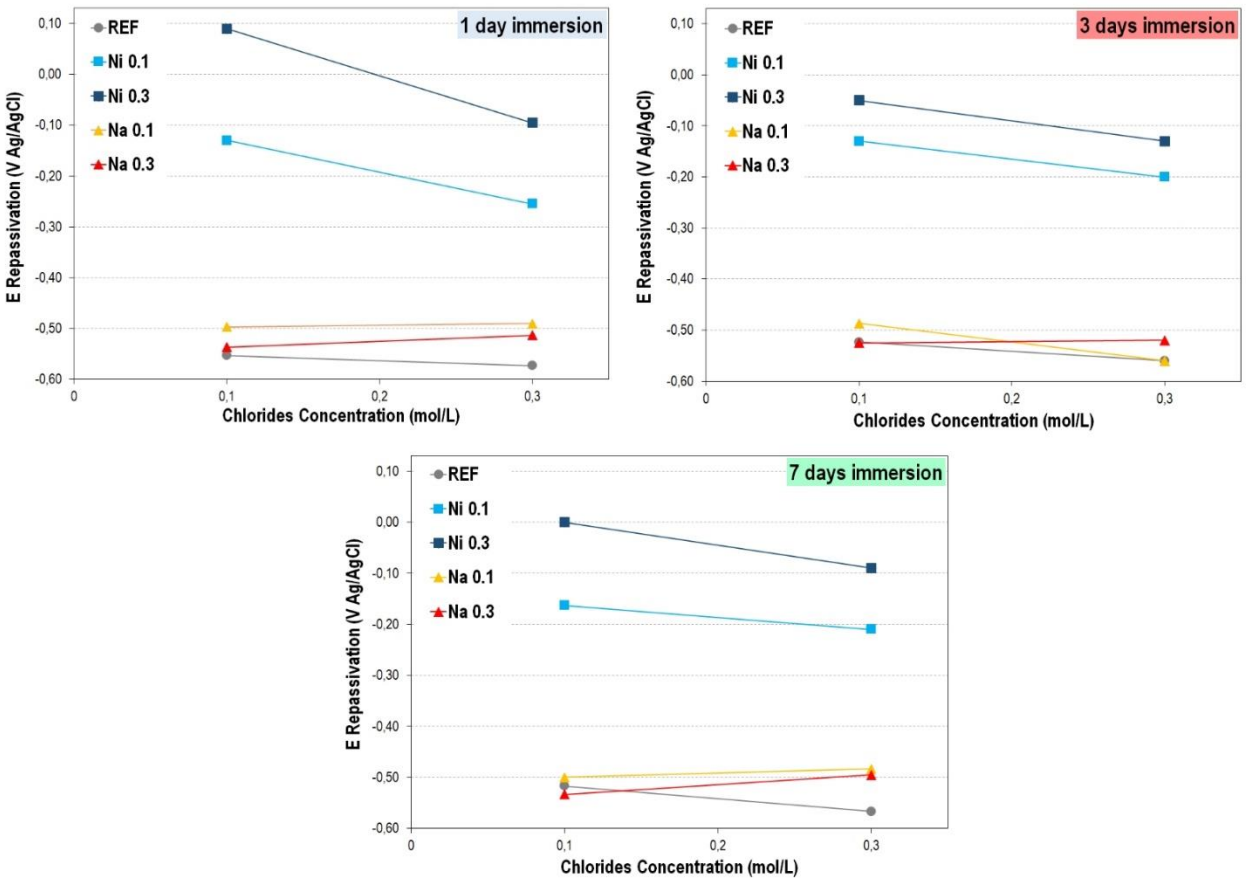

Fig. 5.6 *Repassivation potentials as a function of the chlorides concentration.*

5.3.3 Passive current density

The characteristic curves of the potentiodynamic polarization tests give information about the anodic passive current density; this quantity indicates the current density characteristic of the passivity interval. It is important to clarify that this passive current density is not the corresponding real value that would be measured on the concrete steel reinforcements in passive condition. Since potentiodynamic scan is a rapid polarization test, the recorded passive current densities are referring to the polarizing anodic sample and they thus reach higher values with respect to the corresponding real ones. However, the investigation of the obtained anodic passive current densities through potentiodynamic tests could be useful for the complete analysis of the inhibitors action on chloride-induced corrosion, since lower recorded current densities suggested a higher induced steel protection during the passivity interval of the polarization test.

The obtained current densities for all the test conditions were collected in three plots according to the adopted chlorides concentration; they are illustrated in Figure 5.7.

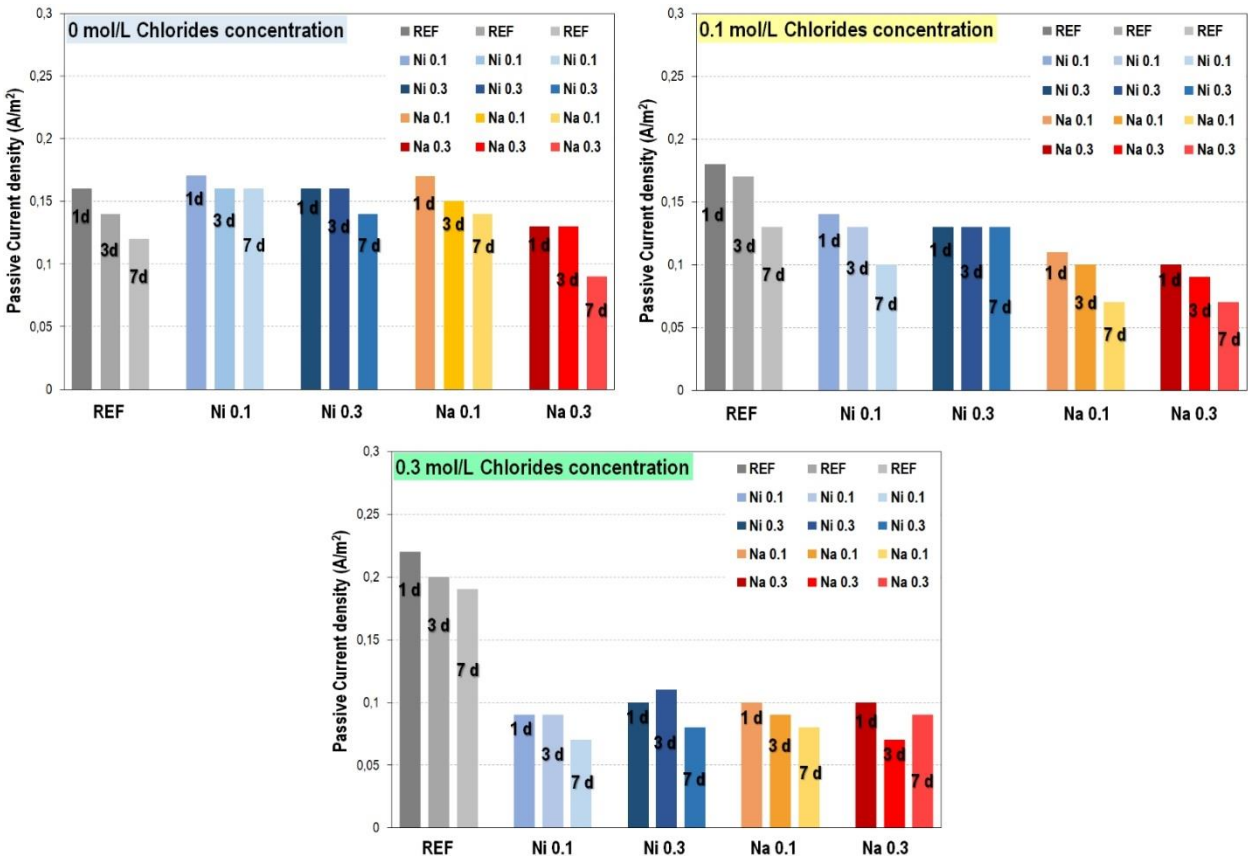

Fig. 5.7 *Anodic passive current densities of potentiodynamic tests.*

The generic decreasing trend of the passive current density as a function of the immersion time of the steel samples in all the solutions is clear: longer residence times into the alkaline environment tend to promote a stronger steel passivation, evident with corresponding lower current density in the characteristic passivity interval. This behaviour is indistinctly visible in the inhibited solutions with both inhibitors, at any concentration, and in the reference tests.

Moreover, the effect of higher chlorides dosages on the passive current densities was investigated. An increasing trend as a function of the chlorides concentration was particularly visible in the REF solutions: for each immersion time, the passive layer of the steel samples resulted less resistant with increasing chlorides dosages. On the contrary, all the inhibited solutions did not show any susceptibility to increasing chlorides concentration, showing a slight decrease in the recorded NI and NA passive current densities. However, no beneficial effect of both the inhibitors can be demonstrated through these results, since just few mA/m^2 of discrepancy from the REF current densities were found for instance with the highest chlorides concentration.

5.3.4 Critical chloride threshold

Long-term polarization tests were used to achieve the results about the steel susceptibility to chloride-induced corrosion in presence of calcium nitrate inhibitor with a more realistic test condition comparable to the state of metallic reinforcements in concrete. Potentiostatic polarization measurements were performed with REF, NA 0.1 mol/L, NI 0.1 mol/L solutions and a combined blend of NI 0.05 mol/L – NA 0.05 mol/L. Polarising 13 steel samples at 0 V Ag/AgCl, with periodic chlorides addition, it was possible to obtain the critical chloride threshold for each solution condition: this quantity is the key factor for the demonstration of calcium nitrate inhibition effectiveness for chloride-induced corrosion.

The critical chloride threshold was calculated considering the minimum chlorides concentration at which the first steel sample initiates local corrosion of pitting nature and the maximum one at which the last specimen corrodes. As a function of the increasing chlorides dosage, the percentage of the corroded samples is reported in Figure 5.8 for all the four different test solutions.

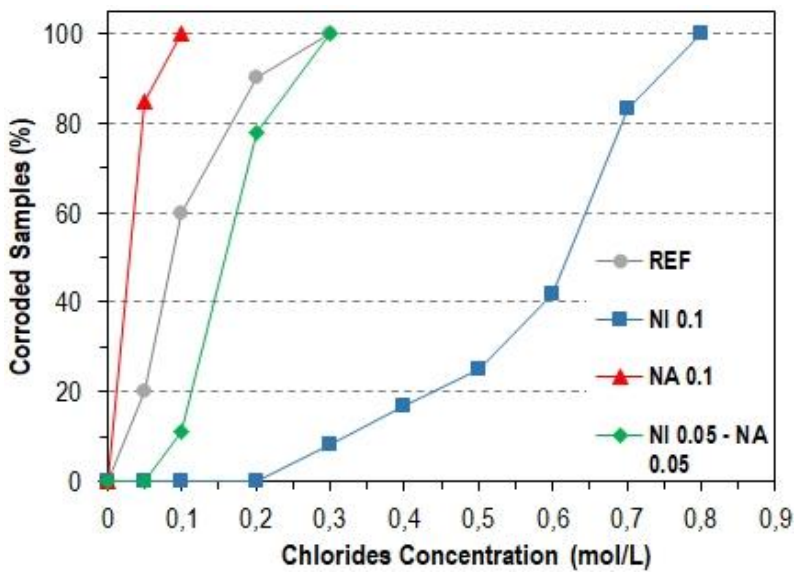

Fig. 5.8 *Percentage of the corroded sample as a function of the chlorides concentration*.

Calcium nitrite demonstrates its good inhibitive effectiveness compared to the reference test also in this type of measurement: a delayed pitting corrosion initiation is visible considering that the maximum sustained chlorides concentration was 0.8 mol/L and the test lasted more than one month.

The effect of calcium nitrate was extremely different, since the trend of corroded samples percentage is shifted to much lower chlorides concentrations; in addition, a worst behaviour with

respect to REF solution was obtained. It is important to highlight that several corrosion phenomena of different nature with respect to pitting corrosion initiated in the NA 0.1 test during the early contamination days: they were not considered in the plot. However, even if only two pitting corrosion events were observed on the steel samples and they took place at the first chlorides additions, they could be considered in the final potentiostatic results comparison. The nitrate ineffectiveness as corrosion inhibitor is thus visible correlating the trend of the obtained corroded samples percentage in the reference test; all the 13 specimens in NA solution failed in presence of a maximum chlorides concentration of 0.1 mol/L, with respect to the 0.3 mol/L chlorides maximum dosage in REF test.

The investigation on eventual synergistic behaviour of the two inhibitors, measured with the fourth potentiostatic test, showed that the addition of calcium nitrite (1:1 molar ratio) in nitrate solution reduces the steel susceptibility to chloride-induced corrosion. A small shift to higher chlorides concentrations is visible in the plot of the corroded samples percentage, indicating a modest improvement of the blend corrosion inhibition with respect to the NA solution. However, a complete absent synergistic effect was observed. Assuming a hypothetic fifth solution with calcium nitrite in 0.05 mol/L (NI 0.05 (hyp)) that could show a halved corroded samples trend with respect to NI 0.1, as illustrated in Figure 5.9, it can be demonstrate that the blend behaviour (green line) is even worst. The presence of calcium nitrate creates thus an antagonistic effect if combined with nitrite ions, identified with the corroded samples anticipation as a function of the chlorides concentration.

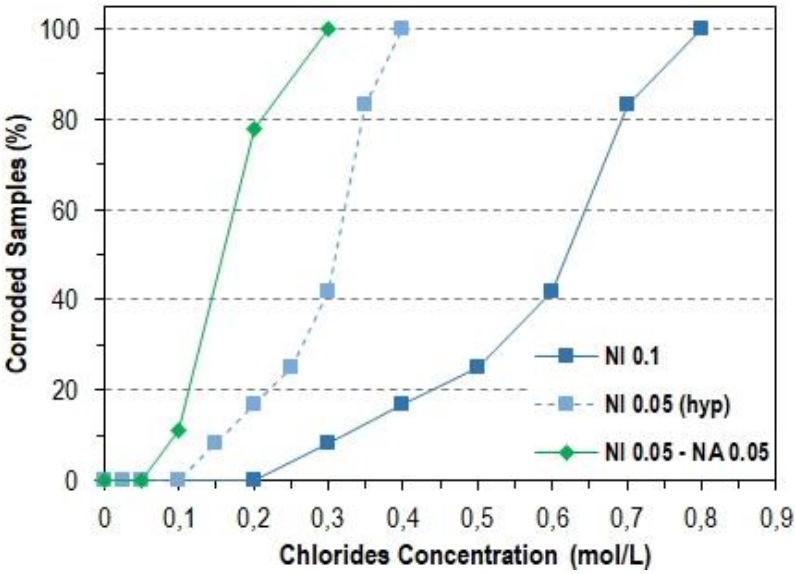

Fig. 5.9 *Corroded samples percentage with the hypothetic nitrite 0.05 mol/L concentration solution.*

For all the four solutions, it was possible to derive the critical chloride threshold at which the steel samples showed pitting corrosion: it was identified with the minimum and maximum chlorides concentration where respectively the first and the last corrosion attack took place on the steel specimens. Since the periodically recorded pH was constantly higher than 12, it was possible to compute the critical threshold values with the $[Cl^-]/[OH^-]$ ratio. The intervals of the critical chloride concentrations are reported in Figure 5.10.

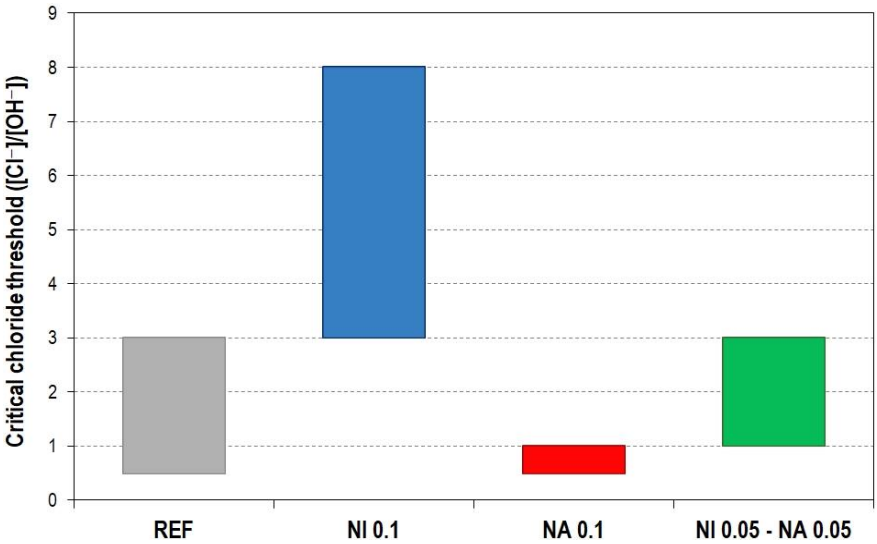

Fig. 5.10 *Critical chloride threshold for the four potentiostatic tests.*

The corrosion inhibition behaviour of the four solutions is evident: comparing the results with the REF test, it was possible to demonstrate the good inhibition efficiency of calcium nitrite solution (0.1 mol/L concentration), with increased maximum chlorides threshold of 63%; calcium nitrate (0.1 mol/L concentration) exhibits its complete ineffectiveness with decreased maximum critical chlorides threshold of 67%. The use of combined nitrite and nitrate shows similar results to the reference test, indicating nonetheless a bad inhibition effectiveness.

At this point, a possible explanation of the calcium nitrate ineffectiveness as corrosion inhibitor could be advanced. The presence of an unaltered steel susceptibility to chlorides may be related to the delayed and feeble metal passivation development induced by the nitrate ions addition and visible in the free corrosion potentials measurements at Paragraph 5.1. This delayed effect is absent in the reference solutions, suggesting that the spontaneous formation of the steel passive layer in the alkaline solution is compromised precisely by the nitrate ions.

The premature corrosion phenomena observed in the NA 0.1 potentiostatic solution, even in the absence of chlorides, may be related to this inhomogeneous passive layer formation that induces

a potential corrosion aggravation of the crevice zones, e.g. at the interface between the metal and the protecting self-adhesive tape. The polarization of the steel samples at 0 V Ag/AgCl was thus sufficient to promote the corrosion instauration in these positions; this would be impossible, as observed, in the free corrosion condition during the immersion period before the potentiodynamic scan.

5.4 Effectiveness on carbonation-induced corrosion

Calcium nitrate effectiveness as corrosion inhibitor was investigated also for what concerns concrete degradation induced by CO_2 contamination. Three series of concrete samples were cast with admixed different inhibitors concentrations; the nitrate admixture effect (in dosage of 2% and 4% by weight of cement) was compared to the nitrite one (2% by weight of cement) and to concrete samples without any inhibitors. The monitoring of the carbonation process diffusion inside the concrete matrix was performed with accelerated tests in the carbonation chamber (4% CO_2) and exposing the specimens to the real aerated atmosphere of Milan.

5.4.1 Accelerated carbonation monitoring

Since carbonation-induced corrosion is related to the slow diffusion of the carbonation process inside the concrete matrix, the plain concrete samples (cast with the different cement compositions) were subjected to accelerated carbonation technique to monitor the CO_2 penetration in a more rapid way. The diffusion of the carbonation process produces a low pH font that gradually penetrates the core of the concrete samples; the penetration rate tends to decrease in time according to the equation (7):

$$d = K \cdot t^{\frac{1}{n}} \tag{24}$$

where d is the depth of carbonation (mm), K (mm/years$^{1/2}$) is a coefficient depending on concrete type and environmental conditions and t is time (years). Usually the equation is approximated to a parabolic trend: $d = K \cdot \sqrt{t}$. For these reason, the depths of carbonation measured with phenolphthalein tests during the periodic withdrawals from the carbonation chambers were plotted as a function of the square root of time (Fig. 5.11); three different plots were built for the three different concrete Series. For a broader view, the carbonation depths measurements of the previous

thesis work were included into the plot; in this way, the complete carbonation diffusion progress was illustrated.

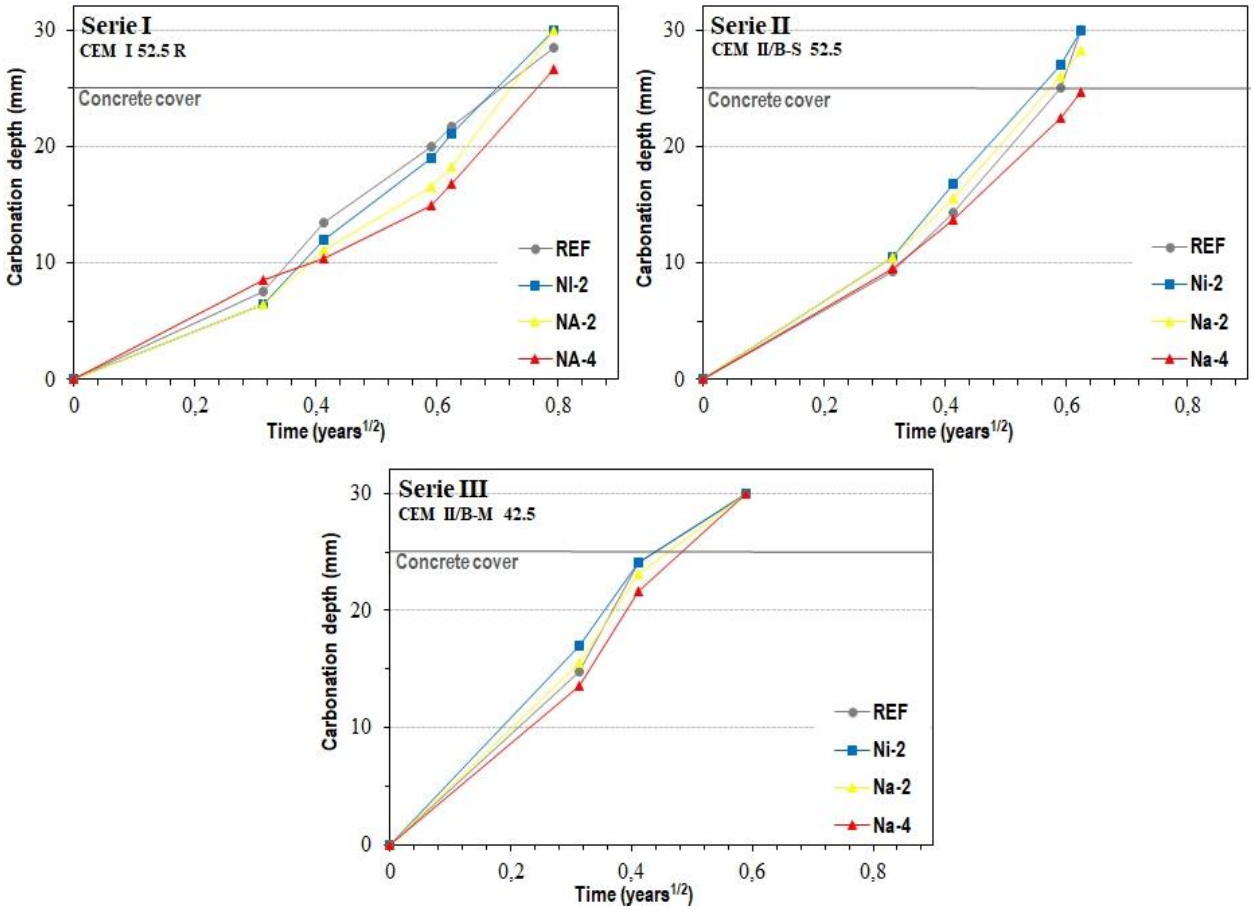

Fig. 5.11 *Carbonation depths as a function of (time)$^{1/2}$ in accelerated carbonation monitoring.*

It is visible that the main differences of the carbonation diffusion trends are among different cement types: Serie I (CEM I 52.5 R, ordinary Portland cement) showed the lowest CO_2 permeability; on the contrary, Serie III (CEM II/B-S 52.5 N, Portland-composite cement) was the less resistant to carbonation penetration and Serie II (CEM II/B-M 42.5, Portland-composite cement) showed medium results. This behaviour was predictable, since the CO_2 diffusion is heavily dependent on the cement composition: in particular, in the previous thesis work, ordinary Portland cements showed the highest mechanical resistances with respect to the other series and this concrete property was assessed to be highly controlled by the material porosity. In the same way, Portland-composite cements of the Serie III were assessed to be the lowest mechanical resistant concrete, with consequent observed high CO_2 permeability [75]. Therefore, a controlled porosity, that influences good mechanical properties, can limit also the carbonation process diffusion.

Concentrating on the individual cement compositions, no big differences in the carbonation depth trends were recorded with different inhibitors admixed; however, in all the three plots, the presence of calcium nitrate in 4% by weight of cement dosage seems to reduce the CO_2 diffusivity to a small extent. Particularly for Serie I and II, an average difference over time of 4 mm in the carbonation depth was observed with respect to the REF concrete. Approximately absent differences in the Series III trends were found, indicating that no carbonation diffusion delayed effect is induced by neither calcium nitrite nor nitrate admixture in both dosages to this cement type.

For a broader view of the carbonation diffusion results, the coefficient *K* (mm/years$^{1/2}$) was determined with the slope of each carbonation depth trend; the obtained values are collected in the histogram in Figure 5.12.

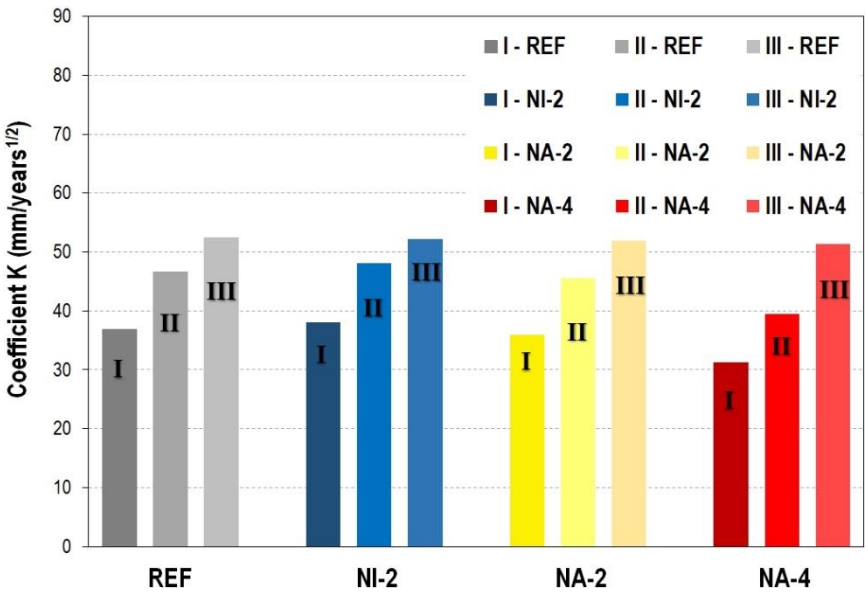

Fig. 5.12 *Coefficient K for the carbonation depth in accelerated tests (Serie I: CEM I 52.5R; Serie II: CEM II/B-S 52.5; Serie III: CEM II/B-M 42.5).*

Since *K* coefficient is highly dependent on the concrete type, the biggest differences are evident with different Series. Nevertheless, a reduced carbonation permeability with the addition of calcium nitrate in 4% by weight of cement dosage is particularly visible in Serie I and II: the *K* coefficient decreases of about 15% with respect to REF samples. A moderate nitrate beneficial effect can be thus demonstrated in the carbonation diffusion process; on the contrary, calcium nitrite shows a total ineffectiveness.

These *K* coefficients should be compared to the corresponding ones related to the carbonation depths measurements on the concrete samples exposed to the external atmosphere; in this way, it

will be possible to understand whether they are in line with the real carbonation process action, corroborating thus the analysis.

5.4.2 Real carbonation monitoring

The carbonation monitoring was performed also on plain concrete prisms exposed to the aerated atmosphere of Milan, part shielded from rain and part exposed, after more than one year from the placing on the rooftop. A single carbonation depth measurement was accomplished with the usual phenolphthalein test and the results were reported in Figure 5.13, divided in the three different Series according to the adopted cement type.

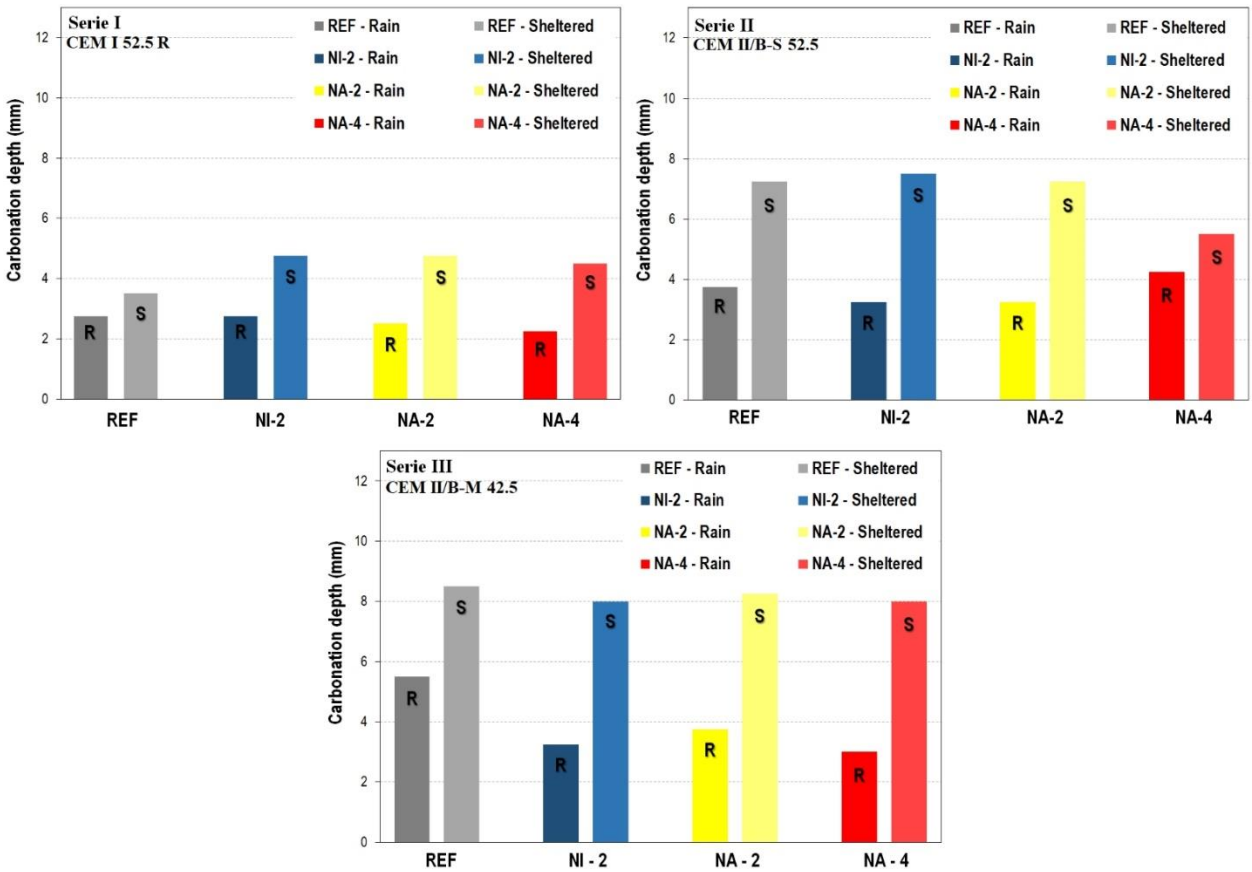

Fig. 5.13 *Carbonation depths measures of concrete samples exposed to atmosphere.*

The results of real carbonation monitoring confirm that the CO_2 diffusion inside concrete is mostly dependent on the cement type: Serie I shows lower carbonation permeability with respect to the other Series, proving the high dependence on the cement porosity.

The *K* coefficients were calculated also for these results as the ratio between the measured carbonation depths (mm) and the square root of time (years$^{1/2}$). They were collected in Figure 5.14, where two histograms are presented according to the different samples exposure conditions.

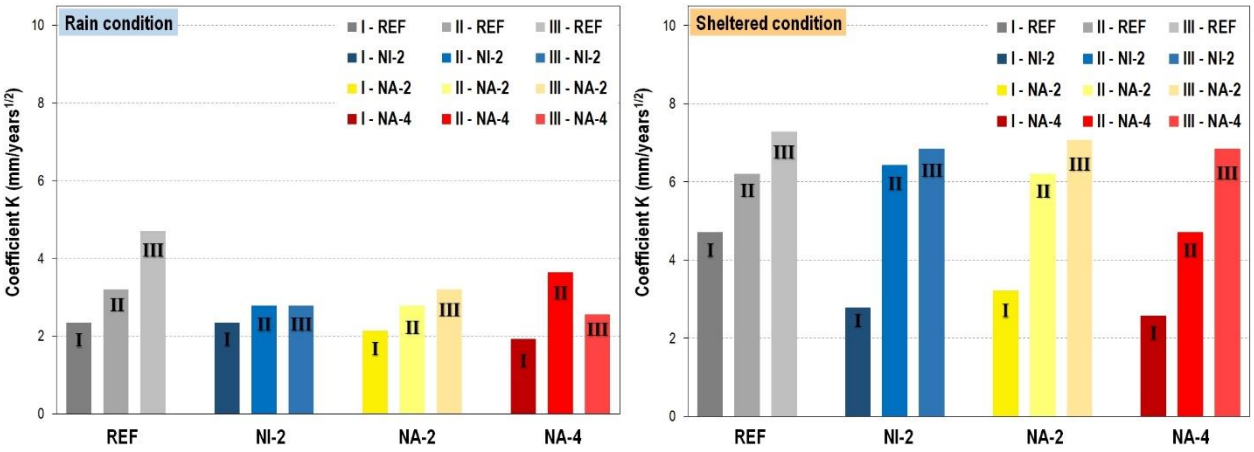

Fig. 5.14 *K coefficients of the real carbonation depth measurements (Serie I: CEM I 52.5R; Serie II: CEM II/B-S 52.5; Serie III: CEM II/B-M 42.5).*

It is visible that a moderate calcium nitrate inhibition effect is present in specific concretes: for instance, concerning Serie I, a carbonation depths percentage reduction of 9% and 18% with respect to REF samples was achieved respectively in NA-2-Rain and NA-4-Rain; in the sheltered condition this effect is further enhanced, with respectively 32% and 45% of reduction. The calcium nitrate positive impact is quite absent in Serie II, except for NA-4-Sheltered that showed a carbonation diffusion reduction of 24% with respect to the reference specimen. However, Serie III seems to be similar to the first Serie: concerning the rain condition, 32% and 45% of carbonation depth decreases were observed admixing nitrate inhibitor respectively at 2% and 4% by weight of cement; for the shielded samples, limited reductions were achieved.

These results seem to demonstrate the presence of calcium nitrate delayed effect on the carbonation process diffusion, especially since an enhanced beneficial action was encountered increasing the admixture dosage in the cement mix. However, the waiting of longer time for additional measurements is fundamental for a complete investigation.

To corroborate the analysis, the above *K* coefficients were compared to the corresponding ones related to the accelerated carbonation process (Par. 5.4.1); in this way, it is possible to establish whether the carbonation chamber atmosphere has accurately simulated an accelerated carbonation process diffusion inside concrete. The scatter plot, collecting the *K* coefficients of the two carbonation conditions, is reported in Figure 5.15, where the real carbonation results

(K_{real}), related to the shielded from rain cements, were plotted as a function of the accelerated carbonation coefficients ($K_{accelerated}$).

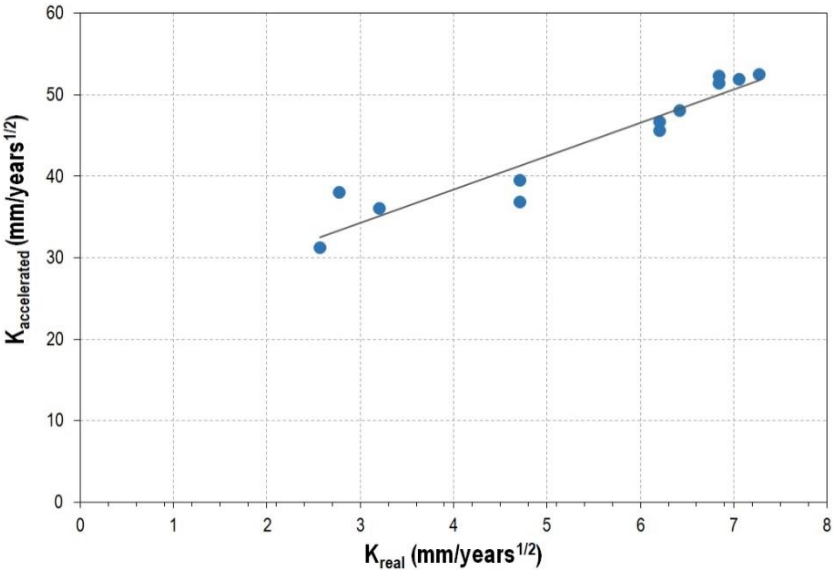

Fig. 5.15 *K coefficients scatter plot of real and accelerated carbonation depth monitoring.*

All the points correspond to the different adopted cement compositions and they show a good fitting with the trend line. This indicates that the accelerated carbonation results are in line with the real carbonation process, demonstrating thus that the technique can simulate in an accurate way an accelerated CO_2 diffusion though shielded from rain concrete. Therefore, the calcium nitrate delayed effect for the carbonation process diffusion can be doubly assessed, especially concerning the ordinary Portland cement (Serie I).

5.5 Effectiveness on rebars corrosion

The effectiveness of calcium nitrate as inhibitor was finally assessed also monitoring the corrosion induced by concrete carbonation of the reinforcements embedded in the cylindrical concrete samples cast with the same compositions of the plain ones. The specimens were introduced into the carbonation chamber to promote the complete carbonation of the concrete cover, removing in this way the alkaline protection for the metal. They were subsequently placed to the external aerated atmosphere of Milan, part shielded from rain and part exposed. The corrosion monitoring of the rebars was performed periodically with free corrosion potential measurements and linear polarization resistance (LPR) tests.

5.5.1 Free corrosion potential monitoring

The technique represents the primary investigation on the corrosion state of the reinforcements. It was possible to assess the active corrosion condition of the metal if its recorded potential was lower than –350 mV CSE; on the other side, low corrosion probability can be demonstrated with collected potentials higher than –200 mV CSE. This analysis is presented in Figure 5.16, where the two thresholds of potential with low and high probability of corrosion were displayed.

It is visible that for all the samples, except for the REF results of the II and III Series, both in sheltered and exposed to rain condition, the first measured free corrosion potential demonstrated the reinforcements active corrosion condition, indicating the total loss of the alkaline concrete cover protection after complete carbonation. The subsequent results are spread over potentials spacing from –200 mV CSE and –500 mV CSE, with some exceptions, indicating that the rebars maintained the active corrosion condition over time. Nonetheless, a generic slow decreasing trend of all the free corrosion potentials in all the specimens was identified, suggesting a progressive worsening of the reinforcements corrosion state in time.

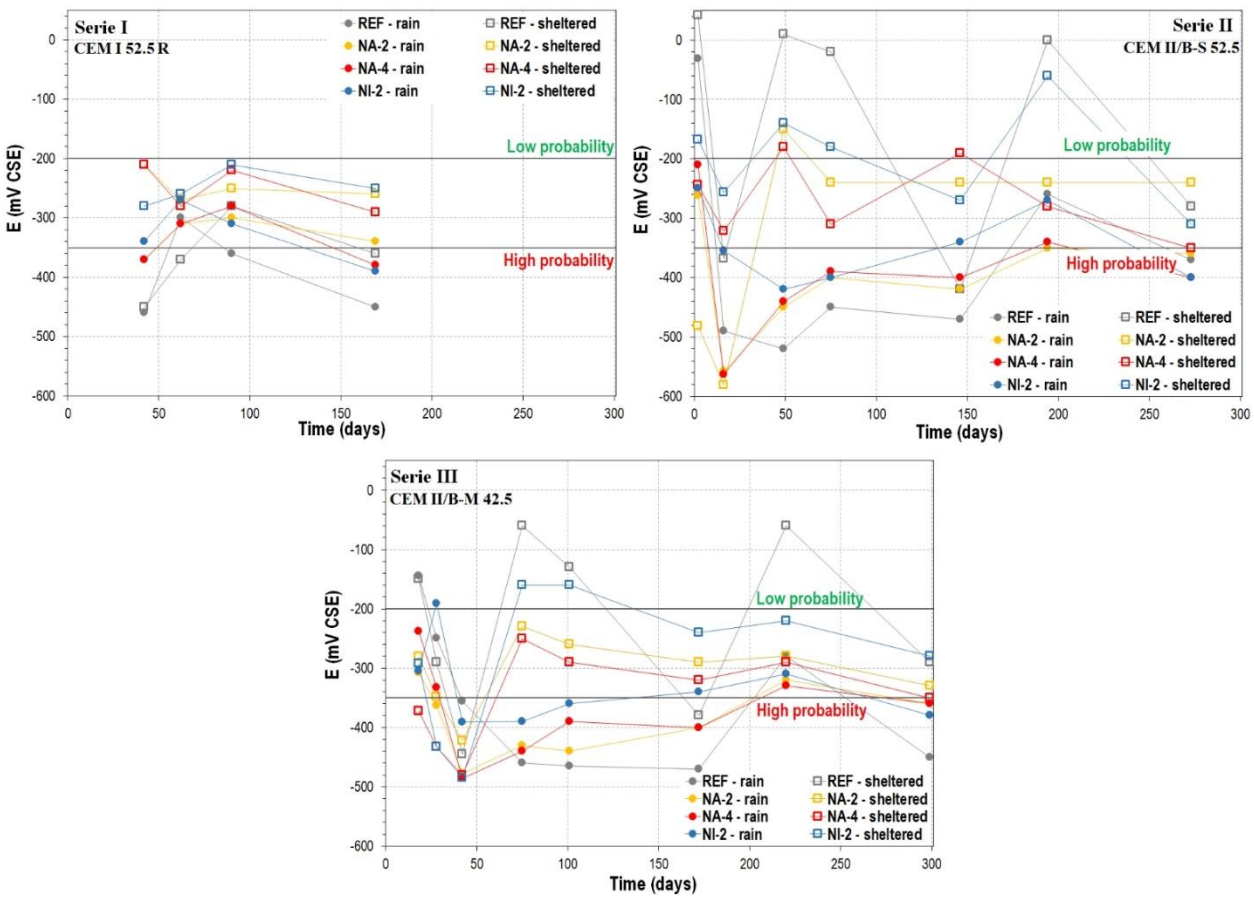

Fig. 5.16 *Free corrosion potentials of the rebars embedded in concrete samples.*

Considering the different concrete compositions, regarding the inhibitors dosages, a total ineffectiveness of calcium nitrate as rebars corrosion inhibitor can be established, since all the NA specimens showed a generic comparable or even worst behaviour with respect to the corresponding REF samples. Even calcium nitrite, whose effectiveness in chloride-induced corrosion is well-known, revealed an ineffective inhibition on the rebars corrosion after complete concrete carbonation.

5.5.2 Penetration rate

A more accurate investigation on the effective corrosion state of the reinforcements inside carbonated concrete was performed with the linear polarization technique (LPR): it allows to obtain, in a precise way, the actual mean corrosion rate i_{corr} (mA/m^2) of the metal through the Stern-Geary relation using the measured polarization resistance R_p (Ω m^2):

$$i_{corr} = \frac{B}{R_p} \tag{25}$$

where B is a constant corresponding to 26 mV, since all the reinforcements were assumed to be in an active condition. The corrosion evaluation was completed with the computation of the mean penetration rates (μm/year), that through the Faraday's law can be obtained multiplying i_{corr} by 1.17 factor. The collected penetration rates are reported in Figure 5.17 as a function of time in three different plots according to the three different Series; corrosion penetrations equivalent to 1 μm/year were highlighted to indicate the threshold for corrosion amounts no more negligible.

It is visible that the obtained results are coherent with the anticipated corrosion evaluation through the free corrosion potentials measures: all the rebars immersed in different concretes showed an active behaviour indicated by corrosion penetration rates higher than 1 μm/year, with the exception of sporadic points that could be neglected. Since the reported quantities are inversely proportional to the obtained polarization resistances illustrated in Paragraph 4.4.2, opposite discrepancies with exposed to rain and sheltered samples results are evident: lower corrosion rates were obtained for the shielded from rain cements, demonstrating once more that the environments with high relative humidity induce huge corrosion rates.

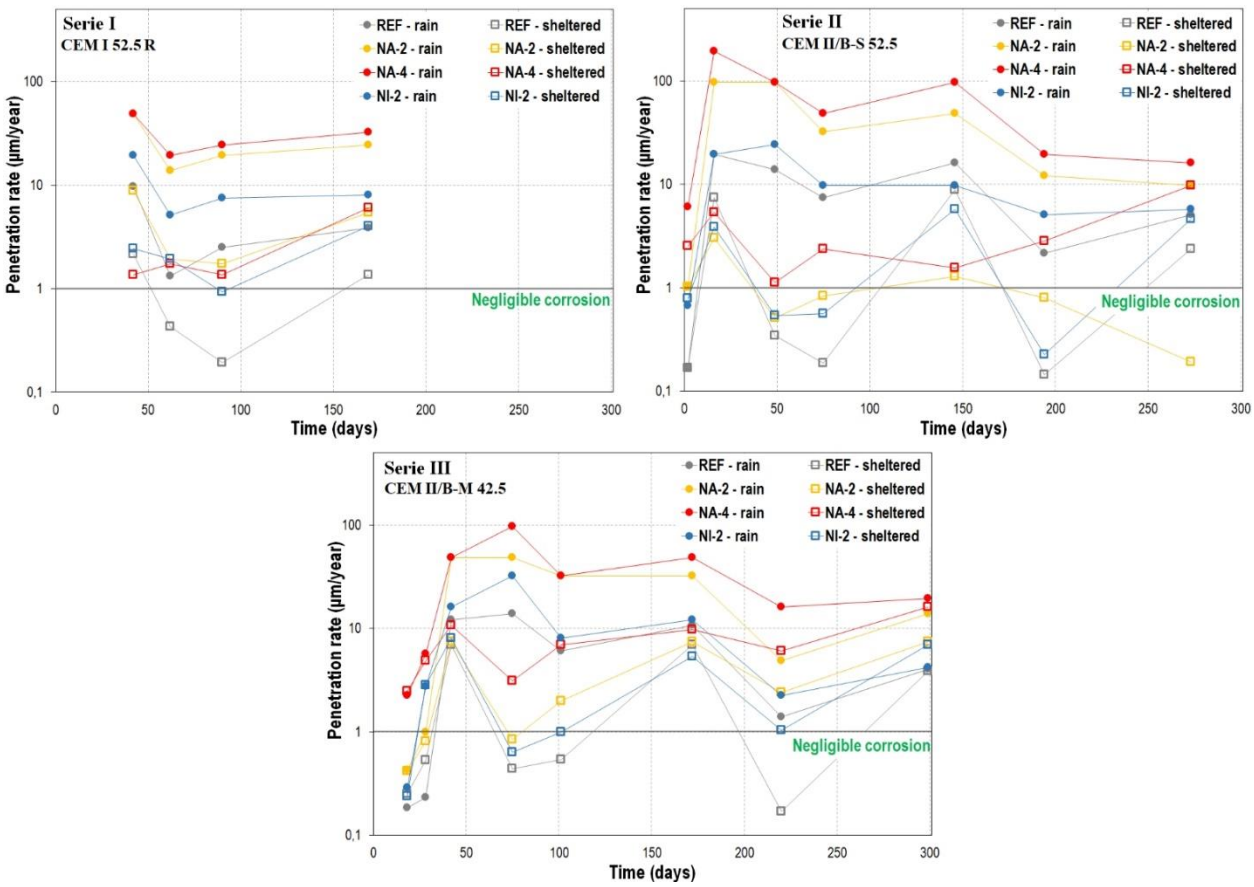

Fig. 5.17 *Corrosion penetration rates of the rebars in carbonated concrete samples.*

Concerning the admixtures' effectiveness on rebars corrosion inhibition, it is possible to demonstrate a general ineffectiveness of both calcium nitrate and nitrite in all the three cements compositions, since evident similar or even higher corrosion rates with respect to REF samples were collected. A generic slow increasing trend over time of the obtained penetration rates can be identified, revealing a progressive aggravation of the corrosive state of all reinforcements embedded in the concrete specimens.

Conclusions

The main purpose of the present work is the investigation of a new class of inorganic concrete corrosion inhibitors, identified by calcium nitrate, that may represent the replacement for the well-established nitrite inhibitor, affected by toxicity issues. Since considerable divergent opinions about reliable nitrate inhibition effectiveness are present in literature, the research focused on the demonstration of eventual calcium nitrate beneficial effects on chlorides and carbonation-induced corrosion, that are the main reasons for concrete degradation.

The experimental tests resorted to simulating concrete environments through the development of alkaline synthetic pore solutions (pH 12.6) and concrete samples, both plain and reinforced, with admixed nitrate compound. To compare the results, parallel tests were implemented without any inhibitor and in presence of admixed calcium nitrite inhibitor. The inhibitors dosages were selected in agreement with many experiments present in literature and considering the suitable concentrations that wouldn't affect the properties of the settled concrete samples. Concerning the simulating concrete pore solutions, calcium nitrite and nitrate were admixed in 0.1 mol/L and 0.3 mol/L concentrations; the steel sample bars were immersed for different residence times in the solutions to promote the surface passive layer development induced by the alkaline condition. It was discovered that the presence of calcium nitrate in the solution delayed the metal passivation, indicated by a slower increase in the free corrosion potentials compared to reference tests. On the contrary, faster passive layer development was observe in presence of calcium nitrite, demonstrating thus its good action as passivating anodic inhibitor.

The cyclic potentiodynamic polarization allowed to investigate the steel susceptibility to localized chlorides-induced corrosion; sodium chloride was added to the pore solutions in two concentrations (0.1 mol/L and 0.3 mol/L) before the scanning start. By comparing the characteristic electrochemical parameters, e.g. pitting potential and repassivation potential, it was possible to demonstrate a poor calcium nitrate inhibitive effectiveness in both concentrations: comparable or even worst pitting potentials with respect to the ones without inhibitor were obtained, ranging from –0.1 V to –0.2 V Ag/AgCl. The absence of evident calcium nitrate inhibitive effectiveness in rapid potentiodynamic tests proved the Justnes' hypothesis of slow reaction kinetic related to the eventual nitrate strengthening effect on the steel surface passivation. The use of long-term polarization tests, e.g. potentiostatic polarization, was thus fundamental.

Potentiostatic polarization technique analyses, in a more realistic way, the steel behaviour in simulating concrete environments in presence of calcium nitrate. Polarizing 13 carbon steel samples immersed in different solutions at 0 V Ag/AgCl, it was possible to obtain the characteristic critical chloride thresholds. In presence of nitrate ions at 0.1 mol/L concentration, a decrease of 66% in the critical chloride threshold was obtained compared to the reference test. This result confirmed and demonstrated, with a more reliable test condition, the total calcium nitrate inhibitive ineffectiveness in chloride-induced corrosion.

On the contrary, the good nitrite inhibitive effect was verified with corresponding polarization tests of potentiodynamic and potentiostatic type, with the same calcium nitrate concentrations. Typical pitting potentials, ranging from 0.1 V to 0.6 V Ag/AgCl, were obtained, with an increment of at least 500 mV with respect to the reference results. The maximum chloride concentration achieved in the potentiostatic polarization test with 0.1 mol/L inhibitor dosage was 0.8 mol/L, indicating a percentage increase of 63% compared to the reference result.

Furthermore, it was investigated an eventual synergistic behaviour of combined calcium nitrite and nitrate inhibitors with a potentiostatic polarization test; the adopted compounds concentration was 0.05 mol/L, in 1:1 molar ratio. The presence of nitrite ions in the blend increased the critical chloride threshold with respect to the nitrate test; however, complete absent synergistic effect was observed, since the steel corrosion behaviour in the blend was even worse than a hypothetic corresponding test with only calcium nitrite in 0.05 mol/L concentration. Therefore, calcium nitrate creates an antagonistic effect if combined with nitrite ions.

Calcium nitrate effect as inhibitive admixture was inspected also concerning the carbonation diffusion process and the induced corrosion. Concrete samples with different cement types (CEM I 52.5 R, CEM II/B-S 52.5 N and CEM II/B-M 42.5) were cast with admixed calcium nitrate at 2% and 4% by weight of cement. For comparison purposes, analogous concrete specimens were fabricated without any inhibitor and admixing calcium nitrite in 2% by weight of cement dosage. Part of the samples were placed into the carbonation chamber (4% CO_2 concentration in controlled atmosphere) for accelerated tests and part were exposed to the external aerated atmosphere, both in shielded and exposed to rain condition. The carbonation process diffusion inside concrete was periodically monitored with phenolphthalein tests on the plain prismatic samples and it was found that the main differences on the carbonation depths trends were among different cement types, demonstrating the heavy CO_2 penetration dependence on the concrete porosity. Moreover, a moderate beneficial effect of calcium nitrate in 4% by weight of cement is present, specifically on

CEM I and CEM II/B-M 42.5 samples: regarding the accelerated carbonation technique, the *K* coefficients showed a percentage decrease of about 15% with respect to REF samples. Coherent results were obtained also in the carbonation monitoring on the exposed to atmosphere samples. In particular, enhanced carbonation process delayed effect was visible increasing the nitrate admixture dosage; carbonation depth percentage reduction by 32% and 45% was observed on CEM I and CEM II/B-M 42.5 samples admixing nitrate inhibitor respectively in 2% and 4% by mass. This beneficial effect was completely absent on admixed cements with calcium nitrite. However, the waiting of longer time for additional measurements is fundamental for a complete investigation.

The general investigation on calcium nitrate inhibitive action concluded with the measurements of the reinforcements corrosion condition after complete concrete cover carbonation. The rebars corrosion condition was assessed with free potential measurements that demonstrated an active corrosion behaviour for all the concrete samples. Periodic linear polarization resistance tests measured the actual corrosion rates, indicating a generic non-negligible corrosion situation in all the specimens. Regarding the different inhibitors effects, it is possible to demonstrate a general ineffectiveness of both calcium nitrate and nitrite in all the cements compositions, since similar or even higher corrosion rates compared to the reference samples were collected.

Bibliography

[1] L. Bertolini, B. Elsener, P. Pedeferri, and R. Polder, *Corrosion of Steel in Concrete: Prevention, Diagnosis, Repair*. Weinheim: Wiley, 2004.

[2] Merchant Research and Consulting Ltd, "Cement Global Market Review 2016/2017," Dublin, 2017.

[3] J. P. Broomfield, *Corrosion of Steel in Concrete: Understanding, Investigation and Repair, Second Edition*. Taylor & Francis, 2006.

[4] F. Bolzoni *et al.*, "Inibitori di corrosione per calcestruzzo armato: 15 anni di sperimentazione @PoliLaPP," *La Metall. Ital.*, vol. 107, no. 3, pp. 3–10, 2015.

[5] J. M. Gaidis, "Chemistry of corrosion inhibitors," *Cem. Concr. Compos.*, vol. 26, no. 3, pp. 181–189, 2004.

[6] H. Justnes and E. C. Nygaard, "The influence of technical calcium nitrate additions on the chloride binding capacity of cement and the rate of chloride induced corrosion of steel embedded in mortars," in *Corrosion protection of steel in concrete*, 1994, pp. 491–502.

[7] V. K. Gouda, "Corrosion and Corrosion Inhibition of Reinforcing Steel: I. Immersed in Alkaline Solutions," *Br. Corros. J.*, vol. 5, no. 5, pp. 198–203, Sep. 1970.

[8] A. Rossi, G. Puddu, and B. Elsener, "The surface of iron and Fe10Cr alloys in alkaline media," in *Proc. Eurocorr 2001*, 2001.

[9] P. K. Mehta and P. J. M. Monteiro, *Concrete: microstructure, properties, and materials*. 2006.

[10] B. Elsener, *Corrosion Inhibitors for Steel in Concrete: State of the Art Report*. 2001.

[11] P. Pedeferri and L. Bertolini, *La durabilità del calcestruzzo armato*. Mcgraw-Hill Libri Italia srl, 2000.

[12] K. Tuutti, "Corrosion of steel in concrete," *Swedish Cem. Concr. Res. Inst.*, 1982.

[13] C. Andrade, C. Alonso, and J. Antonio Gonzalez, "Initial effort to use the corrosion rate measurements for estimating rebar durability," *Corrosion Rate of Reinforcement in Concrete*, 1988. .

[14] D. Nieves-Mendoza *et al.*, "Statistical analysis of factors influencing corrosion in concrete structures," *Int. J. Electrochem. Sci.*, 2012.

[15] R. B. Polder, *Cathodic protection of reinforced concrete structures in the Netherlands - Experience and developments*, vol. 25. 1998.

[16] EN 206, *Concrete - Specification, performance, production and conformity*. 2013.

[17] P. Schiessl and M. Raupach, "Influence of Concrete Composition and Microclimate on the

Critical Chloride Content in Concrete," *Corros. Reinf. Concr.*, no. September, pp. 49–58, 1990.

[18] K. Y. Ann and H. W. Song, "Chloride threshold level for corrosion of steel in concrete," *Corros. Sci.*, vol. 49, no. 11, pp. 4113–4133, 2007.

[19] P. Lambert, C. L. Page, and P. R. W. Vassie, "Investigations of reinforcement corrosion. 2. Electrochemical monitoring of steel in chloride-contaminated concrete," *Mater. Struct.*, vol. 24, no. 5, pp. 351–358, 1991.

[20] L.-O. Nilsson, E. Poulsen, P. Sandberg, H. Sørensen, and O. Klinghoffer, *HETEK, Chloride penetration into concrete, State-of-the-Art. Transport processes, corrosion initiation, test methods and prediction models*. 1996.

[21] C. L. Page and K. W. J. Treadaway, "Aspects of the electrochemistry of steel in concrete," *Nature*, vol. 297, p. 109, May 1982.

[22] C. Alonso, C.; Andrade, "Life time of rebars in carbonated concrete," *Prog. Underst. Prev. Corros.*, vol. 624, 1994.

[23] C. Plage, "Nature and properties of concrete in relation to reinforcement corrosion," *Corros. steel Concr.*, 1992.

[24] A. M. Neville, *Properties of concrete*. Pitman Pub., 1981.

[25] T. A. Söylev and M. G. Richardson, "Corrosion inhibitors for steel in concrete: State-of-the-art report," *Constr. Build. Mater.*, vol. 22, no. 4, pp. 609–622, 2008.

[26] ISO 8044, *Corrosion of metals and alloys - Basic terms and definitions*. 2015.

[27] K. Soeda and T. Ichimura, "Present state of corrosion inhibitors in Japan," *Cem. Concr. Compos.*, vol. 25, no. 1, pp. 117–122, 2003.

[28] R. Myrdal, *Corrosion Inhibitors - State of the art*. 2017.

[29] V. M. Moskwin and S. M. Alekseyeev, "Beton i Zhelezobeton," *J. Impact 2,21*, 1958.

[30] O. S. B. Al-Amoudi, M. Maslehuddin, A. N. Lashari, and A. A. Almusallam, "Effectiveness of corrosion inhibitors in contaminated concrete," *Cem. Concr. Compos.*, vol. 25, no. 4, pp. 439–449, 2003.

[31] L. Mammoliti, C. M. Hansson, and B. B. Hope, "Corrosion inhibitors in concrete - Part II: Effect on chloride threshold values for corrosion of steel in synthetic pore solutions," *Cem. Concr. Res.*, vol. 29, pp. 1583–1589, 1999.

[32] K. Y. Ann, H. S. Jung, H. S. Kim, S. S. Kim, and H. Y. Moon, "Effect of calcium nitrite-based corrosion inhibitor in preventing corrosion of embedded steel in concrete," *Cem. Concr. Res.*, vol. 36, no. 3, pp. 530–535, 2006.

[33] N. Berke and M. C. Hicks, *Estimating the life cycle of reinforced concrete decks and marine piles using laboratory diffusion and corrosion data*. 1992.

[34] I. Callander and F. Gianetti, "A review on the use of C.N corrosion inhibitor to improve

the durability of reinforced concrete," in *The 2nd Annual Middle East Protection and Rehabilitation of Reinforced Concrete Conference*, 1996.

[35] U. Maeder, "A New Class of Corrosion Inhibitors for Reinforced Concrete," *Spec. Publ.*, vol. 163, pp. 215–232, 1996.

[36] A. M. Rosenberg, J. M. Gaidis, T. G. Kossivas, and R. W. Previte, *Corrosion Inhibitor Formulated with Calcium Nitrite for Use in Reindorced Concrete.* 1977.

[37] L. Dhouibi, P. Refait, E. Triki, and J.-M. Génin, *Interactions between nitrites and Fe(II)-containing phases during corrosion of iron in concrete-simulating electrolytes*, vol. 41. 2006.

[38] S. E. Ping Gu R. Hristova, J. J. Beaudoin, R. Brousseau, and B. Baldock, "A Study of Corrosion Inhibitor Performance in Chloride Contaminated Concrete by Electrochemical Impedance Spectroscopy," *Mater. J.*, vol. 94, no. 5.

[39] K. Sagoe-Crentsil, V. Yilmaz, and F. Glasser, "Properties of Inorganic Corrosion Inhibition Admixtures in Steel-containing OPC mortars. Part 1: Chemical Properties," *Adv. Cem. Res.*, vol. 4, no. 15, pp. 91–96, 1992.

[40] A. M. Rosenberg and J. M. Gaidis, "The Mechanism of Nitrite Inhibition of Chloride Attack of Reinforced Steel in Alkaline Aqueous Environments," *Mater. Perform.*, vol. 18, no. 11, pp. 45–48, 1979.

[41] N. Berke and M. C. Hicks, "Predicting long-term durability of steel reinforced concrete with calcium nitrite corrosion inhibitor," *Cem. Concr. Compos.*, vol. 26, no. 3, pp. 191–198, 2004.

[42] M. Ormellese, M. Berra, F. Bolzoni, and T. Pastore, "Corrosion inhibitors for chlorides induced corrosion in reinforced concrete structures," *Cem. Concr. Res.*, vol. 36, no. 3, pp. 536–547, 2006.

[43] C. Alonso and C. Andrade, "Effect of Nitrite as a Corrosion Inhibitor in Contaminated and Chloride-Free Carbonated Mortar," *Mater. J.*, vol. 87, no. 2, pp. 130–137, 1990.

[44] R. Myrdal, *Accelerating admixtures for concrete*. 2007.

[45] V. Dodson, *Concrete Admixtures*, Chapter 4. New York: Van Nostrand Reinhold, 1990.

[46] N. Mailvaganam and R. Rixom, *Chemical Admixtures for Concrete*, Third Edit. London: E&FN Spon, 1999.

[47] R. Craig and L. Wood, *Effectiveness of Corrosion Inhibitors and Their Influence on the Physical Properties of Portland Cement Mortars*. 1970.

[48] M. Collepardi, R. Fratesi, G. Moriconi, V. Corradetti, and C. Luigi, *Use of nitrite salt as corrosion inhibitor admixtures in reinforced concrete structures immersed in sea-water*. 1990.

[49] wikipedia.org, "Nitrate." [Online]. Available: https://en.wikipedia.org/wiki/Nitrate. [Accessed: 09-Feb-2018].

[50] M. V. Diamanti, B. Del Curto, M. Ormellese, F. Bolzoni, and G. Cilluffo, "On the use of nitrates as corrosion inhibitors for concrete rebars," *La Metall. Ital.*, vol. 109, pp. 11–14, 2017.

[51] H. Justnes and E. C. Nygaard, "Technical calcium nitrate as set accelerator for cement at low temperatures," *Cem. Concr. Res.*, vol. 25, no. 8, pp. 1766–1774, 1995.

[52] Y. U. K. D'yachenko, S. G. Enisherlova, G. D. Kucheryaeva, V. B. Rationov, and S. D. Semenova, "Effect of Chloride, Nitrate, and Nitrite on the Corrosion of Prestressed Rebars in Heavy Concrete," *Zashch. Met*, vol. 23, no. 4, pp. 655–659, 1987.

[53] H. Justnes, "Concrete Corrosion Problems solved by Calcium Nitrate," in *25th Conference on Our World in Concrete and Structures*, 2000, pp. 349–356.

[54] D. Talbot and J. Talbot, *Corrosion Science and Technology*. Boca Raton, FL: CRC Press LLC, 1998.

[55] H. Verbruggen, H. Terryn, and I. De Graeve, "Inhibitor evaluation in different simulated concrete pore solution for the protection of steel rebars," *Constr. Build. Mater.*, vol. 124, pp. 887–896, 2016.

[56] R. M. Brown, M. M. Sprinkel, and R. E. Weyers, "Solution Tests of Corrosion-Inhibiting Admixtures for Reinforced Concrete," *Mater. J.*, vol. 99, no. 4, pp. 371–378, 2002.

[57] P. Saura, E. Zornoza, C. Andrade, and P. Garcés, "Steel corrosion-inhibiting effect of sodium nitrate in simulated concrete pore solutions," *Corrosion*, vol. 67, no. 7, 2011.

[58] I. Meland, O. Venncsland, and A. Hofsoy, "KS-prilletarn, Skade-undersokelse MV," *SINTEF Struct. Concr.*, 1995.

[59] J. Vogelsang, "Investigations on Corrosion Inhibitors and Chelating Agents in Alkaline Solution using Cyclovoltammetry," *8th Eur. Symp. Corros. Inhib.*, 1995.

[60] L. Dhouibi, E. Triki, and A. Raharinaivo, "The application of electrochemical impedance spectroscopy to determine the long-term effectiveness of corrosion inhibitors for steel in concrete," *Cem. Concr. Compos.*, vol. 24, no. 1, pp. 35–43, 2002.

[61] P. Montes-Garcia, H. Z. López-Calv, and T. W. Bremner, "Effectiveness of calcium nitrate inhibitor (CNI) in cracked concrete," *Rev. Ing. Constr.*, vol. 24, no. 3, 2009.

[62] T. A. Ostnor and H. Justnes, "Anodic corrosion inhibitors against chloride induced corrosion of concrete rebars," *Adv. Appl. Ceram.*, vol. 110, no. May, pp. 131–136, 2011.

[63] M. Torabzadegan, S. Collepardi, R. Troli, and W. Franke, "Effectiveness of Calcium Nitrate as a concrete corrosion inhibitor according to ASTM G109-07," in *European Corrosion Congress*, 2016.

[64] ASTM G109-07, *Standard Test Method for Determining Effects of Chemical Admixtures on Corrosion of Embedded Steel Reinforcement in Concrete Exposed to Chloride Environments*. 2013.

[65] W. Franke, D. Weger, J. Skarabis, and C. Gehlen, "Study on Calcium Nitrate impact on Carbonation of Concrete," in *1st International Conference on Grand Challenges in*

Construction Materials, 2016.

[66] H. Justnes, "Accelerator Blends for Portland Cement," in *Second International Symposium on Cement and Concrete Technology in the 2000s*, 2000, vol. 1, pp. 433–442.

[67] W. Franke, C. Thiel, F. Duran, and C. Gehlen, "Effect of Calcium Nitrate on the freeze-thaw-resistance of concrete," *Betonw. und Fert. Plant Precast Technol.*, vol. 81, no. 10, 2015.

[68] N. Chikh, M. Cheikh-Zouaoui, S. Aggoun, and R. Duval, "Effects of calcium nitrate and triisopropanolamine on the setting and strength evolution of Portland cement pastes," *Mater. Struct. Constr.*, vol. 41, no. 1, pp. 31–36, 2008.

[69] ASTM C1582, *Standard Specification for Admixtures to Inhibit Chloride-Induced Corrosion of Reinforcing Steel in Concrete*. 2017.

[70] ASTM G61-86, *Standard Test Method for Conducting Cyclic Potentiodynamic Polarization Measurements for Localized Corrosion Susceptibility of Iron-, Nickel-, or Cobalt-Based Alloys1*, vol. 86. 2006, pp. 1–5.

[71] Ente Nazionale Italiano di Unificazione, "UNI EN 10080: Acciaio d'armatura per calcestruzzo - Acciaio d'armatura saldabile - Generalità," *Ente Naz. Ital. di Unificazione*, 2005.

[72] C. L. PAGE, "Mechanism of corrosion protection in reinforced concrete marine structures," *Nature*, vol. 258, p. 514, Dec. 1975.

[73] L. T. Mammoliti, L. C. Brown, C. M. Hansson, and B. B. Hope, "The influence of surface finish of reinforcing steel and pH of the test solution on the chloride threshold concentration for corrosion initiation in synthetic pore solutions," *Cem. Concr. Res.*, vol. 26, no. 4, pp. 545–550, 1996.

[74] A. P. Crane, "Corrosion of reinforcement in concrete construction.," 1983.

[75] N. Celin, "Sperimentazione di un inibitore di corrosione per la protezione delle armature nel calcestruzzo," 2016.

[76] BS EN 197-1, *Cement Part 1: Composition, Specifications and Conformity Criteria for Common Cements*. 2011, p. 50.

[77] Ente Nazionale Italiano di Unificazione, "UNI 9944: Corrosione e protezione dell'armatura del calcestruzzo. Determinazione della profondità di carbonatazione e del profilo di penetrazione degli ioni cloruro nel calcestruzzo.," *Ente Naz. Ital. di Unificazione*, 1992.

[78] ASTM C 876-91, *Standard Test Method for Half-Cell Potentials of Uncoated Reinforcing Steel in Concrete*, vol. 91. 2015, pp. 1–6.

[79] M. Stern and A. L. Geary, "Electrochemical Polarization: I. A Theoretical Analysis of the Shape of Polarization Curve," *J. Electrochem. Soc.*, vol. 104, no. 1, pp. 56–63, 1957.

[80] C. Andrade and J. A. González, "Quantitative measurements of corrosion rate of reinforcing steels embedded in concrete using polarization resistance measurements,"

Mater. Corros., vol. 29, no. 8, pp. 515–519, 1978.

[81] J. A. González, A. Molina, M. L. Escudero, and C. Andrade, "Errors in the electrochemical evaluation of very small corrosion rates-I. polarization resistance method applied to corrosion of steel in concrete," *Corros. Sci.*, vol. 25, no. 10, pp. 917–930, 1985.

[82] www.phys.org, "NIST method sees through concrete to detect early-stage corrosion." [Online]. Available: https://phys.org/news/2017-04-superman-nist-method-concrete-early-stage.html. [Accessed: 19-Mar-2018].

[83] www.cement.org, "Corrosion of Embedded Metals." [Online]. Available: http://www.cement.org/learn/concrete-technology/durability/corrosion-of-embedded-materials. [Accessed: 26-Jan-2018].

[84] Markhamglobal.com, "Marine Concrete Structures and Steel Corrosion," *MARKHAM Adding life to concrete*, 2016. [Online]. Available: https://www.markhamglobal.com/marine-concrete-structures-steel-corrosion/. [Accessed: 18-Feb-2018].

[85] wikipedia.org, "Nitrite." [Online]. Available: https://en.wikipedia.org/wiki/Nitrite. [Accessed: 06-Feb-2018].

Appendix A - Cyclic polarization curves

In this appendix, are reported the characteristic curves E vs i of the cyclic potentiodynamic polarization tests. They are divided according to the solutions compositions, that are identified with the following abbreviations:

- *REF* - reference solutions without any inhibitor;
- *NI 0.1* - inhibited solutions with calcium nitrite ($Ca(NO_2)_2$) in 0.1 mol/L concentration;
- *NI 0.3* - inhibited solutions with calcium nitrite ($Ca(NO_2)_2$) in 0.3 mol/L concentration;
- *NA 0.1* - inhibited solutions with calcium nitrate ($Ca(NO_3)_2$) in 0.1 mol/L concentration;
- *NA 0.3* - inhibited solutions with calcium nitrate ($Ca(NO_3)_2$) in 0.3 mol/L concentration.

The second number (after the dash) is referred to the chlorides dosage: *0.1* and *0.3* respectively for 0.1 mol/L and 0.3 mol/L concentrations. Additional abbreviations were used to identify the immersion time, e.g. *1 d* for one day of immersion, *3 d* for three days and *7 d* for seven days; the symbols *A*, *B*, *C* were used to identify the three identical test solutions for the triple multiplicity.

A.1 Reference solutions

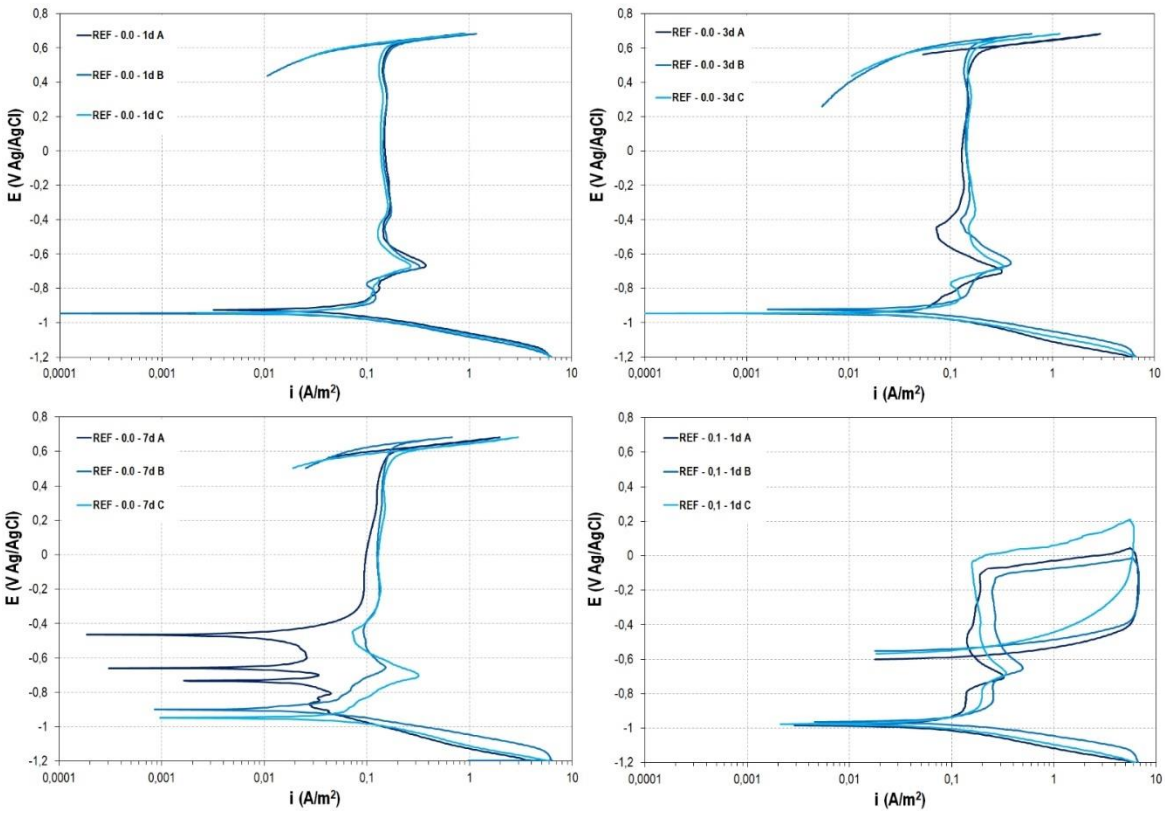

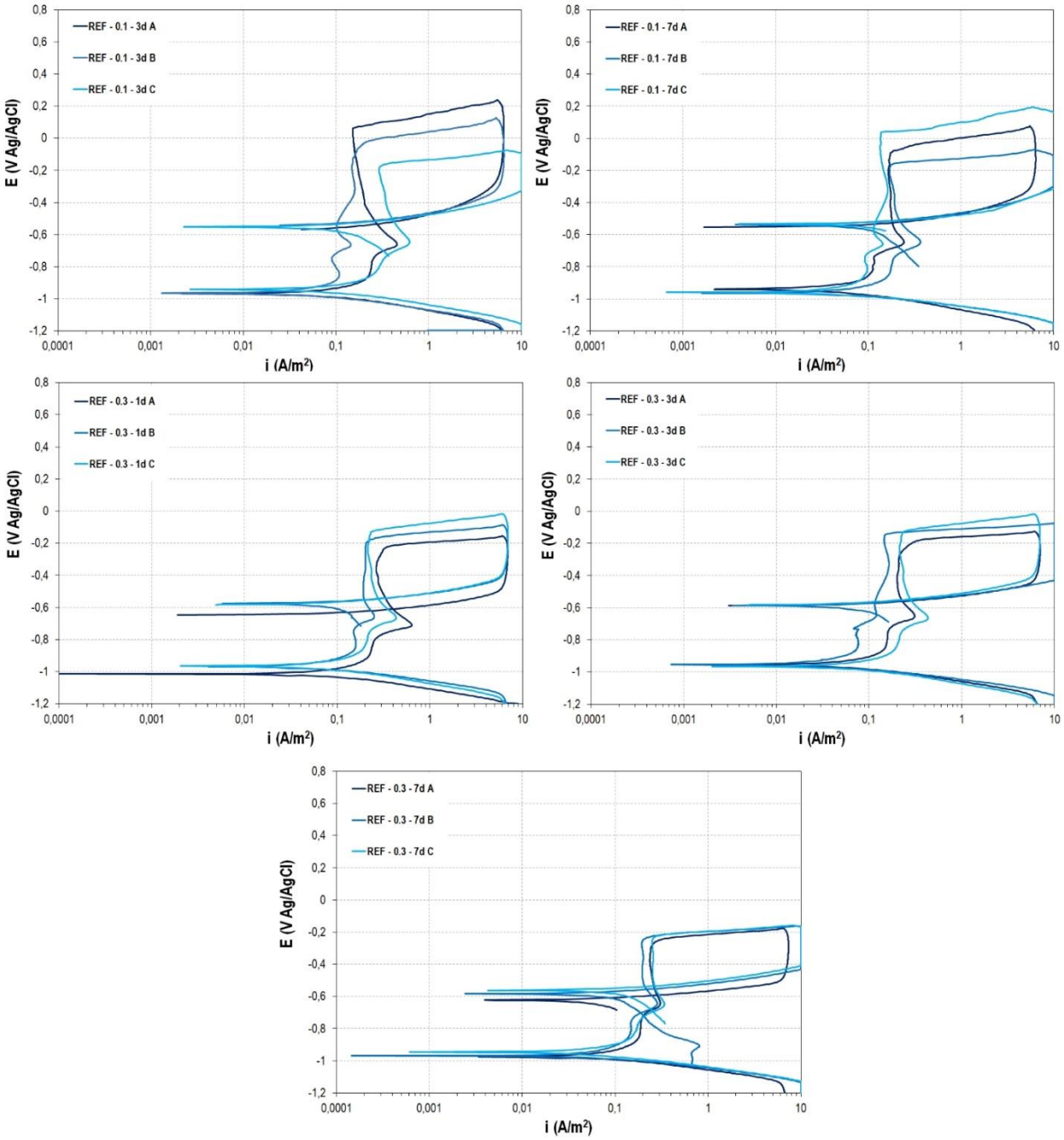

Fig. A.1 *Potentiodynamic characteristic curves of reference solutions.*

A.2 Nitrite inhibited solutions

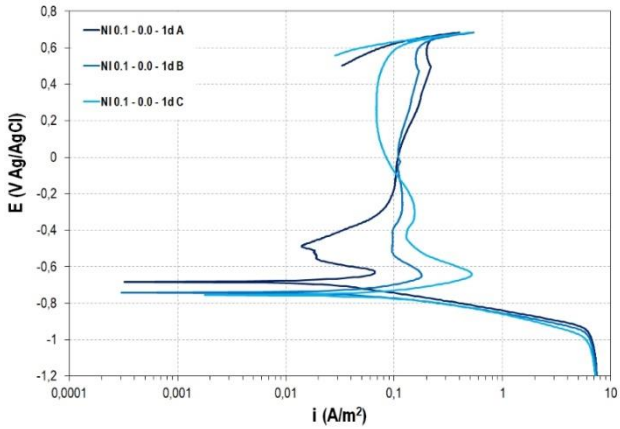

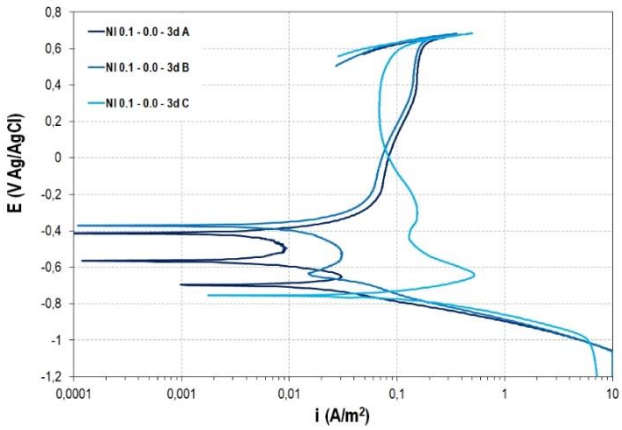

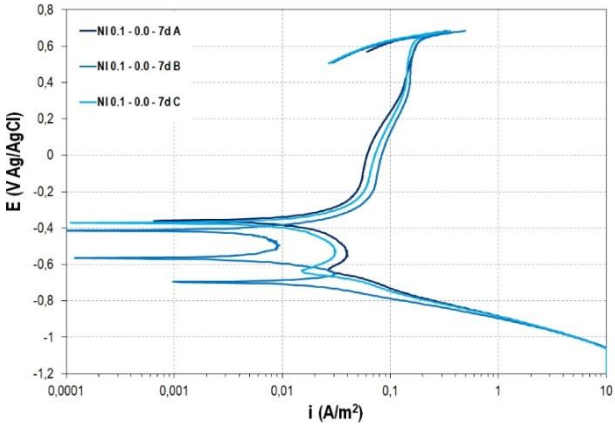

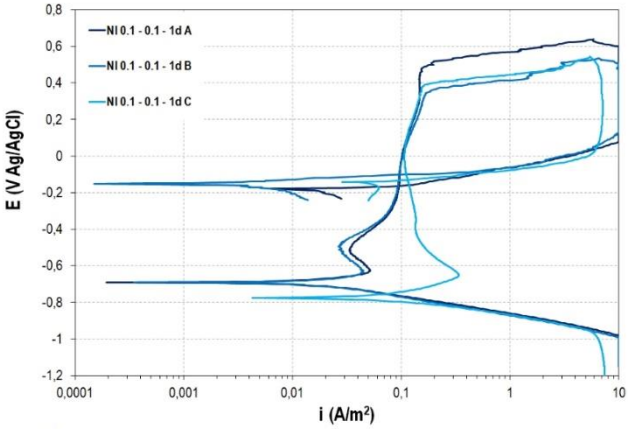

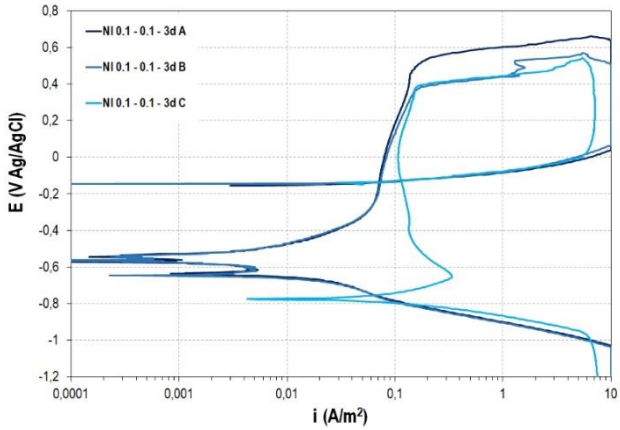

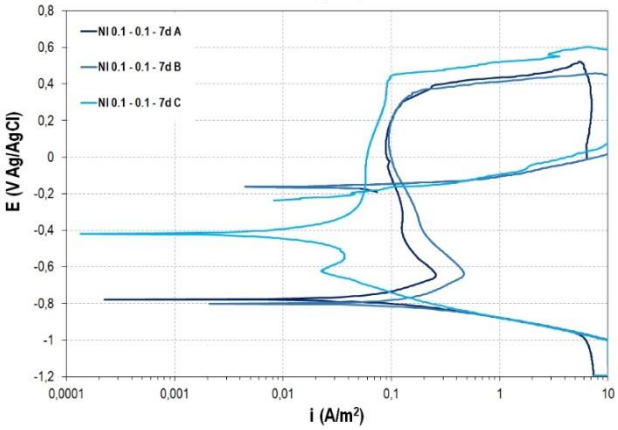

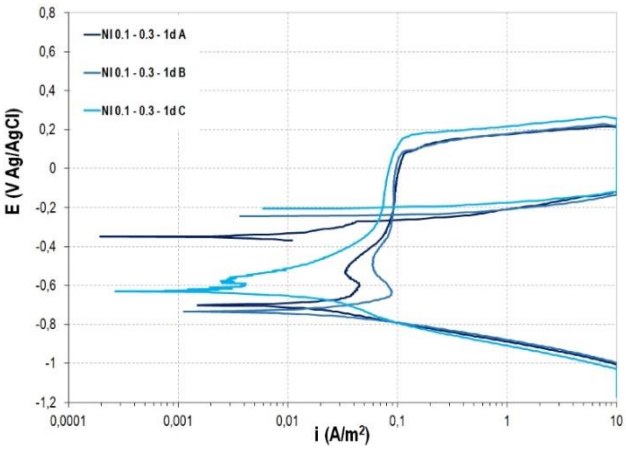

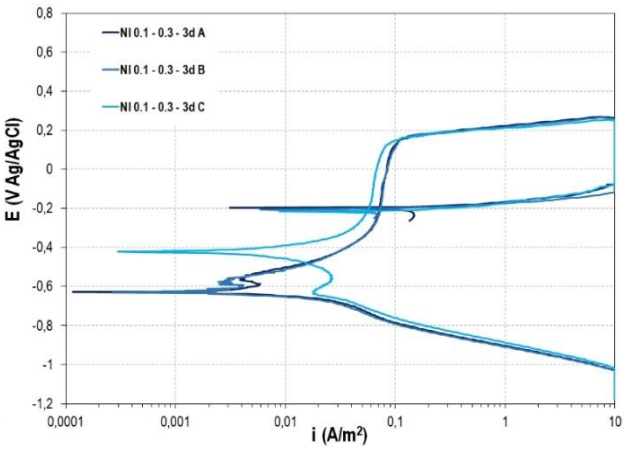

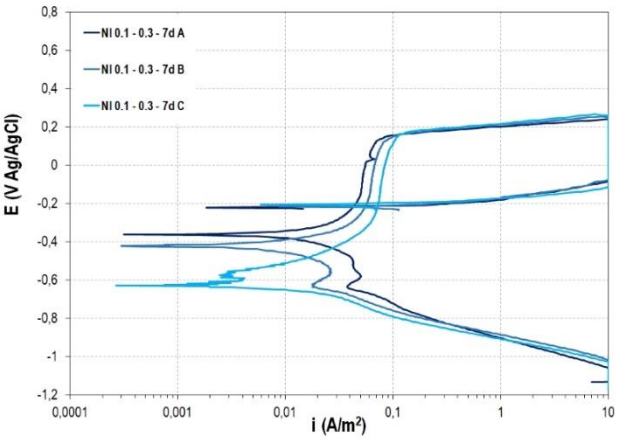
NI 0.1 - 0.3 - 7d A
NI 0.1 - 0.3 - 7d B
NI 0.1 - 0.3 - 7d C
E (V Ag/AgCl)
i (A/m²)

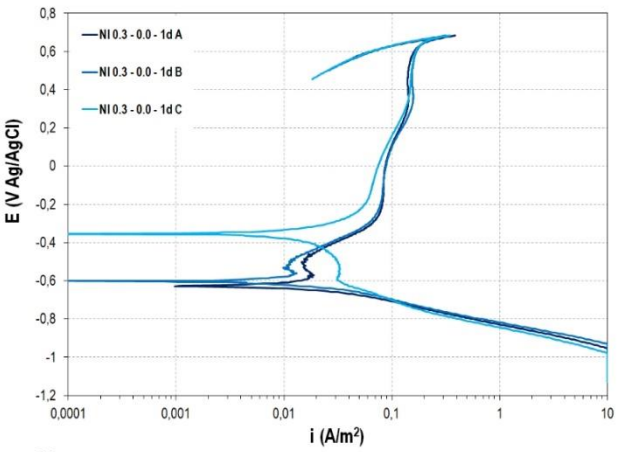
NI 0.3 - 0.0 - 1d A
NI 0.3 - 0.0 - 1d B
NI 0.3 - 0.0 - 1d C
E (V Ag/AgCl)
i (A/m²)

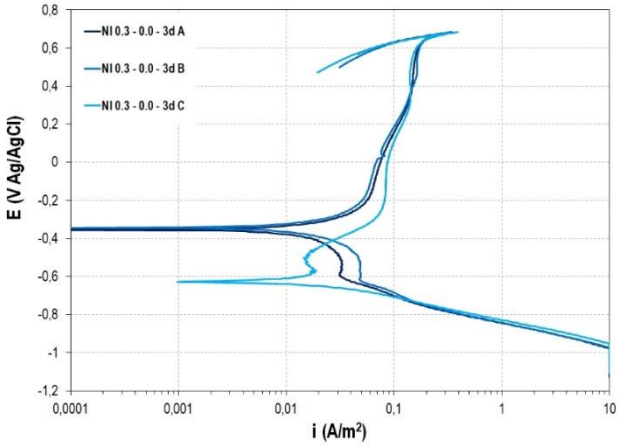
NI 0.3 - 0.0 - 3d A
NI 0.3 - 0.0 - 3d B
NI 0.3 - 0.0 - 3d C
E (V Ag/AgCl)
i (A/m²)

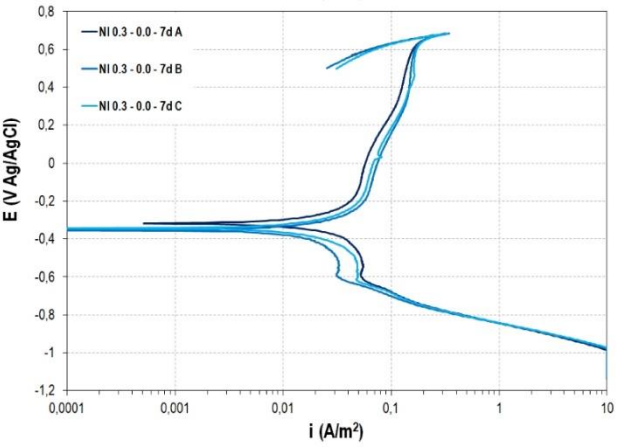
NI 0.3 - 0.0 - 7d A
NI 0.3 - 0.0 - 7d B
NI 0.3 - 0.0 - 7d C
E (V Ag/AgCl)
i (A/m²)

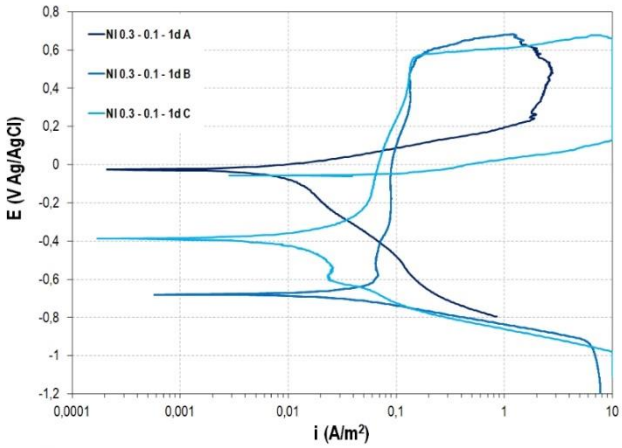
NI 0.3 - 0.1 - 1d A
NI 0.3 - 0.1 - 1d B
NI 0.3 - 0.1 - 1d C
E (V Ag/AgCl)
i (A/m²)

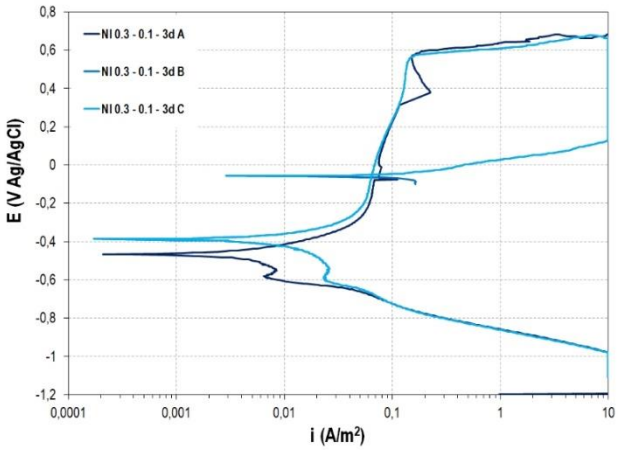
NI 0.3 - 0.1 - 3d A
NI 0.3 - 0.1 - 3d B
NI 0.3 - 0.1 - 3d C
E (V Ag/AgCl)
i (A/m²)

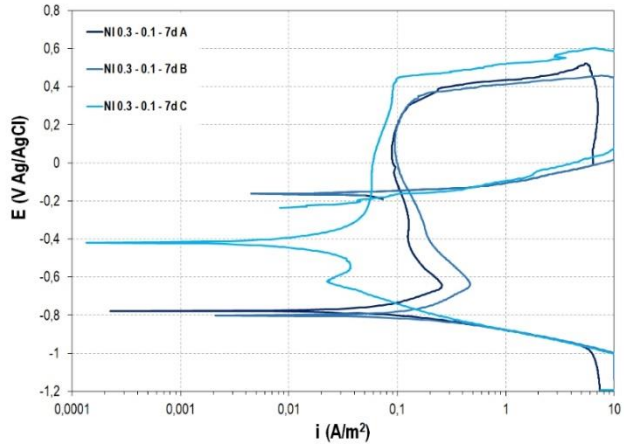
NI 0.3 - 0.1 - 7d A
NI 0.3 - 0.1 - 7d B
NI 0.3 - 0.1 - 7d C
E (V Ag/AgCl)
i (A/m²)

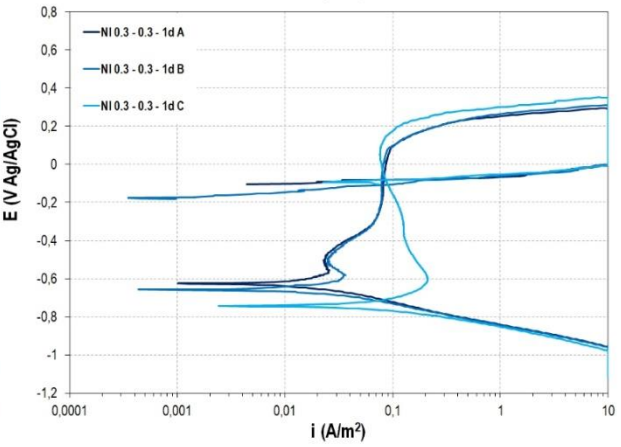
NI 0.3 - 0.3 - 1d A
NI 0.3 - 0.3 - 1d B
NI 0.3 - 0.3 - 1d C
E (V Ag/AgCl)
i (A/m²)

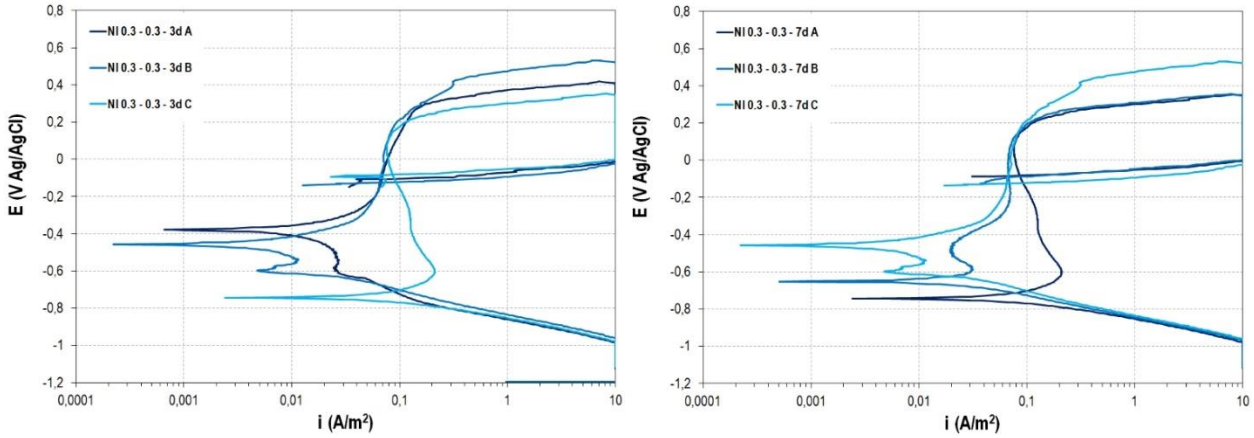

Fig. A.2 *Potentiodynamic curves of calcium nitrite inhibited solutions in 0.1 mol/L and 0.3 mol/L concentrations.*

A.3 Nitrate inhibited solutions

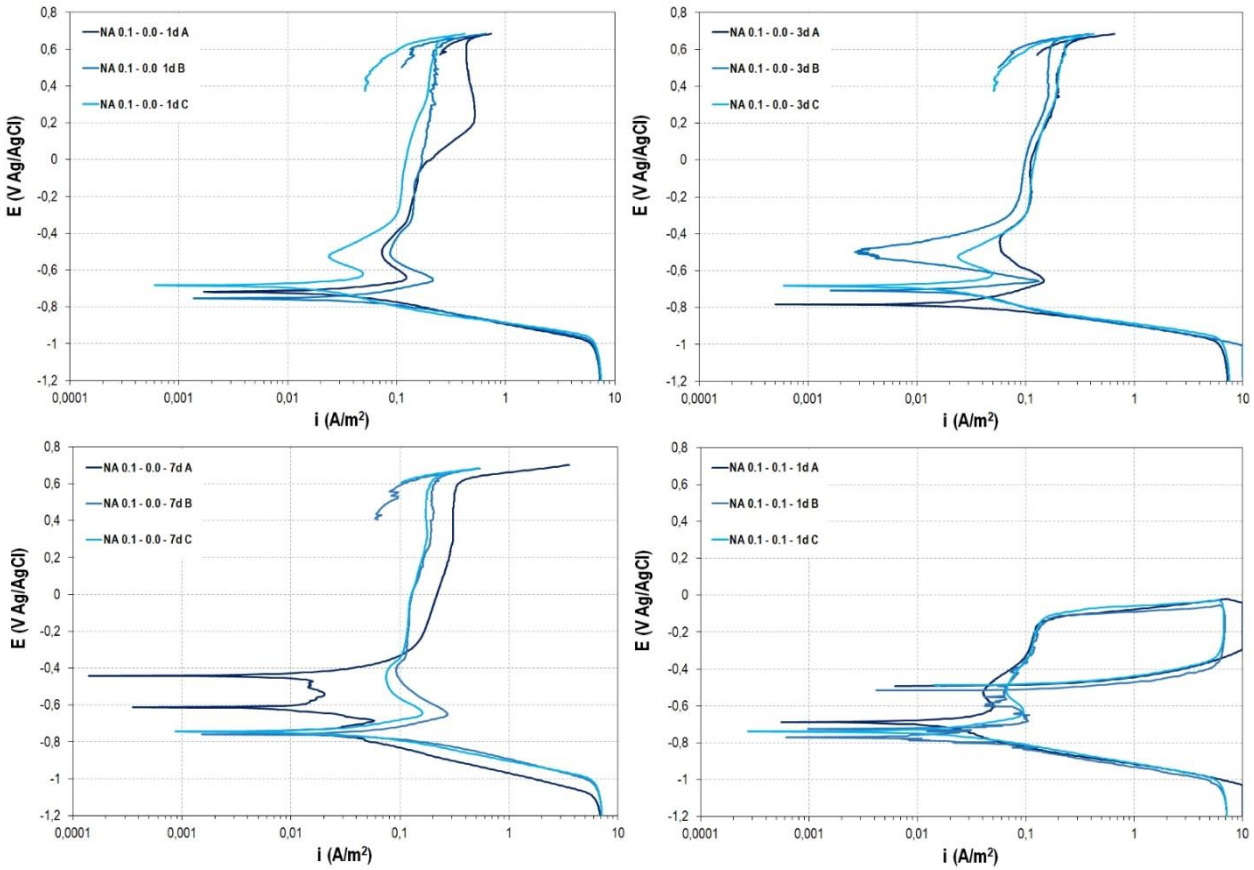

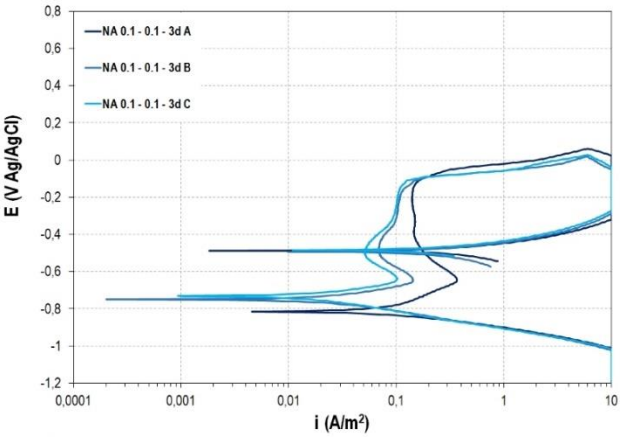
NA 0.1 - 0.1 - 3d A
NA 0.1 - 0.1 - 3d B
NA 0.1 - 0.1 - 3d C
E (V Ag/AgCl)
i (A/m²)

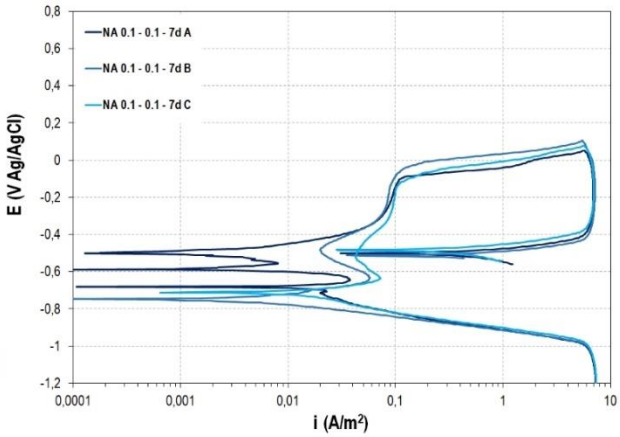
NA 0.1 - 0.1 - 7d A
NA 0.1 - 0.1 - 7d B
NA 0.1 - 0.1 - 7d C
E (V Ag/AgCl)
i (A/m²)

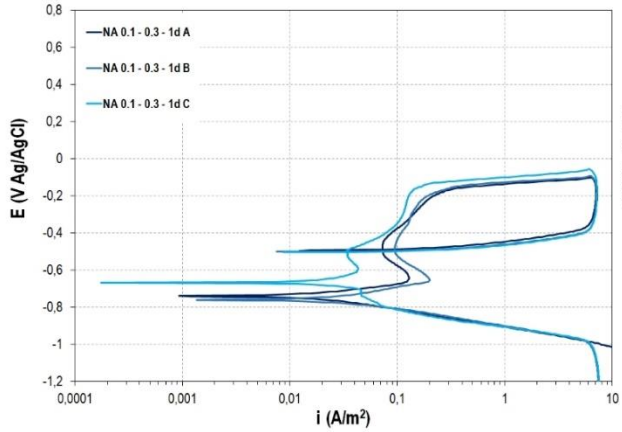
NA 0.1 - 0.3 - 1d A
NA 0.1 - 0.3 - 1d B
NA 0.1 - 0.3 - 1d C
E (V Ag/AgCl)
i (A/m²)

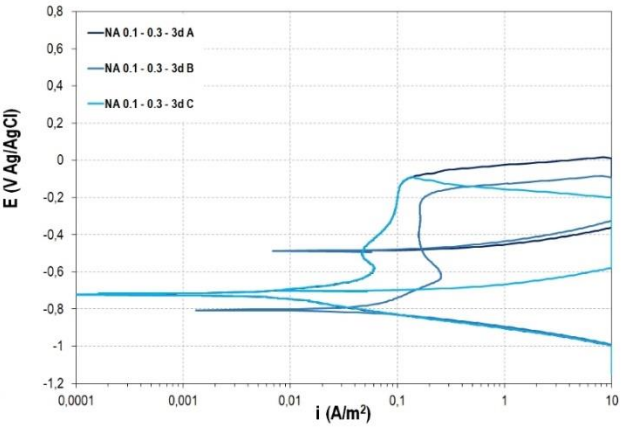
NA 0.1 - 0.3 - 3d A
NA 0.1 - 0.3 - 3d B
NA 0.1 - 0.3 - 3d C
E (V Ag/AgCl)
i (A/m²)

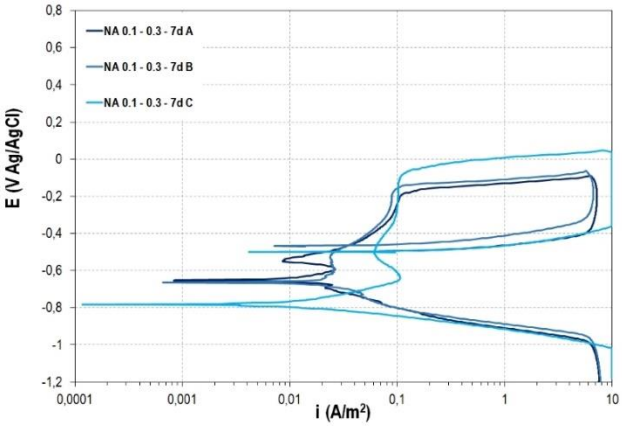
NA 0.1 - 0.3 - 7d A
NA 0.1 - 0.3 - 7d B
NA 0.1 - 0.3 - 7d C
E (V Ag/AgCl)
i (A/m²)

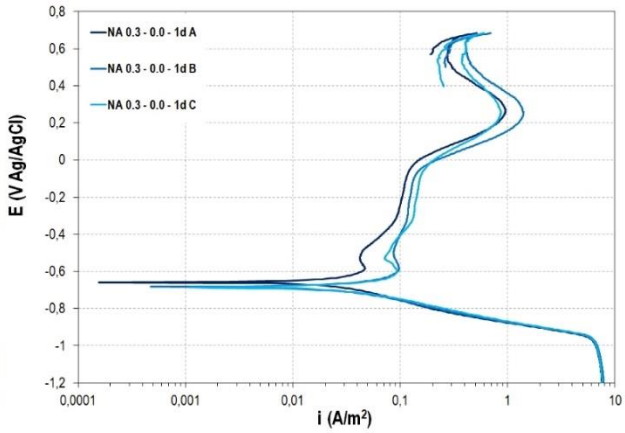
NA 0.3 - 0.0 - 1d A
NA 0.3 - 0.0 - 1d B
NA 0.3 - 0.0 - 1d C
E (V Ag/AgCl)
i (A/m²)

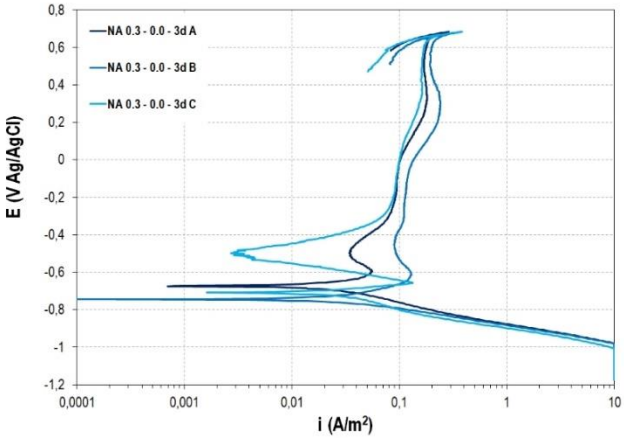
NA 0.3 - 0.0 - 3d A
NA 0.3 - 0.0 - 3d B
NA 0.3 - 0.0 - 3d C
E (V Ag/AgCl)
i (A/m²)

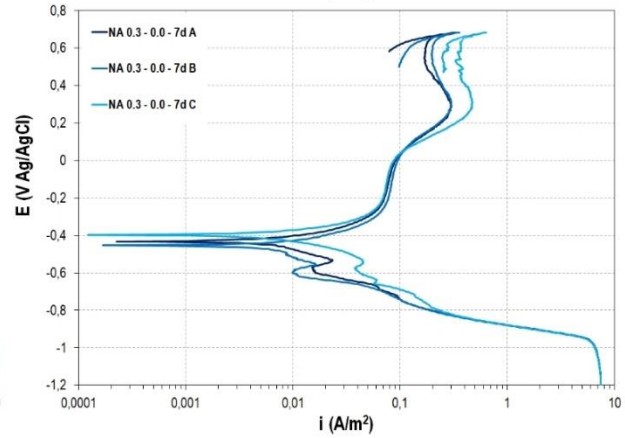
NA 0.3 - 0.0 - 7d A
NA 0.3 - 0.0 - 7d B
NA 0.3 - 0.0 - 7d C
E (V Ag/AgCl)
i (A/m²)

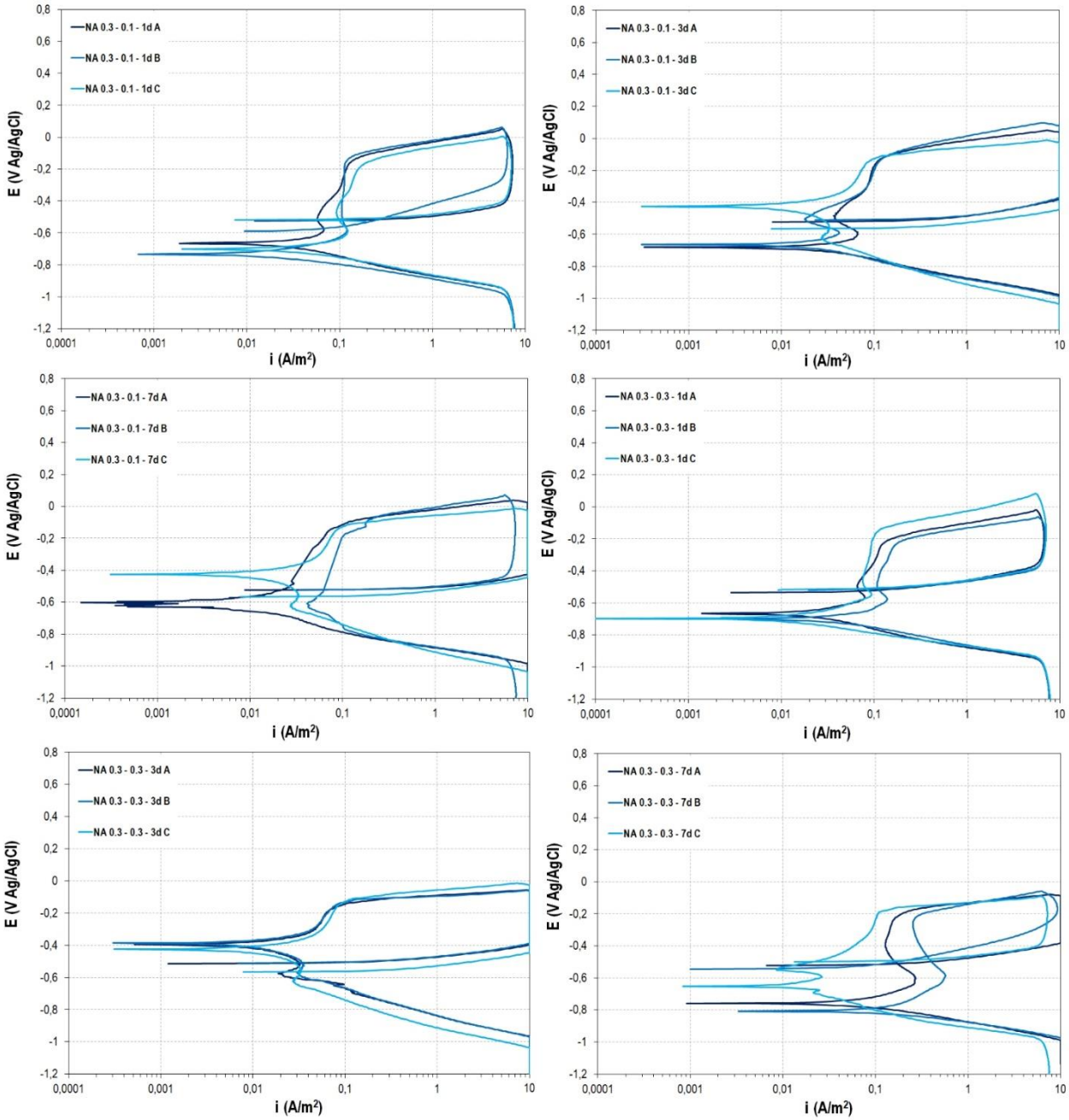

Fig. A.3 *Potentiodynamic characteristic curves of calcium nitrate inhibited solutions in 0.1 mol/L and 0.3 mol/L concentrations.*